universität wien

MASTERARBEIT | MASTER'S THESIS

Titel | Title

Impact of aneuploidy on cell size

verfasst von | submitted by

Lisa Pulferer BSc.

angestrebter akademischer Grad | in partial fulfilment of the requirements for the degree of

Master of Science (MSc)

Wien | Vienna, 2025

Studienkennzahl lt. Studienblatt | Degree programme code as it appears on the student record sheet:	UA 066 865
Studienrichtung lt. Studienblatt | Degree programme as it appears on the student record sheet:	Masterstudium Molecular Biology
Betreut von | Supervisor:	Assoz. Prof. Christopher Campbell PhD

Acknowledgements

I am extremely grateful to my thesis supervisor, Ass.-Prof Christopher Campbell PhD, for providing me with the opportunity to acquire new skills as well as improve my laboratory techniques by working on this project. I highly appreciate the time and expertise he dedicated to addressing my concerns and guiding me through the challenges of this project.

I want to sincerely thank my colleagues for providing a great working environment, which made working in the lab a pleasant experience. I especially want to thank Sophie for teaching me the techniques and the scientific discussions we had regarding my data. I appreciate the valuable feedback you have given me on this thesis and on my presentations. My thanks also go to Ananya, Kathi, Clara, and Rustam, who gave valuable advice and helped me when I was unable to make it to the lab.

Finally, I want to thank my family and friends for supporting me during the highs and lows of my academic journey.

Table of contents

Abstract

Aneuploidy describes the gain or loss of a chromosome, resulting in an abnormal chromosome number through missegregation. Various cancer types have been discovered to be aneuploid. Aneuploidy has been shown to cause various effects on the cell, such as influencing cell size. The mechanisms behind the cell size phenotypes of aneuploidies are poorly understood. Therefore, this study focuses on determining the major genes driving the cell size phenotypes in *Saccharomyces cerevisiae* disomic and double disomic strains. Specifically, focusing on Disomy 12 and Double Disomy of chromosomes 11 and 16, due to these two strains having the largest cell size phenotype.

Throughout the study, the cell size was determined with the CASY cell counter & analyzer. We hypothesized that disomy 12 cell size is due to the overexpression of the ribosomal DNA (rDNA). I discovered that the major drivers of cell size regulation are located on the right chromosome arm. Additionally, through sequential partial arm deletions of the right chromosome arm, four regions were identified contributing to the cell size phenotype, one of which is the rDNA region. The cell size increase of the double disomic strain 11x16 suggests synergistic effects between these two chromosomes are causing this phenotype. However, during this study, I discovered that some double disomic strains, including 11x16, are prone to spontaneously diploidize, making the previously observed phenotype not as significant.

Overall, the findings of this study contribute to the understanding of how aneuploidies regulate their cell size.

Keywords: Aneuploidy, yeast, cell size, chromosome 12, CASY, rDNA, disomy, double disomy, synergistic effects, diploidization

Zusammenfassung

Der Term Aneuploidie wird verwendet, um einen Chromosomengewinn oder -verlust zu beschreiben, der zu einer abnormalen Chromosomenzahl führt. Man fand Aneuploiden in verschiedenen Krebsarten, wie Tumoren. Der Hefestamm, *Saccharomyces cerevisiae*, wird als Modellorganismus verwendet, um Aneuploiden zu erforschen, so wie in dieser Studie. Frühere Studien zeigten, dass Aneuploidien verschiedenste Auswirkungen auf die Zelle haben, wie zum Beispiel auf die Zellgröße. Die Mechanismen hinter der Zellgrößenveränderung in Zellen mit Aneuploiden sind jedoch nicht ausreichend untersucht. Daher liegt der Fokus dieser Studie auf dem Erforschen der Hauptgene, die einen Einfluss auf die Zellgröße in Disomie- und Doppel-Disomie-Stämmen haben, spezifisch für Disomie 12 sowie den Doppel-Disomie-Stamm mit der Chromosomenkombination 16 und 11.

Um die Zellgröße zu bestimmen, wurde der CASY Cell & Analizer verwendet. Eine der Theorien hinter dem Disomie-12-Zellgrößen-Phänotyp beruht auf der Überexpression von der ribosomalen DNA (rDNA) Region. In dieser Studie ergab sich, dass der rechte Arm des Chromosoms hauptverantwortlich für den Phänotyp ist. Die rDNA-Region ist eine von vier Regionen am rechten Chromosomenarm, welche eine Rolle bei der Zellgrößenregulierung hat. Beim Doppel-Disomie-Stamm 11x16-Zellgrößen-Phänotyp wird vermutet, dass die Synergieeffekte zwischen den zwei Chromosomen zur Zellgrößenveränderung beitragen. Während dieser Studie entdeckte man, dass einige Stämme anfällig sind für spontane Diploidisierung. Was die vorherigen Phänotypen nicht so signifikant macht wie vorher angenommen.

Diese Ergebnisse tragen zum Verständnis über die Zellgrößenregulation in aneuploiden Zellen bei.

Schlagwörter: Aneuploidie, Hefe, Zellgröße, Chromosom 12, CASY, rDNA, Disomie, doppelte Disomie, Synergieeffekte, Diploidisierung

1. Introduction

1.1. Aneuploidy - the gain or loss of a chromosome

Missegregation of a chromosome during cell division results in abnormal chromosome numbers in both daughter cells, which is called aneuploidy. Cell division is a highly conserved mechanism where the duplicated chromosomes are separated into both daughter cells. The chromosomes are condensed and held together by cohesion. During the metaphase, the chromosomes align in the metaphase plane and microtubules from the opposite spindle poles attach via the kinetochores (rev. in Hirano, 2015). Correct bi-oriented attachments of the kinetochores are monitored via the spindle assembly checkpoint (rev. in Amon, 1999; rev. in Tanaka, 2002). Cohesion is removed before the chromosomes are separated towards the poles (rev. in Hirano, 2015; rev. in Anjur-Dietrich et al, 2021). Defects of the chromosome segregation machinery or its control systems result in aneuploidy, leading to severe consequences on a cellular and organism level (Torres et al, 2007; Oromendia et al., 2012; rev. in Santaguida & Amon, 2015).

1.2. Aneuploidy causes a variety of diseases in humans

Aneuploidy is one of the major causes of miscarriages (rev. in Hassold & Jacobs,1984). The only viable aneuploid germ-line have gained chromosomes 13 (Patau Syndrome) (Hsu & Hou, 2007), chromosome 18 (Edwards Syndrome) (Lin et al., 2006), and chromosome 21 (Down Syndrome) (rev. in Hassold & Jacobs, 1984). However, the newborns with trisomy 13 and trisomy 18 only survive for up to a few months (Lin et al., 2006; Hsu & Hou, 2007).

Aneuploidy is a hallmark of cancers, with approximately 90% of solid tumors being aneuploid (rev. in Weaver & Cleveland, 2006; Boveri, 2008). However, the relationship between aneuploidies and cancer phenotypes is not yet fully understood. Aneuploidy likely plays an important role in cancer initiation and progression (rev. in Gorden et al., 2012). Furthermore, mutations can be driven by aneuploidy (Watson et al. 2024). Taking this into account, chemoresistance in cancer cells may arise not only from genome mutations but also from aneuploidy (Ippolito et al., 2021). The degree of aneuploidy, as well as the presence of specific aneuploidy combinations, influences

the failure or success of various treatment methods (Lukow et al., 2021). Taking advantage of the consequences of aneuploidies, an early detection method for cancerous lesions could be established before it has fully adapted (rev. in Ben-David & Amon, 2020; Lukow et al., 2021).

1.3. Effects of aneuploidy

Both the gain and the loss of a chromosome can impact cellular fitness in yeast as well as in human cell lines (Torres et al, 2007; Stingele et al., 2012). The gain of an entire chromosome is more tolerated than losing a chromosome (monosomy) (Beach et al., 2017). Monosomies with a diploid background, which have lost a larger chromosome, lead in most cases to cell death (Torres et al, 2007; Beach et al., 2017; Koller et al., 2025). The resulting fitness defects scale with the number of aneuploid genes, indicating that there is a relationship between relative gene expression levels and aneuploidy (Beach et al., 2017). As a result of the stress caused by gene expression levels, cell cycle progression may be impacted, such as delays in G1 to S phase transition (Torres et al, 2007; Thorburn et al., 2013; Beach et al., 2017; Sommer, 2021). Aneuploid strains exhibiting a delay in the G1 stage likely have a dysregulated macromolecule biosynthesis pathway (Beach et al., 2017). To pass the G1/S checkpoint, a certain number of cyclins, such as CLN3, must be produced for the cell to proceed. However, due to low expression levels of CLN3 in some aneuploid strains, a G1 delay occurs (Thorburn et al., 2013; Sommer et al., 2021).

The downregulation and overexpression of genes in aneuploid strains causes protein imbalance, which in turn affects cell cycle progression and reduces fitness (Torres et al., 2007; rev. in Torres et al., 2008). To maintain a proper cellular function, dosage compensation is achieved by downregulating the transcription or by degrading the excess proteins (rev. in Torres et al, 2008; Muenzner et al., 2024). Due to the large number of misfolded proteins as well as the strained turnover pathways, the cells are under proteotoxic stress (Oromendia et al., 2012). Since the cell cannot keep up with the demand to degrade the misfolded proteins, the proteins form aggregates. For these to be removed, autophagy of the protein aggregates is induced (Santaguida et al., 2015). Overall, aneuploidy puts the cells under enormous stress, which triggers the upregulation of the stress response pathways and downregulates genes involving cell cycle progression and cell proliferation (Sheltzer et al., 2012).

1.4. Aneuploidy as an adaptation mechanism

Aneuploidy is an adaptive mechanism under specific conditions, such as low nutrient availability or exposure to high temperatures, that result in the selection of growth-promoting genetic alterations. These alterations can become highly beneficial for the cell (Sheltzer et al., 2011; Chen et al., 2012; Yona et al, 2012; Chen et al., 2015; Sirr et al., 2015; Voordeckers et al, 2015; Rojas et al., 2024). Aneuploid cells can gain a growth advantage, allowing them to dominate the population through continuous proliferation. However, if the conditions change, the previously gained advantage of aneuploid cells over non-genetically altered cells may turn into a disadvantage (rev. in Torres et al, 2008; Sheltzer et al., 2011; Rojas et al., 2024). Specific chromosomes are more likely to be gained under specific conditions, suggesting that certain genes on these chromosomes are required for survival under those conditions, e.g. drug resistance, environmental stress, pathogenic taxa (Chen et al., 2012; Yona et al, 2012; Chen et al., 2015; Zhu et al., 2016; Peter et al., 2018; Koller et al., 2025). In addition to aneuploidy, genetic alterations in strains with an abnormal number of chromosomes have been shown to improve the negative effects of aneuploidy (Torres et al., 2007; Torres et al., 2010).

Natural occurring yeast, like *Saccharomyces pastorianus*, has been found to have adapted to its environment via aneuploidy. *S. pastorianus* is a yeast strain used in beer brewing. Specific chromosomal copy number combinations influence the properties and flavor of the product (van den Broek et al. 2015).

A similar principle can be applied to cancer cells. Their cellular fitness has decreased due to aneuploidy (Stingele et al., 2012). However, by overexpressing specific genes, cancer cells gain a competitive advantage, which makes them thrive. Taking this into account, administration of drugs such as chemotherapeutics over a long period may lead cancer cells to alter specific dosage-sensitive genes, which drive the selection for these specific aneuploidies. This makes the cancer cells resistant to therapy (Lukow et al., 2021). By characterizing specific aneuploidy phenotypes and the genes that drive them, new cancer screenings and novel therapies can be developed (rev. in Ben-David & Amon, 2020).

1.5. Cell size regulation in aneuploid cells

Cell size as a parameter that can be applied to distinguish cancer cells from non-cancerous cells. Experiments have been conducted to determine if there is a possibility of recognizing various ploidy levels by their size. Human cells that undergo whole genome duplication (tetraploid) have a larger cell size compared to diploid cells (Duncan, 2023). Cancer cells from the NCI-60 panel, which have been confirmed to exhibit various forms of aneuploidy, have been found to increase their cell size notably compared to euploid cells (Tsai et al., 2019). Like cancer cells, yeast strains with various ploidy profiles have an increased cell size (Zadrag-Tecza et al. 2018).

There are three main models for how genes can regulate yeast cell size homeostasis: “sizers”, “timers”, and “adders”. Sizers regulate their size by accumulating inducers and thereby diluting inhibitors to pass, for example, the G1/S phase checkpoint and enter the S phase (Facchetti et al., 2017; Chandler-Brown et al., 2017; Pérez et al., 2022). Timers initiate molecular events after a fixed amount of time. Adders regulate the cell size through a fixed size increase, combining both sizer and timer models (Chandler-Brown et al., 2017; Facchetti et al., 2017; Pérez et al., 2022).

An example of the sizer mechanism in yeast is at the START transition, where the accumulation of cyclins, e.g. CLN3, in G1 triggers the transition to S phase (Turner et al, 2012). During the accumulation of the activator CLN3, the inhibitor Whi5 is diluted while the cell increases in volume (Wang et al., 2009; Chandler-Brown et al., 2017; Facchetti et al., 2017). The transition between the cell cycle phases is triggered once the accumulated cyclins reach their maximum number in the nucleus (Pérez et al., 2022). Therefore, the cell’s largest size is obtained when the amount of CLN3 reached its highest level. A positive feedback loop is established for the cells to grow to a fixed cell size when the threshold for the START transition is reached (Wang et al., 2009; Facchetti et al., 2017). This is also referred to as the critical cell size (Hartwell & Unger, 1977). However, size control in yeast is not mainly due to the accumulation of Whi5, which indicates the sizer model may be too simplistic (Barber et al., 2020; Sommer et al., 2021).

Cell cycle mutants, which have been genetically manipulated to block the cell at various cell cycle stages, continue to increase their cell volume, mass, and protein content,

suggesting a connection between cell size and cell division (Johnston et al., 1977). As previously mentioned, yeast strains with whole-genome duplication across various ploidy states were found to increase in cell size (Wu et al., 2010; Zadrag-Tecza et al. 2018). The increased volume of the cells is caused by the increased transcription rates to maintain the cells' cellular homeostasis (Wu et al., 2010). However, when these cells with various levels of ploidy further increased in cell size this led to the cell's death via bursting (Zadrag-Tecza et al. 2018).

In aneuploid yeast cells, the increased cell size can be caused by the resulting protein imbalance, causing the cells to experience hypo-osmotic stress, leading to the swelling of the cells (Tsai et al., 2019). Furthermore, a connection between cell cycle entry delays and cell size in aneuploids was discovered (Thorburn et al. 2013). Defects in cell cycle entry of disomic strains are perturbed in the G1 phase by interfering with the activation of the Cln3-CDK cascade and cell growth. This delay resulted in an increased critical cell size, which correlates with the degree of aneuploidy, suggesting that the additional chromosomes influence cell size (Thorburn et al. 2013). However, strains have been engineered with additional yeast artificial chromosomes (YACs), encoding human genes, where no changes in cell size were found. These findings indicate that although a correlation between cell size and the degree of aneuploidy was found, there is no relationship between cell size and the amount of DNA present (Thorburn et al. 2013). The Bachelor thesis of Nina Stanišić (2023) concluded that cell size regulation in aneuploids is chromosome-specific, indicating that specific genes drive various cell size phenotypes.

1.6. Ribosomal DNA and cell size phenotype of chromosome 12.

Among the various single disomic strains associated with increased cell size, the largest cell size phenotype has been identified to be the result of gaining an extra copy of chromosome 12 (Nina Stanišić, 2023). Disomy 12 was found to have twice the size of the haploid cell and exceeded the size of the diploid control by 20fL. The phenotype is a result of overexpressing at least one gene, which influences the cell size. The *Saccharomyces cerevisiae* chromosome 12 is one of the largest chromosomes, with a length of 1078kb. Located on the right chromosome arm is the conserved rDNA region, which occupies a total of 60% of the full chromosome's length (Petes, 1979). The region consists of approximately 150 repeated copies of 9.1kb rDNA sequences (Albert

et al., 2013; rev. in Kobayashi, 2014). In an rDNA copy, the ribosomal RNAs 5S and 35S are encoded. 35S is further processed into three mature rRNA species, 18S, 25S, and 5.8S(rev. in Kobayashi, 2014). Since the largest region on the chromosome is where the rDNA repeats are located, it can be suspected that the region drives the cell size phenotype. The Bachelor thesis of Nikola Yordanov (2024) compared full chromosome arm deletion strains, where the right arm was identified to be the main contributor to the cell size increase.

Disomy 12 has been found to have a high variability in ribosomal DNA (rDNA) copy numbers (Thorburn et al. 2013). This is due to the rDNA region being a relatively unstable genomic element that needs active maintenance. Variations in the copy numbers can result from environmental and genetic factors (rev. in Nelson et al., 2019; Thornton et al., 2025). Excess rDNA copies prevent transcriptional replication conflicts by forming extra-chromosomal rDNA circles. These circles are formed through intra-chromatid recombination between distant rDNA copies. If the rDNA copies decline, for example, due to DNA damage, the circles can be reincorporated into the chromosome via homologous recombination to maintain a certain amount of rDNA repeats (rev. in Kobayashi, 2014; rev. in Nelson et al., 2019).

Extra-chromosomal rDNA circles can impact the cell in various ways, such as aging (Sinclair & Guarente, 1997). The number of rDNA circles increases with the age of the mother cell, since these do not have a centromere and can not be transferred to the daughter cell. Therefore, the rDNA circles accumulate in the mother cell over time (Shcheprova et al., 2008). Excess amounts of rDNA circles interfere with cell proliferation by influencing the expression of G1/S phase genes (Neurohr et al., 2018). Detrimental effects for cells occur after reaching over 360 copies and by the time of cell death, the cell has accumulated approximately 1500 copies. This indicates that accumulating rDNA circles speeds up the aging process of the yeast cell, which ultimately leads to cell death (Sinclair & Guarente, 1997; Morlot et al., 2019).

The cell volume of cell size mutant strains changed proportionally to the increase or decrease of rDNA repeats (Pérez-Ortín, 2021). Nina Stanišić (2023) analyzed strains in which rDNA circles have been overexpressed have increased in cell size. However, overexpressing rDNA circles comes with a variety of other problems for the cell. A large

amount of rDNA circles becomes highly toxic to the cells, which could in turn influence the cell size (Sinclair & Guarente, 1997; Shcheprova et al., 2008; Neurohr et al., 2018; Morlot et al., 2019).

1.7. Aim of my project

Although there are a variety of models describing cell size regulation, limited information regarding how aneuploid cells regulate their size or what specific genes drive the cell size phenotype is known. Therefore, this study will provide insights into how cell size regulation influences aneuploidies in the yeast model organism *S. cerevisiae*. Previously, Nina Stanišić (2023) confirmed that cell size phenotypes are chromosome-specific. This result indicates that specific genes encoded on the overexpressed chromosomes disrupt the regulation of the cell size mechanism. The overall goal is to identify specific genes and the driving mechanism of cell size in cell size phenotypes in aneuploidies by using Campbell lab's *S. cerevisiae* single disomy and double disomy collections.

The Campbell lab previously identified the largest cell size phenotypes in the single disomy collection as disomy 12 (Nina Stanišić, 2023). Although the data gathered by Nina Stanišić (2023) and Nikola Yordanov (2024) suggest that the rDNA may be playing a major role in the cell size phenotype. However, other genes and their alternative cell size regulatory pathways cannot be excluded. Therefore, in this study, I focus on engineering disomic chromosome 12 full and partial chromosome arm deletion strains (Linder et al., 2017) to narrow down the regions involved in cell size regulation.

For the double disomy collection, the largest cell size phenotype was discovered to be the chromosome combination 11 and 16 (11x16) (Nina Stanišić, 2023). This chromosome combination resulted in a significantly larger cell volume than the haploid control as well as the diploid control. Disomy 16 has no size phenotype. However, disomy 11 is significantly larger than the haploid control. No information is available about the cell size mechanisms involved in the double disomic strains. It can be suspected that synergistic effects occur, meaning that each chromosome contains at least one gene that in combination, influences cell size. To identify these genes, I will

engineer full and partial chromosome arm deletion strains (Linder et al., 2017) and measure the changes in cell size.

2. Methods and Materials

2.1. Yeast strains and Molecular Barcoded Yeast ORF library

The aneuploid yeast strains used in this study were taken from the Christopher Campbell Lab Yeast (CCY) collection, which includes the disomy collection, the double disomy collection as well as the newly established Aneuploid Chromosome Dissection Collection (ACDC). The ACDC includes full and partial arm deletions of 14 out of 16 disomic chromosomes. The main contributors of the ACDC library are Clara Hackethal, Manuela Sophie Koller, Rodina Genidy, Rustam Tuktarov and Lisa Pulferer. The missegregation inductions of all 14 disomic parent strains were engineered by Katharina Nittnaus (2024). All yeast strains in this study have a S288c background. A detailed description of all strains used in this study is provided in the supplementary Table S4 and S5. Strains were kept on selective media plates to continuously select their aneuploidy. All yeast strains were grown at 30°C. Overnight cultures (ON) were incubated for approximately 16h at 30°C and 200rpm. For the experiments, liquid selective media with different amino acid combinations, liquid synthetic complete media (SC), and yeast extract peptone adenine dextrose (YPAD) media were used (Table S8).

The Molecular Barcoded Yeast ORF library (MoBY) was used as a template to perform the desired deletions for the partial and full arm deletions (Table S7) (Ho et al. 2009). Each MoBY plasmid encodes one specific gene, two unique barcodes, and a kanamycin (G418) cassette. Media containing G418 and chloramphenicol (CHL) were used to grow these bacterial strains (Ho et al. 2009). Bacterial cultures (*Escherichia coli* containing the MoBY plasmid) were grown at 37°C for a maximum of 16h, due to the antibiotics losing their effectiveness over time and, in turn, resulting in the loss of the plasmid in the cell. Liquid overnight cultures were additionally shaken at 200rpm. Details about the different growth media used are in Table S8.

2.2. Designing full and partial chromosome arm deletion strains

The full arm deletions were designed by combining two DNA fragments. One fragment containing the homology region where the cut was made, while the other fragment consisted of the G418 cascade and a unique UPTAG and DOWNTAG. The unique barcodes, as well as the G418 cascade, were taken from the established MoBY library.

Both fragments had to be amplified individually and were combined through overlap extension PCR.

Partial arm deletions were designed every 75 kb. Therefore, genes in that interval were cross-referenced to the MoBY library to find a plasmid encoding that specific gene, which was used as a homology region. Further, the barcodes, UPTAG and DOWNTAG, of the plasmid had to be unique. After confirming by sequencing that the correct gene and tags were integrated into the plasmid, primers were designed approximately 200 bp into the gene from the stop codon. This was done to amplify the homology region at the genes' 3' end and the barcodes along with the G418 cassette.

2.3. Genetic manipulation

2.3.1. Plasmid extraction

The QIAquick® Spin Miniprep method by Qiagen (Düsseldorf, Germany) was used to extract the MoBY plasmids. The overnight grown liquid *E.coli* cultures were pelleted in an Eppendorf tub by centrifugation at 20-25°C for 3 min at full speed (14.650 rpm). The pellet was resuspended in 250µL Buffer P1 (50mM tris(hydroxymethyl) aminomethane hydrochloride (Tris-HCl), 10 mM ethylenediaminetetraacetic acid (EDTA), pH 8.0, 100µg/ml RNase A). The same amount of Buffer P2 (200 mM sodium hydroxide (NaOH), 1% sodium dodecyl sulfate (SDS)) was added and mixed thoroughly by inverting the tube to lyse the cells. To stop the lysis reaction, 350µL of Buffer N3 (4.2M guanidine hydrochloride (Gu), 0.9M potassium acetate (KOAc), pH 4.8) were added and mixed. To separate the cellular wall from the genetic material, the tube was centrifuged in a tabletop centrifuge at full speed for 14 min. The supernatant was transferred into the spin column and centrifuged for 60s at full speed. The flow-through was discharged, and 750µL of PE buffer (100 mM Tris-HCl, pH 7.5, 80% ethanol (EtOH)) was added for washing. The column was spun for 60s at full speed and the flow-through was discharged. For no PE buffer to remain, the tube was spun again. For eluting the plasmid, the column was placed into a fresh 1.5mL Eppendorf tube, and 35µL of water was applied directly to the membrane. After waiting for at least a minute at room temperature, the tube was spun down with the same settings as the previous centrifugation step. Each plasmid concentration and purity were determined via Nanodrop.

2.3.2. Polymerase chain reaction (PCR)

The DNA fragment used in this study was amplified through polymerase chain reaction (PCR) using the Phusion High-Fidelity DNA Polymerase (ThermoFisher) or the Q5 polymerase (New England Biolabs, Ipswich, USA).

2.3.2.1. Amplification of a single fragment

The primers were designed and ordered from Microsynth (see primer list in Table S6). The templates used were either extracted MoBY plasmids or the genetic material from specific yeast strains, extracted with NaOH.

Each reaction consisted of the following master mix final concentrations: 200µM dNTPs (New England Biolabs, Ipswich, USA), 0.02U/µL Polymerase, 1µl or 0.5µL template DNA (MoBY plasmid was 1:20 diluted), 0.2µM forward and reverse primer (Microsynth, Balgach, Switzerland). The Phusion polymerase had the 1 × HF Reaction Buffer (Thermo Fisher Scientific, Waltham, USA), and the Q5 polymerase needed 1x Q5 Reaction Buffer (New England Biolabs, Ipswich, USA) in the master mix. The reaction volume was filled up to 50µL with ddH_2O. The standard PCR program, which was the same for both polymerases, was programmed on an Analytik Jena Biometra TOne 96 thermal cycler. The program started with initial denaturation of the DNA at 98°C for 30s, followed by 34 cycles of a denaturation step at 98°C for 5 to 10s, primer annealing at 52°C for 10-30s, and the extension step at 72°C for 15-30s/kb. The final extension step lasted 5 min followed by cooling the cycler down to 4°C to preserve the samples. The annealing temperatures were adjusted depending on the assay, and the extension time depended on the fragment length of the PCR product.

2.3.2.2. Overlap extension PCR

This PCR was applied when combining two fragments into a single product. Master mix conditions did not differ from normal PCR (chapter 2.5.1). The two templates were added at an equimolar ratio. The total volume for template DNA was not to exceed 2µL. Primers were only added after the first 15 cycles. The overlap extension PCR program: initial denaturation at 98°C for 30s, followed by 15 cycles of denaturation at 98°C for 7s, annealing at 64°C for 20s, and 1 min of extension at 72°C. After primers were added 20 cycles of the previous steps were repeated. The annealing temperature decreased to 52°C, and the extension time was extended to 1 min and 20s.

2.3.3. Gel electrophoresis

Agarose gel electrophoresis was used to verify proper insertion or deletion fragments amplified by PCR. The PCR product was loaded onto a 0.8% agarose (GERBU) gel with PeqGreen (VWR, Radnor, USA) dye. A total sample volume of 8µL was used, consisting of 5µL PCR product and 3µL of Orange G (total volume 50 mL: 0.2g Orange G, 30% glycerol, 35 mL ddH2O, AppliChem). The PCR product bands were companied to 1kb Plus DNA Ladder (New England Biolabs). Gels were run at 90V for 30min and imaged with the Gel DocTM XR+ (BIO RAD, Hercules, USA).

2.3.4. Enzymatic digest with DpnI

To remove the remaining parental plasmid in the PCR product a DpnI digest was performed. 1µL DpnI (Biolabs) was added to a 50µL PCR reaction and kept at 37°C for one hour. In some cases, an additional PCR was performed to increase the DNA fragments concentrations.

2.3.5. Sequencing

To determine that the MoBY plasmids UP- and DOWNTAGS were correct, as well as that the amplified gene region did not have any mutations, the PCR products were sent for sequencing. 2µL of PCR product, 10µL of purified water, and 3µL of 20µM OCC3862 primer (Table S6) were transferred into a 1.5mL Eppendorf tube. The sequencing was performed by Microsynth (Balgach, Switzerland). If the sequencing quality was insufficient, the PCR product was purified via the PCR purification and the sequencing was repeated.

2.3.6. PCR product purification

The QIAquick® PCR purification method by Qiagen (Düsseldorf, Germany) was used to remove remaining master mix components, that influence the sequencing quality. 1 volume PCR reaction was mixed with 5 volumes of PB Buffer (5M Gu-HCl, 30 % Isopropanol) and transferred into a column. The samples were centrifuged with the tabletop centrifuge at full speed (14000 rpm) for 60s and the resulting flow-through was discharged. 750µL Buffer PE was added and the column was spun with the previous settings. The flow-through was discharged and the centrifugation step was repeated to remove the remaining buffer before transferring the column 1.5mL Eppendorf tube. To elute the PCR product 15µL of distilled water was applied to the center of the

membrane and incubated at room temperature for at least a minute. The purified sample was obtained after centrifugation, and the concentration was measured with the Nanodrop.

2.3.7. Yeast transformation protocol

Overnights cultures of the parent strains were grown in media that maintained their specific aneuploidy. Depending on the growth rate of the aneuploid strain, 700µL to 850µL of overnight culture was used to inoculate 50 mL of YPAD media. The flask was incubated for approximately 5 hours at 30°C and continuously shaken at 200 rpm till an optical density (OD) of 0.6 was reached. The culture was transferred into a 50 mL Falcon tube and centrifuged for 3 min at 2000 rpm (4°C). The supernatant was discharged, and the cells were resuspended in 5 mL of TE (10 mM Tris, 1 mM EDTA, pH 7.5). The tube was placed into the centrifuge and spun down with the same settings as previously stated. The supernatant was aspirated. The cells were washed with 5 mL of TE/LiAc (100mM Lithium acetate (LiAc), 10 mM Tris, 1 mM EDTA, pH 7.5), spun down, and the supernatant was removed. Per transformation, 100µL of TE/LiAc was used to resuspend the cells in. During the yeast cell preparation, the carrier DNA, denatured salmon sperm DNA (ssDNA, Invitrogen, Carlsbad, USA), was prepared by heating the ssDNA tube to 95°C on a heating block for 5 min, followed by transferring the tube onto ice. Each transformation reaction consisted of 10µL of PCR product (100ng - 1µg DNA), 5µL of ssDNA, and 100µL of cell suspension. 700µL of PEG/LiAc/TE (100mM LiAc, 10 mM Tris, 1 mM EDTA, pH 7.5, 40% Polyethylene glycol (PEG) 4000) was added, mixed thoroughly through inversion, and incubated for 30 min at 30°C without shaking. To the reactions, 80µL of dimethyl sulfoxide (DMSO) was added, mixed by inversion, and incubated for 15 min in a 45°C water bath. Cells were collected by centrifugation in a tabletop centrifuge at 5000 rpm for 2 min and the aspiration of the supernatant. Resuspension was done with 100µL SOS (6mM calcium chloride ($CaCl_2$), 0.3x YPA). For the arm deletions, the entire volume was plated on YPD plates, incubated at 30°C for one to two days, depending on the strain's growth, before replica-plating them on resistance marker selective media, e.g., G418. When transforming the haploid strains with the auxotrophic markers, these strains were plated directly onto the corresponding auxotrophic marker plates and incubated at 30°C for at least two days.

2.3.8. DNA extraction via NaOH

For each sample, 20µL of 0.02M NaOH was proportioned into PCR tubes. A clump of cells was taken from the fresh patches that had grown on the auxotrophic marker plate and mixed with NaOH. The samples were boiled at 100°C for 10 min in an Analytik Jena Biometra TOne 96 thermal cycler. To pellet the cellular material, the tubes were spun down in a minicentrifuge for 10 minutes.

2.3.9. Mating strains

Strains were mated to obtain different aneuploid chromosome combinations or diploid control strains containing different auxotrophic marker combinations. To mate two strains, they must be of opposite mating types, a or α. The strains were streaked out in a cross on YPAD plates. After incubating the strains at 30°C for a day, they were replica-plated on combined or single drop-out plates, depending on which auxotrophic markers the resulting mated strain had. Single colonies were picked, checked via qPCR to determine if the strain is indeed aneuploid, and then frozen. Diploids that contain the marker combinations were directly frozen.

2.3.10. Mating type test

Two YPD plates and the strains to test were prepared. Either the strain CCY80 or CCY81 was spread evenly across the plate. A clump of cells was diluted in 20µL ddH_2O and a 3µL drop was pipetted onto the YPD plate. The strains CCY801 and CCY802 were used as controls. The plates were incubated at 30°C for up to two days, and the growth observed indicated that the plated strain and the sample had mated. Growth was observed when the patched strain was the opposite mating type of the tested strain. Meaning the tested strain was of the opposite mating type of the patched strain. If no growth was seen both the mated strain and the tested strain are of the same mating type.

2.4. Confirmation of aneuploidy

2.4.1. Copy number variation analysis - quantitative PCR (qPCR)

Primers were prepared by combining 2µl of 100nM forward and 2µl of 100nM reverse primers with 72µL ddH2O (primers listed in Table S6). For an even distribution of the primers in the liquid, the tubes were vortexed and centrifuged with the minicentrifuge for a few seconds. The components of a 1x qPCR master mix are 7µL ddH2O, 10µL Luna universal qPCR master mix (New England Biolabs, Ipswich, USA), and 1µL of extracted template DNA. To ensure an even distribution of all master mix components, each sample tube was vortexed and then spun down. 18µL of the master mix was added to each well. Samples were either measured in duplicates or triplicates. 2µL of the primer mix was added to the designated wells. The plate was covered using an optically clear heat-sealing foil and sealed with the PX1 PCR Plate sealer (3s, 180°C). Before placing the plate into the qPCR machine (Eppendorf Mastercycler realplex4 epGradient S), it was centrifuged (Megafuge 1.0 R, Thermo Fisher Scientific) for a few seconds to spin down any droplets on the walls of each well. The standard qPCR program began with the initial denaturation performed at 95°C for 5 min, followed by 39 cycles of denaturation at 95°C for 15s and annealing of the primers at 60°C for 1 min. Afterwards, a melting curve was established for each primer pair. The samples were heated up to 95°C over 20 min. The output was the measured CT-values of each sample.

For confirmation of aneuploidy, the fold changes were used, which were obtained by normalizing the CT output to the unmodified chromosome arm and to the haploid values. A fold change of 1 obtained for a modified strain indicates that the chromosome arm has not been deleted. However, if a change to 0.5 was shown, the deletion was successful.

The rDNA copy numbers were determined via qPCR in Disomy 12, haploid and diploid cells by amplifying the rDNA regions 5S, 18S, and 35S 3'. Additionally, the ACT1 gene, located on chromosome 6, was amplified as a reference since there is only one copy. The fold changes were determined by normalizing the obtained CT-values to the ACT1. Two to the power of negative CT-value normalized to the ACT1, was taken. The resulting value is the relative rDNA copy number of each gene. To obtain the fold changes, the relative copy numbers are normalized to the haploid values.

2.4.2. Determination of the DNA amount via Fluorescence-activated cell sorting - FACS

The strains in question were grown overnight in selective media at 30°C and 200rpm. 500µL of the overnight culture was transferred into 10mL fresh YPAD media and incubated up to 5 hours at 30°C till an OD of 1 was reached. 300µL of cells were transferred into a 2mL Eppendorf tube before being spun down for 2 min at 2000 rpm, and the supernatant was removed. To resuspend the cells, 300µL of sterile H_2O was used. While vortexing, 700µL of 100% ethanol was added. The tubes were either incubated at room temperature for 1 hour or placed into the 4°C fridge for up to a month. The cells were pelleted, the supernatant was discharged, and the pellet was resuspended in 1 mL 50 mM Sodium Citrate (pH 7). The mixture was sonicated (Bandelin sonopuls, Berlin, Germany) with 3x 1s pulses at 35% and centrifuged at 14000 rpm for 1 min. Supernatant was removed and the cells resuspended in 100µL 50mM Sodium Citrate containing 250µg/mL RNase A (Thermo Scientific) and 1mg/mL Proteinase K. The tubes were mixed via inversion and incubated at 37°C overnight. The cells were centrifuged, supernatant discharged, resuspended in 1 mL 50 mM Sodium Citrate containing 1µM Sytox Green, and incubated for 1 hour at room temperature in the dark. Into the FACS designated tubes, 150µL of this sample solution was mixed with 1 mL of 50 mM Sodium Citrate. The samples were measured on the BD LSRFortessa™ Cell Analyzer.

2.5. CASY - Cell size measurement

To measure the cell size of yeast cells, overnights were grown in dropout, YPAD, or synthetic media. The OD of the overnight-grown strains were measured and diluted in 2mL media to have a starting OD of 0.1 for haploid strains, 0.12 for diploid strains, and 0.15 for chromosome-specific aneuploidies. The dilution was incubated at 30°C with shaking (200 rpm) for 5 hours. Each strain's OD was measured. The sample volume, which was transferred into the 10mL CASY Ton, was previously calculated (see Table S1) for all samples to have a similar number of cells for each measurement. The tubes were sonicated (Bandelin sonopuls, Berlin, Germany) for 10s at ~15% of power. Cell size of the samples was measured using a CASY cell counter & analyzer (OMNI Life Science GmbH & Co KG, Bremen, Germany). A 60µL capillary was used. To ensure nothing plugs the capillary, a weekly cleaning procedure with CASYclean was performed. By adjusting the amount of sample diluted into the CASYton, the error

message “high concentration” was less frequent. Nevertheless, if it occurred, the sample was diluted 1:1 by removing 4.6 mL of the sample CASYton mixture and refilling the volume up to 10 mL with CASYton. The cell volume and cell size were calculated by the program, where a size range from 3µm to 9µm was selected. The data obtained from CASY was analyzed in much more detail with the Python script, written by Manuela Sophie Koller. The script calculated a Gaussian curve fit over the data points measured by CASY. The Gaussian peak was used as the cell size for that strain in further analysis.

2.6. Computational analysis and statistical analysis

SnapGene was used to design primers and align the sequencing results of target genes.

To identify the fragment sizes of the PCR product, the gel images were visualized with Fiji/Image J (Version 2.14.0/1.54f).

The FACS data was analyzed and visualized via FLOWJO 11 (Version 11.0.0).

Python (3.12.4 64-bit) calculated Gaussian curves and the Gaussian peak of the cell size raw data. The script, working-file.py, additional used various other modules for the Gaussian curves and Gaussian peak to be calculated. The imported packages numpy, matplotlib.pyplot, scipy.optimize, pandas, sys, and os were used. Permission has been granted to use the script in this thesis.

To design graphs and conduct additional statistical analysis the GraphPad Prism program (Version 10.5.0 (673) was used.

The open-source program Biorender was used to create illustrations.

Microsoft Excel, Word and PowerPoint (Version 16.99.2) were used to summarize the data obtained in this study.

3. Results

Previously, the Campbell lab discovered that cell size phenotypes are chromosome-specific and only mildly correlate with the number of open reading frames (ORFs) on a chromosome. Hence, cell size phenotypes are caused by the overexpression of specific genes. Therefore, the main objective of this study is to investigate how aneuploidy impacts cell size regulation in both large disomic and double disomic cell size phenotypes.

3.1. Optimization of the CASY method

To obtain accurate cell size measurements, the CASY cell counter & analyzer (CASY) (OLS OMNI Life Science GmbH) was used, which calculates cell volume based on the change in conductivity between two electrodes. To determine the most reproducible experiment conditions, the three parameters: sample dilution, growth media, and incubation time, had to be optimized, as all three could influence cell size.

3.1.1. Samples should contain $5.40x10^3$ to $5.40x10^4$ cells to achieve an optimal cell size analysis.

Optimal sample concentration is necessary for the CASY system to distinguish between cell aggregates and large single cells (OLS CASY cell counter & analyzer Operators Guide). At a higher cell concentration, the system generated an error message to alert the operator of the possibility of cell aggregates having formed. Therefore, I determined the optimal cell count for a robust and reproducible CASY cell size measurement. The size of the same strain at different sample concentrations was measured (Table 1). The CASY raw data were fitted to a Gaussian curve to calculate the average size of the cells in a sample, using a customized Python script. The optimal theoretical cell concentration was between $5.40x10^3$ to $5.40x10^4$ (Table 1). In this range, no error message from the system was obtained. With this information, the appropriate dilution volume table (Table S1) was established. Furthermore, a cell size increase can be seen with increased cell concentration. This can be explained by the biological variability as well as the possibility of the formation of aggregates, leading to a shift in cell size.

Table 1: Determination of the optimal number of cells for the CASY cell counter analyzer by making various dilutions from a sample with an OD of 0.45 and 0.64. The theoretical cell amount in the total solution and the theoretically measured cells in a 400µL sample volume have been calculated. The cell concentration indicates if the measurement cell concentration was sufficient (+) and if CASY indicated a too high concentration (-). The cells counted value corresponds with the cells CASY measured in a 400µL sample. The Gaussian peak diameter, peak volume and the standard deviation were obtained with the Python script.

Sample Nr	OD	V dilution [µL]	total V [mL]	Theoretical total cells	Theoretical measured cells	cell conc	Cells counted	Gaussian peak volume [fL]	Gaussian peak diameter [µm]	Standard dev.
1	0.45	20	10	1.35E+04	5.40E+03	+	4.79E+03	97.4	5.71	0.58
2	0.45	60	10	4.05E+04	1.62E+04	+	1.20E+04	97.6	5.71	0.58
3	0.45	80	10	5.40E+04	2.16E+04	+	1.62E+04	97.6	5.71	0.59
4	0.45	100	10	6.75E+04	2.70E+04	+	1.93E+04	99.9	5.76	0.61
5	0.45	150	10	1.01E+05	4.05E+04	+	2.81E+04	102.2	5.80	0.63
6	0.45	200	10	1.35E+05	5.40E+04	+	3.64E+04	103.0	5.82	0.62
7	0.64	70	10	6.72E+04	2.69E+04	+	2.06E+04	102.6	5.81	0.58
8	0.64	100	10	9.60E+04	3.84E+04	-	2.88E+04	102.4	5.80	0.61
9	0.64	110	10	1.06E+05	4.22E+04	-	8.62E+04	102.5	5.81	0.62
10	0.64	150	10	1.44E+05	5.76E+04	-	9.94E+04	107.5	5.90	0.65

3.1.2. Growth media impact cell size more than the incubation times.

After determining the optimal cell amount in a sample for fewer error messages, attention was directed towards refining the experimental parameters, growth media and incubation time, to ensure reproducible data. Considerable differences between cell size measurements with different growth media and the duration of the incubation times were observed during the preliminary experiments. The nutrient availability for the cells can differ depending on the media composition, which can have an impact on cell growth. Additionally, the growth media is used to actively select for aneuploidy to ensure that the gained chromosomes are not lost during the experiment. As for the incubation times, cells with decreased proliferation could need more time to reach their critical cell size.

I tested the impact of different overnight media on the cell size of a haploid, diploid, and two randomly selected single disomy strains (single disomy of chromosomes 11 and 14) with restored auxotrophic markers histidine, uracil, lysine, and leucine. Strains were grown overnight in YPAD, synthetic media lacking histidine, uracil, leucine, and lysine (-HIS/-URA/-LYS/-LEU) or synthetic complete media (SC). The dilution was

performed in the same media used for the overnights (Figure 1A). Yeast grown in YPAD resulted in generally larger cells than grown in synthetic media (Figure 1A). The difference in cell sizes between strains was not affected by the culture media and was consistent across the different media conditions (Figure 1B and Supplement Figure S1). Since the strain-to-strain differences in cell size are not affected by the media conditions, -HIS/-URA/-LYS/-LEU media was used to grow cells into log phase for the size measurements. Strains that were auxotrophic for lysine and leucine were grown overnight in selective media lacking only histidine and uracil (-HIS/-URA), since growing cells in -HIS/-URA/-LYS/-LEU conditions compared to -HIS/-URA did not affect the relative difference in cell size (Figure 1C and 1D). When neither of these two selective media options could be used, due to the strains having different markers incorporated, the experiment was conducted with YPAD. The media change from selective media to YPAD increases the cell volume compared to the strains diluted in the same overnight media (Figure 1C). The change in nutrient availability of the media influences the cell size. For higher reproducibility, no media change was conducted.

Three incubation times, 4 hours, 6 hours, and 8 hours were tested to determine their effects on cell size (Figure 1C). The incubation time had a minor effect on the cell size, which is likely caused by the proliferation speed of the individual cells as well as the starting number of cells. To keep the incubation time as short as possible but still providing the cells with enough time to proliferate, a 5-hour incubation time was chosen.

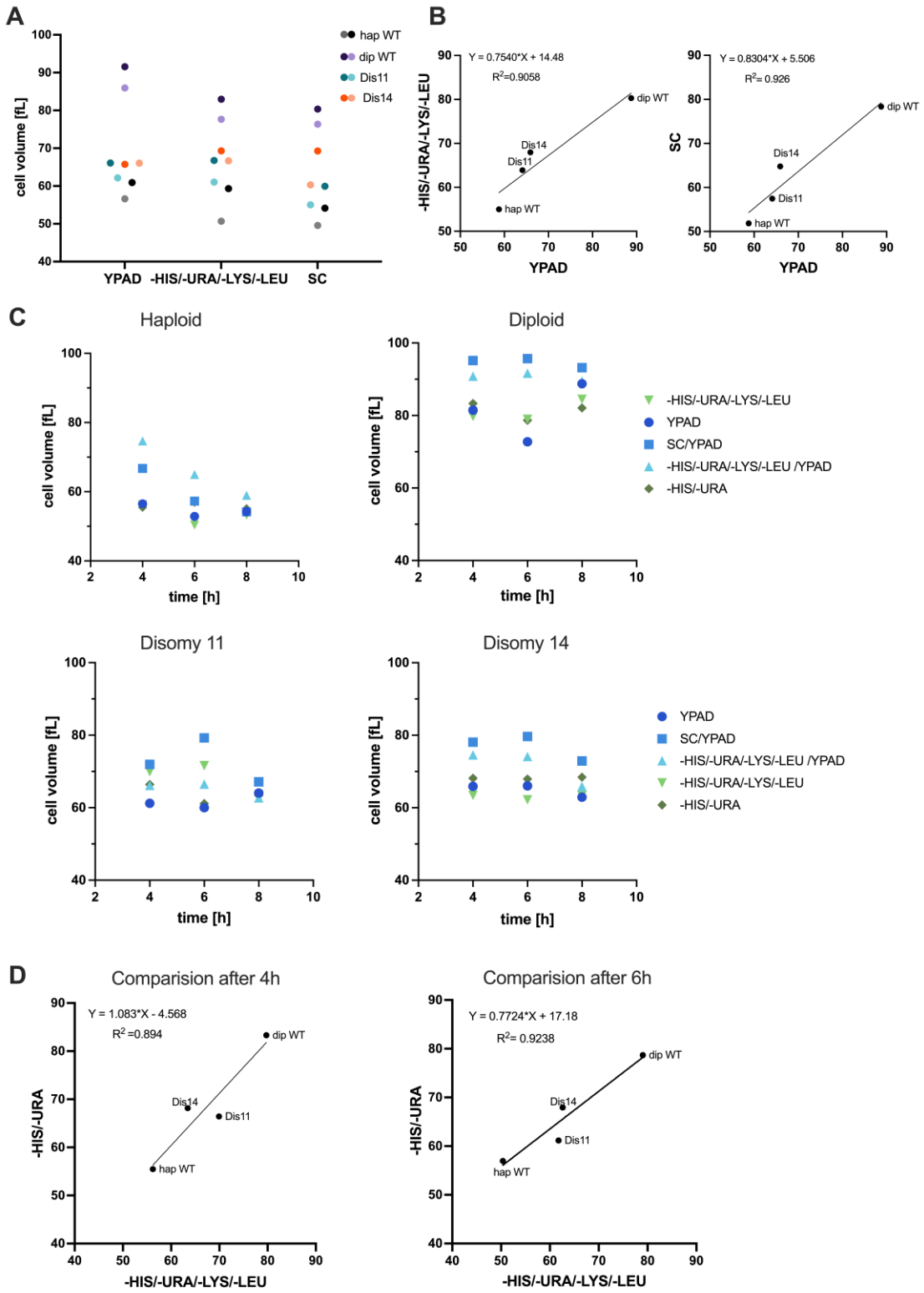

Figure 1: Cell size is influenced by the media and incubation times. Hap WT…CCY5419, dip WT…CCY3837, disomy 11…CCY5848, disomy 14…CCY5848 **A**: The graph depicts the cell size (fL) of the four strains grown in three different types of media, YPAD, SC, and -HIS/-URA/-LYS/-LEU. Each strain is colored differently to distinguish between the experiment repetitions; the lighter colors were measured in one set, and the darker colors belong to the second data set. **B**: Comparisons between cell size of strains in different growth media (SC or -HIS/-URA/-LYS7-LEU to YPAD). The cell size differences in different media conditions were compared with a linear regression model. n =2 **C**: Cell size measurements of all four strains incubated for three different time points in various media.

D: Comparison of cell sizes of the strains measured after 4 and 6 hours between the -HIS/-URA and -HIS/-URA/-LYS/-LEU media with a linear regression model. n=1

3.2. Restored auxotrophic markers influence cell size

Previously, lab members induced aneuploidy by replacing the centromere with an artificial centromere containing a galactose-inducible promoter (Anders et al., 2009) and reincorporating specific auxotrophic markers. After induction, the markers were used to select for strains that had become aneuploid. In the single disomic strains, histidine and uracil, lysine and leucine, or all four markers were reincorporated into the genome to select for aneuploidy. The double disomic strains were engineered to contain all four markers. Preliminary cell size measurements of haploids and diploids containing various auxotrophic combinations showed cell size variability. Therefore, speculation that the reinstalled auxotrophic markers influence cell size due to incorrect reintegration or mutations in the sequences arose. The successful restoration of the auxotrophic markers into the yeast genome was confirmed. Further, to determine if there is an influence on cell size, haploid and diploid strains were engineered containing various auxotrophic marker combinations, and their size was determined.

3.2.1. Incorporation of markers into the chromosome

The most obvious cell size difference was observed between the haploid strains auxotrophic for histidine and uracil (CCY3863) and the strain auxotrophic for lysine and leucine (CCY3862). A size difference was also observed for the haploid strain where all auxotrophic markers had been restored (CCY5419), which was engineered by using the same PCR products as for the other two strains. Therefore, I analyzed the strains CCY3862 and CCY3863 to determine whether the restored markers have been incorporated into the chromosome. This was achieved by amplifying the gene fragment using primers located outside of the integration site or on the original plasmid backbone. Through gel electrophoresis, these fragments were visualized and subsequently sent for sequencing for further confirmation. All markers were successfully integrated into the genome without any mutations except for uracil. The strain CCY3862 uracil gene was confirmed to be encoded on a centromeric plasmid by growing on FOA plates (Figure 2A). Stains containing incorporated uracil markers are unable to grow on FOA plates, such as the diploid control strain. This result led to the engineering of haploid and diploid strains where the URA gene has been

incorporated into the genome (Figure 2B). However, the promoter region, which is usually used as a homology region, was fully deleted in S288c strains. Therefore, fragments from the strains CCY433 and CCY801, which each had a different URA3 mutation, ura3-52 mutation and ura3-1, were amplified. I further engineered haploid and diploid strains containing uracil and the other three auxotrophic marker combinations to obtain a variety of controls for future experiments.

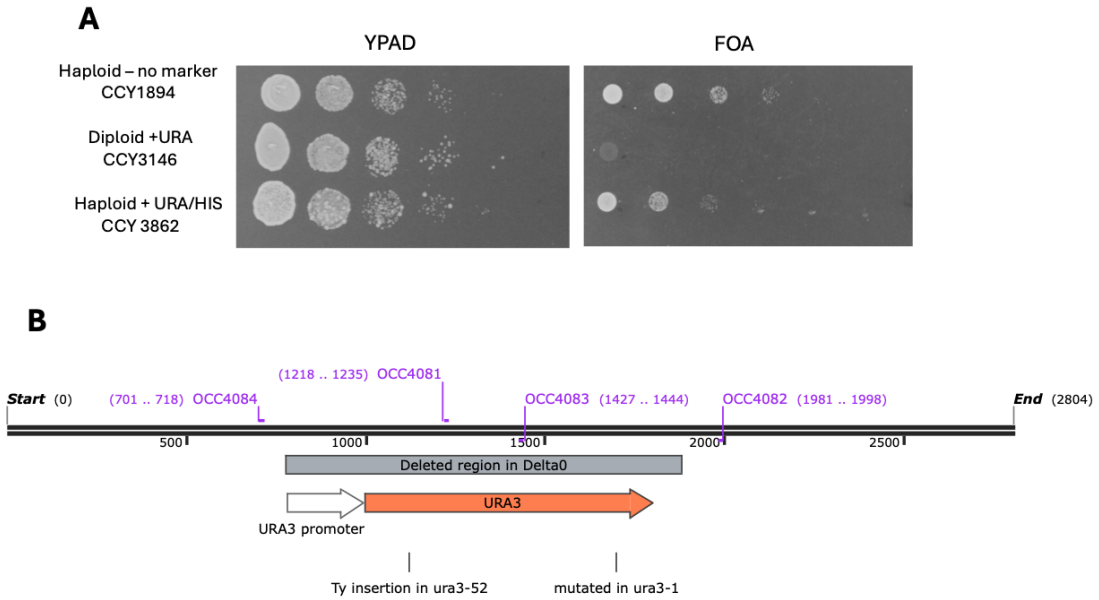

Figure 2: URA3 marker has not integrated into the chromosome; instead, it is encoded on a plasmid. **A**: Images of a haploid without markers, a diploid containing an incorporated URA gene, and the haploid strain with both URA and HIS markers grown on YPAD and FOA plates. **B**: SnapGene map of the URA3 gene (orange). The S288C strains URA3 gene and its promoter region have been fully deleted, highlighted in gray. Mutation sites of yeast transposon (Ty) insertion in ura3-52 and ura3-1 are indicated. The primers are highlighted in purple.

3.2.2. Uracil encoded on a plasmid affects cell size.

By measuring the cell size of all haploid and diploid strains containing various reincorporated auxotrophic marker combinations via CASY, their influence on cell size was determined (Figure 3). Further, a statistical analysis, One-way ANOVA, was performed.

Uracil encoded on a plasmid in the haploid strains increases the size of the cell (Figure 3A). A significant difference was statistically determined between the HIS/LYS/LEU/URA (plasmid) and HIS/LYS/LEU/URA strain (P=0.0370). The strain containing the marker combination HIS/URA (plasmid) has a larger cell size than the HIS/URA strain. However, the statistical analysis did not show a significant difference

between these two data sets (P = 0.9623). Nevertheless, the increase in cell size is likely due to the URA gene encoded on a plasmid. Outliers in the LYS, LEU, and URA strains were seen. The outlier for the URA strain is smaller in size, likely due to contamination. The outliers for the LYS and LEU strains do not exceed 70 fL, and the other measurements fall within the range of the haploid strain without any markers. This makes the likelihood that these cells are diploid very low. Since it was also one out of three replicates, it is more likely that it was an outlier than a problem with the strain itself. However, the cells might have formed clumps due to an error during sample preparation, resulting in the formation of aggregates that shifted the Gaussian curve peak to a larger cell volume.

Uracil encoded on a plasmid did not cause the diploid strains to have a significant size increase (Figure 3B). It seems that the diploid cell can compensate for the plasmid's affect, due to the chromosome copy numbers. The diploid LYS/LEU strain auxotrophic for histidine and uracil does not reach a similar cell size compared to the other diploid strains. There could be two explanations. First, the auxotrophic marker combinations LYS/LEU cause diploid strains to be smaller. Second, there is a problem with the strain itself. However, the haploid single markers LYS and LEU were obtained from the diploid LYS/LEU strain, and both haploid marker strains did not show a significant difference from the other haploids, except for the two outliers. However, before this strain can be used as a control, the cell size decrease has to be investigated.

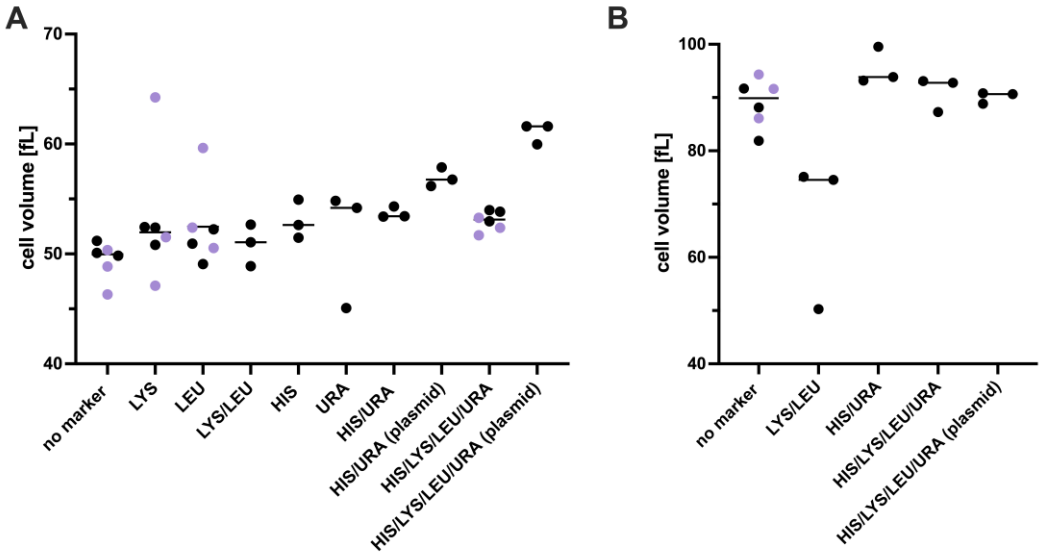

Figure 3: Haploid strains have a larger cell volume (fL) when uracil is located on a plasmid. For direct comparison of all strains, all have been cultivated in YPAD media. For each strain, three biological replicates were measured, and the median was calculated (shown as a black line). **A**: Cell size measurement of haploid strains with various

auxotrophic markers via CASY analysis. The marker combinations listed have been incorporated into the strain. The colors, black and purple, indicate that two different strains with the same marker combinations were measured. The comparison through a One-Way ANOVA analysis of HIS/URA/LYS/LEU and HIS /LYS/LEU/URA(plasmid) strains resulted in a significant difference of P= 0.0370. No-marker … CCY1894 (black) and CCY1895 (purple); LYS… CCY7476 (black) and CCY7477 (purple); LEU… CCY7478 (black) and CCY7479 (purple); LYS/LEU… CCY3863 (black); HIS … CCY7312 (black); URA… CCY7373 (black); HIS/URA… CCY7372 (black); HIS/URA (plasmid)… CCY3862 (black); HIS//LYS/LEU/URA … CCY7475 (black) and CCY7492 (purple); HIS//LYS/LEU/URA (plasmid)… CCY5419 (black) **B**: The cell size of diploid strains with various auxotrophic marker combinations was determined via CASY. The marker combinations listed have been incorporated into the strain. The colors, black and purple, indicate that two different strains with the same marker combinations were measured. No-marker … CCY1914 (black) and CCY803 (purple); LYS/LEU… CCY7435 (black); HIS/URA(plasmid)… CCY7433 (black); HIS//LYS/LEU/URA … CCY7434 (black); HIS//LYS/LEU/URA (plasmid)… CCY3837 (black)

3.3. Chromosome-specific effects are the main driver of cell size phenotypes in single disomic strains.

The previous lab member, Nina Stanišić (2023), measured the cell size of disomic and double disomic strains, where a weak correlation between the ORFs on aneuploid chromosomes and their cell size was discovered ($R^2 = 0.19$). It was concluded that the cell size phenotypes of aneuploid cells are chromosome-specific. Recently, the Aneuploid Chromosome Dissection Collection was established by Clara Hackethal, Manuela Sophie Koller, Rodina Genidy, Rustam Tuktarov, and Lisa Pulferer. This collection includes full and partial arm deletions of 14 out of 16 chromosomes, which are auxotrophic for lysine and leucine. To confirm the similarity of the single disomy collection and the ACDC collection, I measured the cell size of the ACDC parent strains used to engineer the full and partial chromosome arm deletions (Figure 4A). I observed a weak correlation ($R^2 = 0.12$) between the cell size and the number of ORFs on the aneuploid chromosome of the ACDC strains (Figure 4A). To compare the two collections, the average cell sizes were plotted against each other, and the linear regression fit was performed. The statistical test showed a high correlation between these two data sets ($R^2 = 0.8734$) (Figure 4B). The differences observed can be attributed to the different growth media used. The single disomy collection was incubated overnight in selective media, and then a media change to YPAD was performed, which has been shown to influence cell size. Nevertheless, this data indicates that insights gained from one collection can be applied to the other dataset. Additionally, the ploidy of the ACDC disomic strains was confirmed by FACS (Supplementary Figure S3).

I tested whether cell size phenotypes are dependent on the relative change in copy numbers of a chromosome. Therefore, the cell size of trisomic (2N+1) and tetrasomic (2N+2) strains aneuploid for chromosomes 1 and 12 was determined (Figure 4B and C). The disomic strain of chromosome 1 (1N+1) has the smallest cell size phenotype of the disomic strains tested (Figure 4A and 4C). The CLN3 gene, which is encoded on the chromosome, is involved in checkpoint regulations of G1 to S phase and has been shown to influence the cell volume (Thorburn et al., 2013; Facchetti et al., 2017). Overexpressing chromosome 1 one-fold (1N+1) is smaller than the haploid wildtype. The trisomic strain (2N+1), where chromosome 1 is overexpressed 0.5-fold, is slightly smaller than the diploid control (2N). The tetrasomic strain (2N+2) is slightly larger than the diploid. The control strains, where CLN3 was heterozygously deleted in a disomy 1 strain (1N+1 +/-CLN3), lead to an increase in cell size compared to the disomic strain. Similarly, the heterozygous deletion of CLN3 in a diploid (2N +/-CLN3) also increases cell size compared to the diploid control. The availability of only one clone for certain strains represents a minor limitation, which should be considered when interpreting the data. These results show that CLN3 is the main driver of the disomy 1 cell size phenotype.

The strongest cell size phenotype we observed in a haploid background was the increase in cell size of disomy 12 (Figure 4A and 4C). The single disomic strain of chromosome 12 (1N+1) cell volume is similar to the diploid wild type (2N). The cell size increase from a disomic strain to a trisomic strain (2N+1) is not as pronounced as cell size increase of the tetrasomic strain (2N+2), which contains two extra copies of chromosome 12. The tetrasomic strains cell volume increases to the size of the tetraploid (4N) strains. It can be concluded that the cell size scales with the number of copies of chromosome 12.

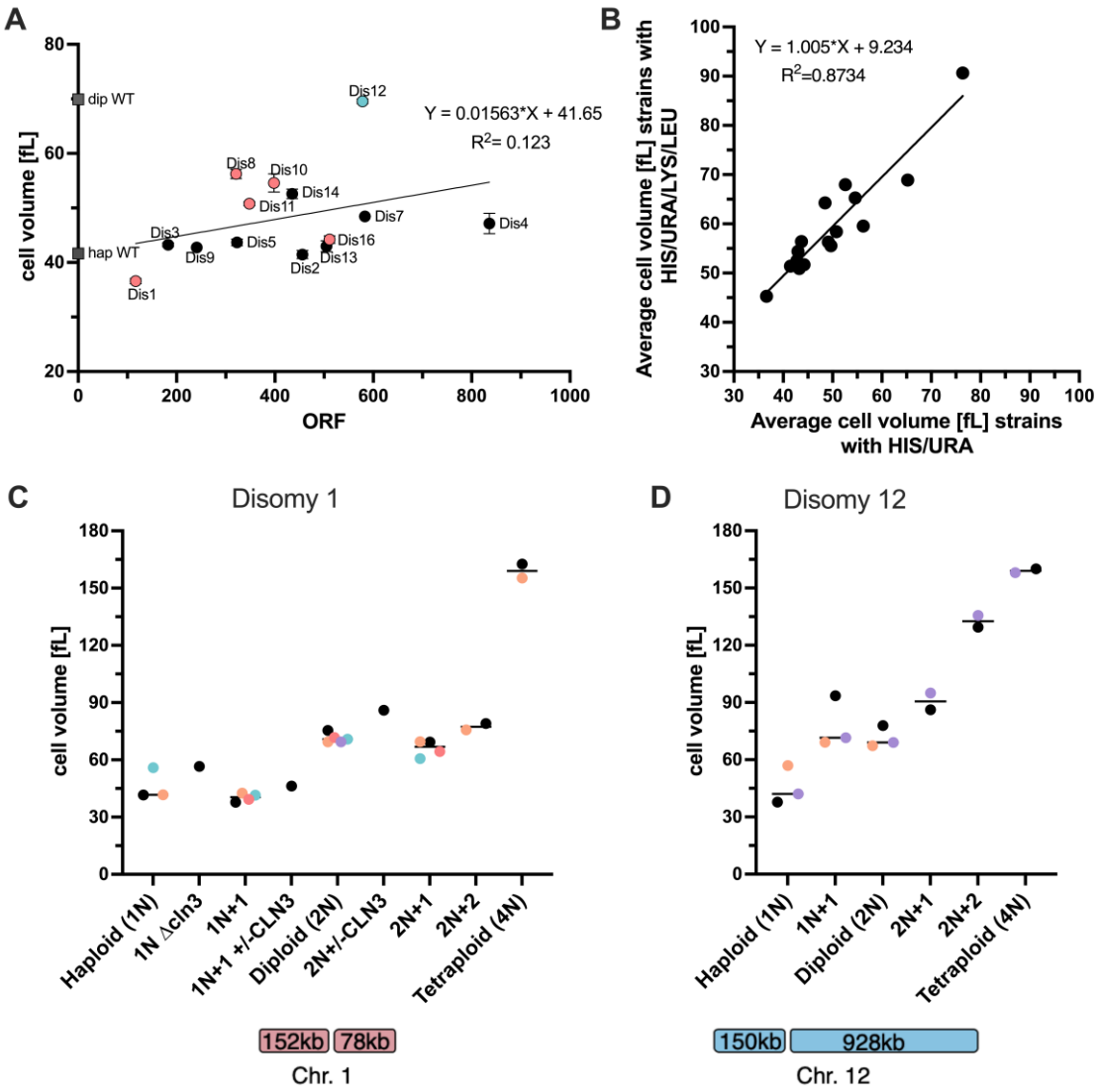

Figure 4: Cell sizes phenotypes dependency on copy number changes of chromosomes. **A**: Weak correlation between the ORF of disomic strains and cell volume. Disomic strains highlighted in pink are disomic strains with a cell size phenotype, or when combined with another chromosome, result in a cell size phenotype (see Figure 10A). Blue emphasizes the largest disomic cell size phenotype, Disomy 12. The strains were grown in -HIS/-URA media without a media change. Disomy 1…CCY6157; Disomy 2…CCY1956; Disomy 3…CCY1959; Disomy 4… CCY6144; Disomy 5…CCY6178; Disomy 7…CCY6312 ; Disomy 8…CCY1909; Disomy 9… CCY6530; Disomy 10…CCY1927; Disomy 11…CCY6223; Disomy 12… CCY6103; Disomy 13…CCY6317; Disomy 14…CCY6180; Disomy 16…CCY6160; Haploid…CCY7372; Diploid…CCY7433 **B**: High correlation between the average cell volume of the single disomy collection (previous data from Nina Stanišić (2023)) and the ACDC collection. The single disomy collection was grown overnight in -HIS/-URA/-LYS/-LEU media and diluted in YPAD. The ACDC strains were grown overnight and diluted in -HIS/-URA media. **C**: Plotted cell size data of various chromosome 1 ploidy levels and strains having CLN3 full or heterozygous deletion. No triplicates were measured. Strains were grown in YPAD and -HIS/-URA/-LYS/-LEU, depending on the auxotrophic markers of the strains, overnight and diluted in YPAD. Each color corresponds to a different strain with the same ploidy. Haploid (1N)… CCY1894 (black), CCY1895 (orange), and CCY5419 (blue); 1N ΔCLN3… CCY5564 (black); 1N+1 … CCY2188 (black), CCY5851 (orange), CCY6156 (blue), and CCY6157 (red); 1N+1 +/-CLN3…CCY5565(black); Diploid (2N)…CCY803 (black), CCY1914 (orange), CCY3837 (blue), CCY6236 (red) and CCY6237 (purple); 2N+/-CLN3…CCY5563(black); 2N+1…CCY6230 (black), CCY6231 (orange), CCY6234 (blue), and CCY6235 (red); 2N+2…CCY6232 (black) and

CCY6233 (orange); Tetraploid (4N)… CCY6265 (black) and CCY6269 (orange) **D**: Various ploidy levels of chromosomes 12 and their cell size. Only a single measurement per strain was done. Each strain has a different color. Strains were grown in YPAD and -HIS/-URA/-LYS/-LEU, depending on the auxotrophic markers of the strains. Haploid (1N)…CCY1894 (black), CCY1895 (purple), and CCY5419 (orange); 1N+1 …CCY5845 (black), CCY6102 (purple) and CCY6103 (orange); Diploid (2N)…CCY803 (black) CCY1914 (purple) and CCY3837 (orange); 2N+1…CCY6104 (black) and CCY6106 (purple); 2N+2…CCY6105 (black) and CCY6135 (purple); Tetraploid (4N)…CCY6265 (black) and CCY6269 (purple)

Cell size phenotypes are chromosome-specific, indicating that specific genes drive cell size. Therefore, various pathways can be responsible for each cell size phenotype. Various chromosomes result in larger or smaller cell size phenotypes. In this study, I mainly focused on larger phenotypes, due to the cell volume changes being larger. The chromosomal regions involved need to be narrowed down to identify the driver genes of the cell size phenotypes. The ACDC collections disomic strains with full chromosome arm deletions were engineered through homologous recombination (Figure 5A) (Linder et al., 2017). A significant change in the measured cell size is expected if the responsible chromosome arm is deleted. If both arms are involved, a decrease in cell size will be observed for each arm deletion strain, however, this change will not be as pronounced.

I tested the disomic strains for chromosomes 8, 10, 11, and 16 to narrow down the chromosome arm involved in cell size regulation (Figure 5B-5E). Disomy 8, 10 and 11 have a larger cell size phenotype, while Disomy 16 has no cell size phenotype (Figure 4A). Both chromosome arm deletion strains of Disomy 8 decrease in cell size. However, their measured value was similar, indicating genes driving cell size are located on both arms (Figure 5B). Disomy 10, although previously identified as a disomic strain having a cell size phenotype, did not have a significant size change compared to the haploid wildtype (Figure 5C). Genes encoded on disomy 11 left chromosome arm contribute to the cell size phenotype (Figure 5D). Disomy 16, no significant cell size change was observed (Figure 5E). Overall, these findings successfully identified chromosome arms involved in the cell size phenotype, especially for chromosomes 8 and 11, which can provide valuable directions for future approaches.

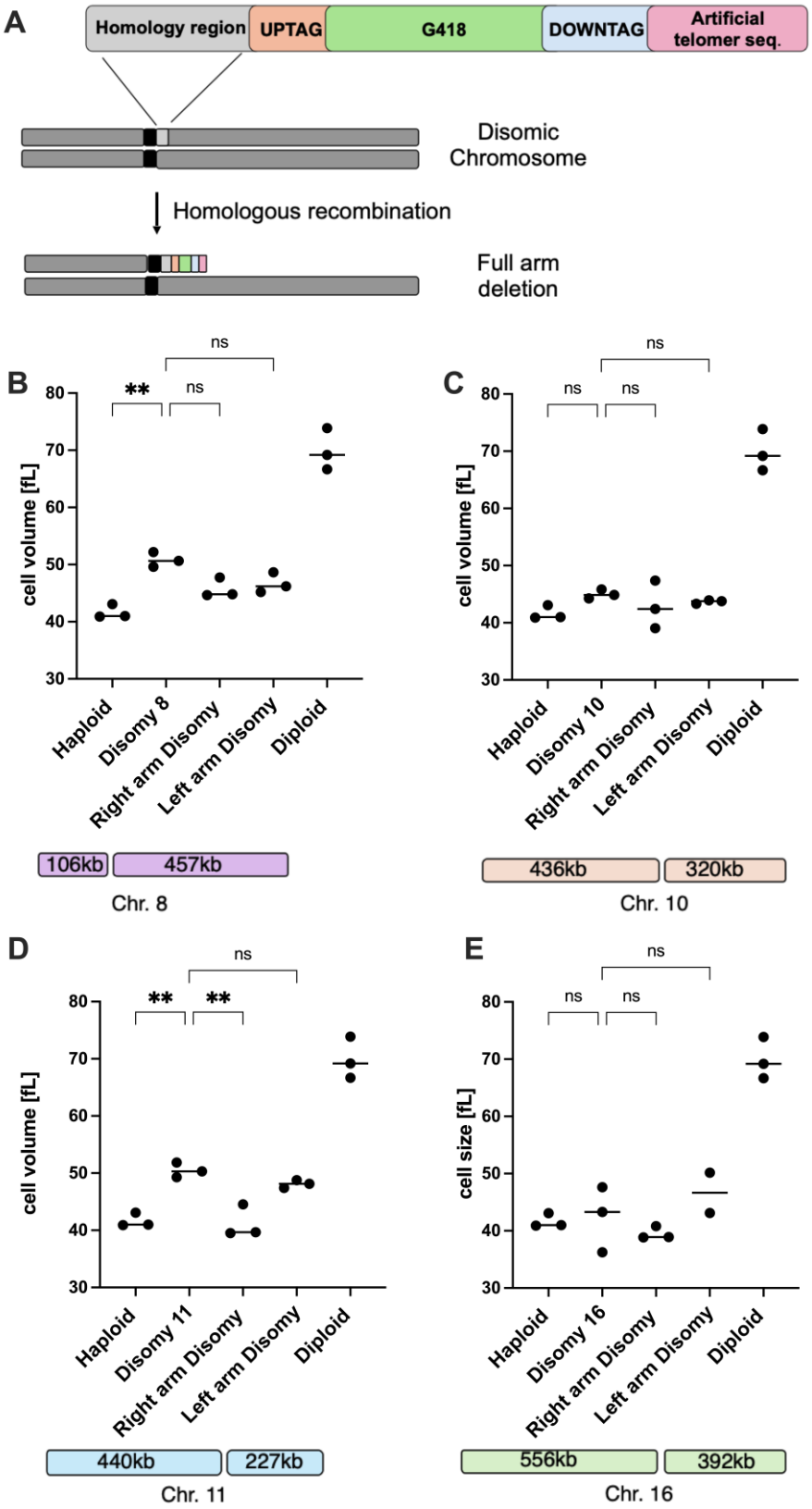

Figure 5: Full chromosome arm deletions of four disomic strains. **A:** Schematic of the method for performing a full chromosome arm deletion by homologous recombination (Linder et al., 2017; Ho et al., 2009). The fragment that was exchanged has a 500bp homology region (gray) connected to an UPTAG (orange), resistance marker (green), DOWNTAG (blue), and an artificial telomere sequence. **B-E:** Cell size measurement of Disomy 8, 10, 11, 16, and their full chromosome arm deletions. Measurements were performed in triplicate. Haploid and Diploid were control strains. All strains were cultivated in -HIS/-URA media. **B**: P value of Disomy 8 compared to the haploid is 0.0026.

No significant differences were found between the full arm deletions and the parent strains. haploid …CCY7372; diploid…CCY7433; Disomy8…CCY1909; Right arm Disomy 8…CCY7194; Left arm Disomy 8…CCY7196 **C**: No significant cell size differences have been determined between the haploid and Disomy 10. The full arm deletions do not show a large change in the cell size. Haploid …CCY7372; Diploid…CCY7433; Disomy 10…CCY1927; Right arm Disomy 10…CCY7304; Left arm Disomy 10…CCY7306 **D**: Disomy 11 is significantly larger than the haploid (P = 0.0049). By deleting the left arm (right arm Disomy), a decrease in the disomic strain can be seen (P = 0.0352). Haploid … CCY7372 ; Diploid…CCY7433; Disomy 11…CCY6223; Right arm Disomy 11…CCY7079; Left arm Disomy 11…CCY7080 **E**: Disomy 16 does not have a cell size phenotype. There is a minor cell size change when deleting the left chromosome. However, the statistical analysis shows no significant change. Haploid …CCY7372; Diploid…CCY7433; Disomy 16…CCY6160; Right arm Disomy 16…CCY7077; Left arm Disomy 16…CCY7147

3.4. Multiple regions on disomy 12 are responsible for the cell size phenotype.

Chromosome 12 is one of the largest yeast chromosomes. The entire ribosomal DNA (rDNA) is located on the right chromosome arm of chromosome 12. Previously, Nina Stanišić (2023) and Nikola Yordanov (2024) have tried to determine if rDNA is the main contributor to the increase in cell size by determining the rDNA copy numbers of the disomy 12 strains. The obtained results did show a possible involvement of the rDNA. However, it is unclear if the rDNA region is the only driver of the disomy 12 cell size phenotype.

3.4.1. Reproducibility of the disomy 12 measurements

Due to the dynamic process of the cells forming rDNA circles, there was a concern that the cell size measurements could lack reproducibility. To address this, the cell size of a single colony was tracked for three days using the experimental setup depicted in Figure 6A. I observed a high variability in cell size between the biological replicates of disomy 12, but not for the wildtypes and the single disomy of chromosome 4, across the entire experiment (Figure 6B and 6C). By tracking the cell size of single colonies over three days, we can show that the cell size of disomy 12 single colonies does not stay constant. The average variation of each cell size per day was taken, resulting in an overall cell size variation range of 7.31fL per day. For future measurements, three biological replicates were taken when determining cell size. The reason for the large variability is unclear. A potential explanation could be an increase in extrachromosomal rDNA circles in the disomy 12 strains. However, this has to be confirmed in future experiments.

Next, I conducted a FACS experiment to determine if a shift in the peaks for single colony cells of different cell sizes would show a variation in the amount of DNA (Figure 6D). The difference between single colonies could provide information regarding the rDNA contents of the cells. However, no obvious variation was detected. Different from the euploid strain, the disomy of chromosome 12 had a double peak in the G1 and G2 phase, independent of the growing FACS cultures from single colonies. This could indicate that a problem during the sample preparation may have occurred. However, neither of the controls, except for the single disomy 12, shows any double peaks, indicating that there was no problem during the sample preparation. Another reason for the double peaks could be related to overexpressed rDNA and the formation of rDNA circles. However, this data does not provide sufficient evidence to confirm this statement.

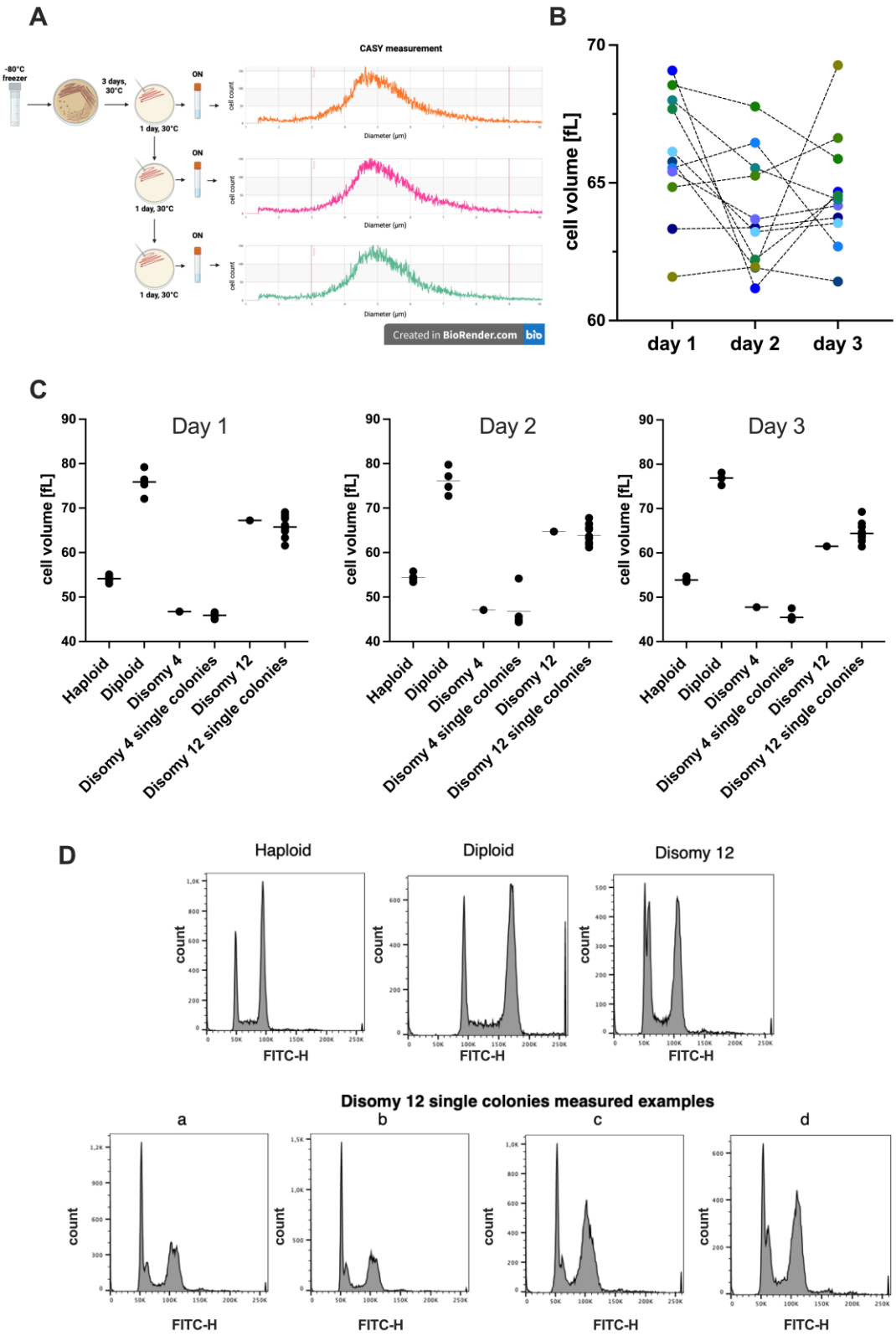

Figure 6: Disomy 12 single colony experiment. **A**: Experimental setup for analyzing single colonies of disomy 12. Designed in BioRender (https://BioRender.com). **B**: Disomy 12 single colony cell size measurements over the three days. High day-to-day variability. **C**: Three-day cell size measurement of single colonies. As controls, haploid, diploid, and disomy 4 were used. Grown in -HIS/-URA selective media. Haploid …CCY3682; Diploid …CCY3837 disomy 4… CCY6144 disomy 12… CCY6103 **D**: FACS measurements of four of the disomy 12 single colonies. Controls used were haploid, diploid, and disomy 12. a,b,c,d…examples of disomy 12 single colonies

3.4.2. Engineering disomy 12 full and sequential partial chromosome arm deletion strains

It remains unclear if the rDNA is a driver of the chromosome 12 cell size phenotype. To test which arm of chromosome 12 contributes to the large cell phenotype, both chromosome arms were deleted in the disomic strains (Figure 4A). To identify the multiple chromosomal regions contributing to cell size, we engineered sequential partial chromosome arm deletions of disomy 12 (Figure 7A, 8A and 8B). Full and partial chromosome arm deletions were confirmed by qPCR (Figure 7B). The CT-values are normalized to the haploid and the unmodified chromosome arm, resulting in a fold change value of 1 (black bar). A 0.5-fold decrease was expected when the deleted chromosome arm (orange bar). When achieving a value of around 0.5-fold, the partial arm deletion was deemed successful. If the transformation has failed, the chromosome fold change would be 1, indicating two copies remain.

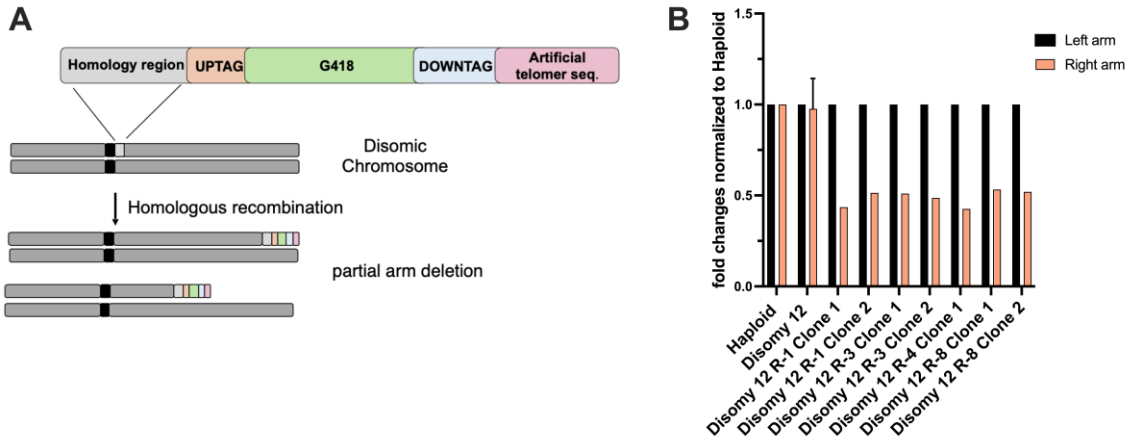

Figure 7: Engineering partial arm deletions. **A**: Method to obtain partial arm deletions (Linder et al., 2017; Ho et al., 2009). The fragment which will be exchanged has a 500bp homology region (gray) connected to a UPTAG (orange), resistance marker (green), DOWNTAG (blue), and an artificial telomere sequence. **B**: qPCR results of partial arm deletions for the cut sites 1, 3, 4 and 8. The fold changes of the chromosomal copy number are obtained when normalized to the haploid. The black bar represents the unmodified chromosome arm, which is present as 2 copies in the aneuploid strains and one copy in the haploid. The orange bar represents the measured fold change of the modified chromosome arm, in this case the right arm. The expected decrease in fold change lies at 0.5, indicating only one copy of this arm remained in the strain. Haploid…CCY7372; Disomy 12…CCY6103; Disomy 12R-1…CCY7436 (clone 1) and CCY7437 (clone 2); Disomy 12R-3…CCY7438 (clone 1) and CCY7439 (clone 2); Disomy 12R-4…CCY7440 (clone 1); Disomy 12R-8…CCY7441 (clone 1) and CCY7442 (clone 2)

3.4.3. The right chromosome arm encodes the main regulators of disomy 12 cell size phenotype.

The cell volume of the engineered full and partial arm deletions of disomy 12 were measured to narrow down the regions contributing to the cell size phenotype (Figure 8).

By comparison between the full left and right chromosome arm deletions, I was able to determine the arm responsible for disomy 12 cell size phenotype. The left chromosome arm cell size change is mild compared to the deletion of the full right arm, which fully abolishes the phenotype (Figure 8C and 8D). The mild decrease in size of disomy 12 with a left arm deletion can be mapped between the cut sites, Disomy 12-1 and the full arm deletion (Figure 8C). I identified four chromosome regions that were associated with decreased cell size on the right chromosome (Figure 8D). This suggests that in the deleted region of 147kb to 224kb, 224kb to 383 kb, 584kb to 731kb, and 731kb to 812 kb, genes are located that influence cell size regulation. The sequential deletions show that the rDNA locus has a strong effect on cell size but is not the only cause for the larger cell size phenotype. A list of candidate genes was compiled, cross-referencing the previously annotated genes known to influence cell size from the *Saccharomyces* Genome Database (SGD) with the narrowed-down regions (Figure S3 and Table S2). The majority of the proteins encoded in these regions are part of pathways involved in the cell cycle, cell wall synthesis and maintenance, and transporters.

Since rDNA copy numbers are highly variable, the rDNA genes, 5S, 18S, and 35S 3'end, were amplified via qPCR to determine variations in the number of rDNA repeats in the left and right full and partial arm deletion strains (Figure 8E and 8G, Figure 8F and 8H). Copy numbers of rDNA were compared because regulatory elements of the rDNA locus are located in different regions across the chromosome. Due to the majority of rDNA repeats being located on the right chromosome arm, it was predicted that the sequential chromosome arm deletion, deleting the rDNA region, would result in a decrease in rDNA levels. For the left arm, a stable level of rDNA was expected. Nevertheless, the sequential chromosome arm deletion strain Disomy 12L-1 showed a decreased fold change of rDNA for all three genes (Figure 8E). After deleting the main rDNA region on the right chromosome arm, a reduction of the rDNA repeats was

measured (Figure 8F). However, the partial arm deletions up to 224kb (Disomy 12R-3) show a decrease in rDNA fold changes. At the cut site Disomy 12R-4 (297kb), the rDNA fold changes increased more than the single disomy control. The relative rDNA copy numbers indicate how many more copies of the rDNA genes are present compared to the ACT1 gene, which is located on chromosome 6 (Figure 8G and 8H). The relative copy numbers of the haploid are in an expected range of 100-200 copies (rev. in Nelson et al., 2019). It can be expected that the total rDNA copy numbers for a diploid are double the number of the haploid. In this case, the relative copy numbers are plotted, making the values of the diploid similar to those of a haploid, since the ACT1 gene is used as a reference and set to a value of 1. To obtain the diploids total copy number, the value has to be multiplied by a factor of two due to the two copies of ACT1. Nevertheless, the values for the euploids are reasonable. The single disomy 12 strain rDNA copy number values should be double the amount of the haploid due to the extra chromosomal copy. However, this is not the case. No major copy number changes are expected for the left and right partial arm deletions except when removing the main rDNA region, which is located between the right arm cut sites 584kb-731kb. Additionally, decreases in rDNA copy numbers for various cut sites located on both chromosome arms can be seen. However, after deleting the rDNA region, a steep decline in the copy numbers of each gene can be observed. This data suggests that the amount of rDNA copy numbers is affected by multiple regions. It is possible that the variability of the data could be due to the formation of rDNA circles. However, this can not be confirmed by this data, and further methods are required for confirmation.

Overall, these results concluded that the rDNA region on the right arm has been successfully deleted for the sequential partial arm deletion cuts Disomy 12R-10, Disomy 12R-11, Disomy 12R-12 and Disomy 12R-F.

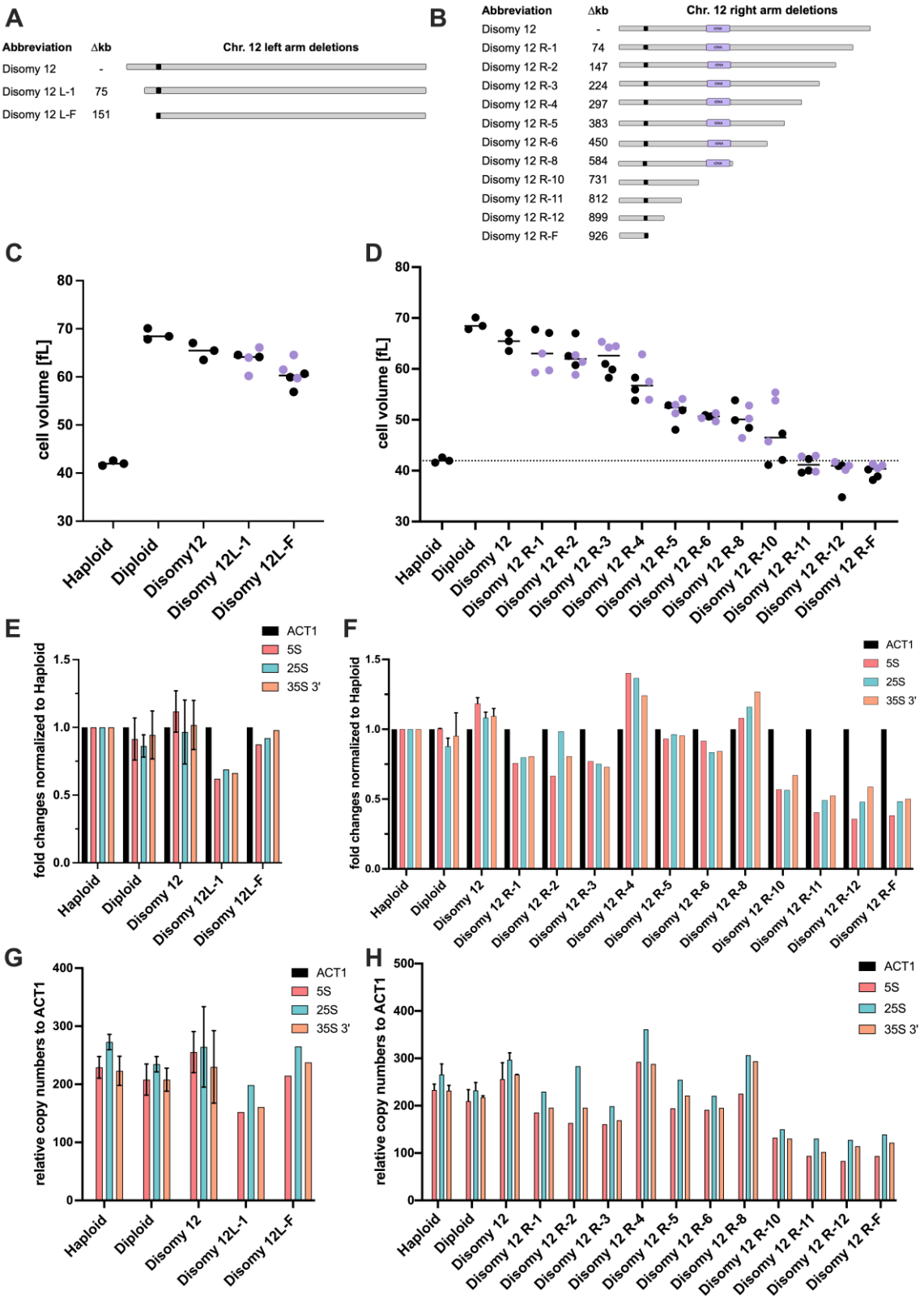

Figure 8*:* The major genes, which drive the cell size phenotype of disomy 12, are located on the right chromosome arm. **A**: Schematic overview of the cut sizes, the kilobases that have been deleted, and abbreviations of the left chromosome arm. **B**: Schematic overview of the cut sizes, the kilobases that have been deleted, and abbreviations of the right chromosome arm. The rDNA region is highlighted in purple. Additionally, regions have been enhanced that could play a role in the cell size phenotype. **C**: Cell size measurement with CASY. Each strain was measured in triplicate. The cells were cultivated in -HIS/-URA media. Haploid …CCY7372; Diploid …CCY7433; Disomy 12

…CCY6103; Disomy 12L-1 … CCY7320 (black)and CCY7321 (purple); Disomy 12L-F… CCY7202 (black) and CCY7203 (purple) **D**: The cell size of each partial arm deletion was determined with CASY. The measurement was performed in triplicate, and clones of strains with the same genotype can be differentiated through the black and purple colors. Haploid … CCY7372; Diploid …CCY7433 ; Disomy 12 …CCY6103; Disomy 12R-1 …CCY7436 (black) and CCY7437 (purple); Disomy 12R-2 …CCY7534 (black) and CCY7535 (purple); Disomy 12R-3 …CCY7438 (black) and CCY7439 (purple); Disomy 12R-4 …CCY7440 (black) and CCY7472 (purple); Disomy 12R-5 …CCY7536 (black) and CCY7537 (purple); Disomy 12R-6 … CCY7532 (black) and CCY7533 (purple); Disomy 12R-8 …CCY7441 (black) and CCY7442 (purple); Disomy 12R-10 …CCY7443 (black) and CCY7473 (purple); Disomy 12R-11 …CCY7444 (black) and CCY7445 (purple); Disomy 12R-12 …CCY7446 (black) and CCY7474 (purple); Disomy 12R-F…CCY7204 (black) and CCY7205 (purple) **E**: Left chromosome arm rDNA fold change normalized to the haploid WT from qPCR data of the left chromosome arm deletion strains. rDNA expression level changes were analyzed by amplifying three rDNA genes, 5S (pink), 18S (blue), and 35S 3'(orange). The values have been additionally normalized to the ACT1 gene. **F**: The fold changes of rDNA (5s (pink), 18s (blue), and 35s 3'(orange)) were determined via qPCR for the right chromosome arm. The values were normalized to the haploid WT and the ACT1 gene. **G-H**: The relative copy numbers of the three rDNA genes, 5s (pink), 18s (blue), and 35s 3'(orange), normalized to ACT1 (black gene) and the haploid. **G**: The relative rDNA copy numbers for each left partial chromosome arm deletion. **H**: Relative rDNA copy numbers for the right partial chromosome arm deletion.

3.5. Cell size phenotypes are the results of synergistic effects in double disomic strains.

Aneuploidy is not limited to the gain or loss of one chromosome. Different chromosome combinations can result in more pronounced cell size phenotypes due to the occurrence of synergistic effects between the overexpressed chromosomes. Therefore, I studied the synergistic effects of various chromosomal combinations has on cell size with the double disomy collection, specifically investigating the chromosomal combination 11 and 16.

3.5.1. The double disomy strain, 11x16, exhibiting the largest cell size phenotype has undergone diploidization.

The largest double disomic cell size phenotype resulted from the chromosomal combination of 11 and 16 (Figure 10A). To determine which overexpressed genes, cause this increase in cell size, the idea was to engineer full and partial arm deletions for the 11x16 strain. However, for easier genetic manipulation, the disomic strains for chromosomes 11 and 16 were mated to confirm the phenotypes replication (Figure 10B). The 0.5-fold overexpression of the two chromosomes in the double trisomy strain is not sufficient to reproduce the double disomic strain’s significant cell size increase. Hence, I engineered full arm deletion with the original double disomic strain. However,

the qPCR results performed to confirm the deletion of the chromosome arm never showed the expected fold change for the chromosome (Figure 10C). Repeatedly obtaining a fold change of 1.5 for chromosomes 11 or 16, where a fold change of 2 was expected due to the two chromosome copies, led to the conclusion that the strains may have mutated during the transformation process or during the freezing and thawing procedure. For that reason, FACS was performed to determine the amount of DNA in the strains, since a shift in FACS profiles can be seen for haploid and diploids (Figure 10D). The results confirmed that all six double disomic strains of chromosomes 16 and 11 have independently undergone diploidization.

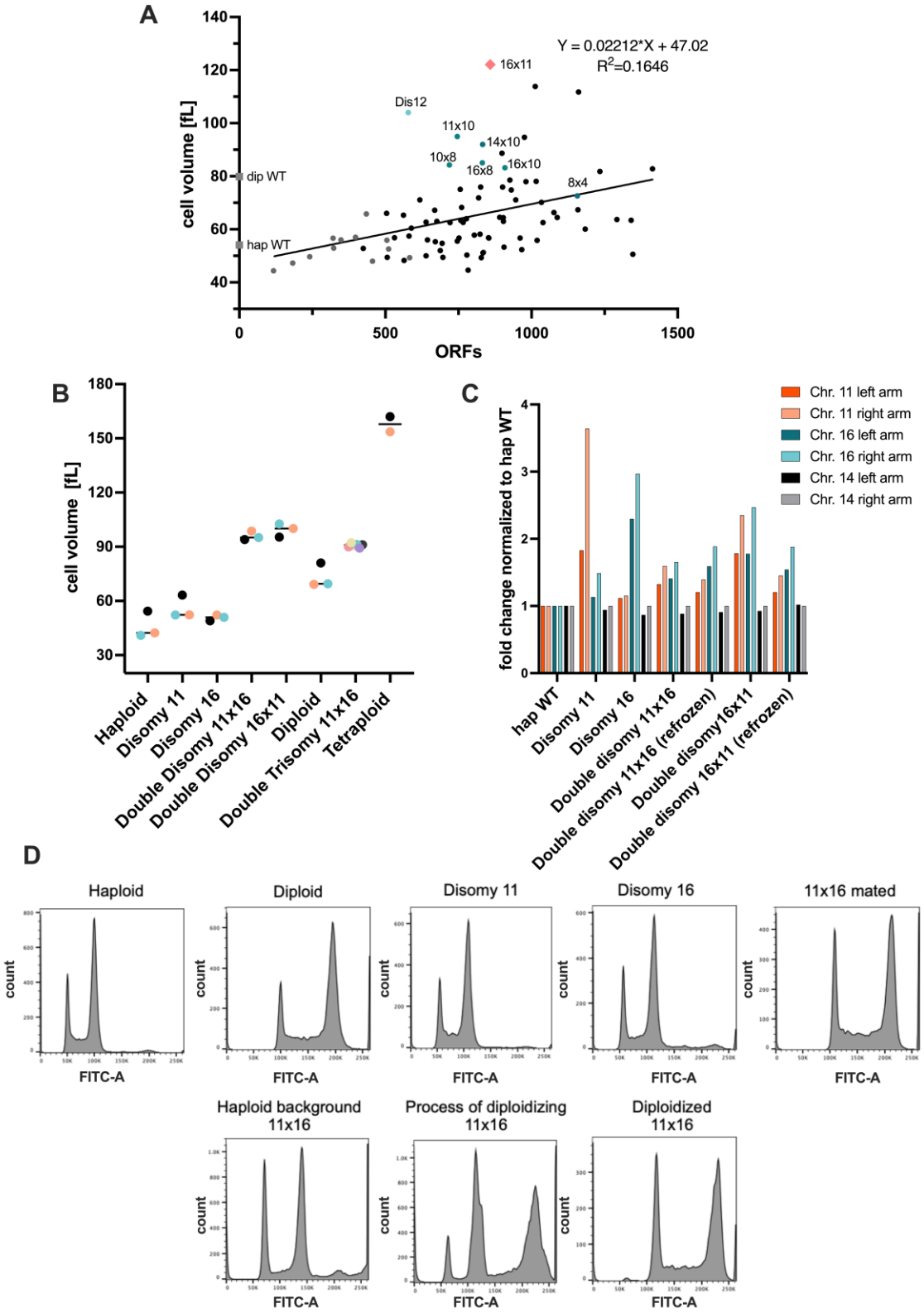

Figure 9: The most significant cell size phenotype in the double disomy collection, 11x16, has diploidized. **A**: Updated graph from Nina Stanišić (2023). Strains that have been discovered that have been diploidized have been removed, apart from the double disomic strain 11x16. **B**: Cell size (fL) measurement of the double disomy strains 11x16 and 16x1, as well as the double trisomy strain 11x16. Each strain was only measured once. To distinguish between strains, various colors were used. As control strains, haploid, diploid, tetraploid, Disomy 11, and Disomy 16 strains were measured. Haploid … CCY5419, CCY1894, and CCY1895; Diploid …CCY803, CCY1914, and CCY3837 ; Disomy 11…CCY6223, CCY6225, and CCY5843; Disomy 16… CCY6160, CCY6162, and CC5886;

double disomy 11x16 …11x16-1, 11x16-2, 11x16-3; double disomy 16x11 …16x11-1, 16x11-2, 16x11-3; double trisomy 11x16… CCY 6958, CCY 6959, CCY 6960, CCY 6961, CCY 6962, and CCY 6963 Tetraploid… CCY6265 and CCY6269 **C**: To determine the ploidy of the samples, Disomy 11, Disomy 16, double disomy 11x16, and double disomy 16x11, a qPCR analysis was performed. The values were normalized to chromosome 14 and the haploid strain. **D:** FACS graphs show the different stages of the cell cycle by measuring the DNA content. The first peak corresponds to the G1 phase, and the second peak is the M+G2 phase. Between those two peaks, the S phase is located. As controls a haploid, diploid, Disomy 11, Disomy 16, and a double trisomy 11x16 (mated) strain were used. The double disomy strains of 11x16 showed that they have diploidized or are in the process of diploidizing, as seen in the image. Only one strain was found to still have a haploid background.

3.5.2. Cell size phenotypes in double disomies caused by synergistic effects.

It is unclear how synergistic effects are involved in cell size regulation in double disomic strains. It could be due to the overexpression of genes involved in the same pathway or genes driving cell size through two individual cellular mechanisms. The larger cell size phenotypes in double disomic strains are likely combinations with chromosomes 8 or chromosome 10 (Figure 10A). It was decided to exclude combinations with chromosome 12 due to the strong cell size phenotype of the disomic strain.

I measured the cell sizes of the double disomic strains chromosomal combinations 4x8, 8x10, 10x11, 8x16, 10x14, and each chromosomes disomic strains from the single disomy collection were measured as a control to determine if the phenotype could be caused by synergistic effects (Figure 10A- 10E). The two double disomic strains 4x8 do not have the same cell size, making it impossible to determine if a synergistic effect results in the phenotype (Figure 10A). Both strains need further investigations to exclude spontaneous diploidization. The chromosome combination 8x10 and 10x11 increases their size when both chromosomes are gained (Figure 10B and 10C). The double disomic strain 10x14 has a larger cell size increase compared to the controls (Figure 10E). However, this can be likely due to the media change that was performed before optimizing the CASY parameters. This data from the double disomic strains 8x10, 10x11 and 10x14 suggests that overexpressing genes on these chromosomes influences cell size pathways. In contrast to the other measured double disomic strains, 8x16, the cell size phenotype does not result in a cell size increase. Instead, the combination cell size lies between the two disomic controls (Figure 10D). This chromosomal combination data suggests that genes located on these two chromosomes balance out each other’s effects. Overall, the chromosomal

combinations utilized in this thesis are interesting candidates to study synergistic effects in double disomic strains.

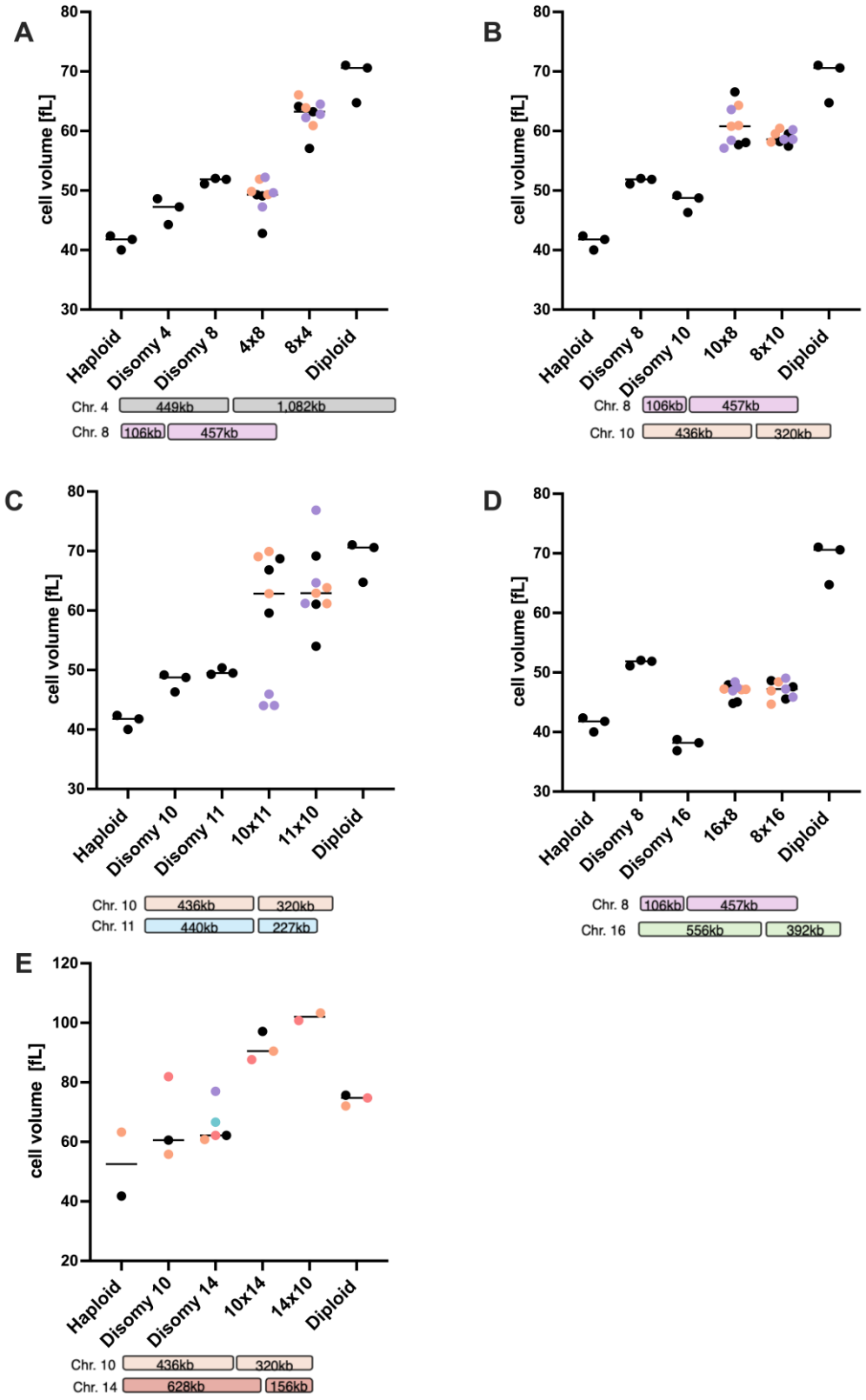

Figure 10: Cell size phenotypes of double disomy strains, with a variety of chromosome combinations. **A-D**: The cell volume of the double disomy strains 4x8, 10x8, 10x11, 16x8, and 10x14 and their respective disomy controls

were measured via CASY analysis. Each strain was analyzed in triplicate. To distinguish between strains with the same genotype, each was highlighted with a different color. The statistical test, one-way ANOVA, was applied for all to determine significant differences. **A:** Cell sizes of the double disomy chromosome combination 4x8. Between the double disomic strains 4x8 and 8x4, a significant difference can be seen (P =<0.0001). Double disomic strain 8x4 has a significant difference to the Disomy 4 (P = <0.0001) and Disomy 8 (P = <0.0001). Haploid … CCY7475; Diploid … CCY7434; Disomy 4 … CCY5859; Disomy 8 … CCY5866; double disomic strains 4x8 (clones 1 to 3) and 8x4 (clones 1 to3) **B**: Cell sizes of the double disomy chromosome combination 8 and 10. A significant difference between the double disomic strains to the haploid (P =<0.0001) and disomy controls is seen (P =<0.0001 and 0.0011 for 8x10 vs Disomy 8). Haploid … CCY7475; Diploid … CCY7434; Disomy 8 … CCY5866; Disomy 10 …CCY5874; double disomic strains 10x8 (clones 1 to 3) and 8x10 (clones 1 to3) **C**: Cell sizes of the double disomy chromosome combination 10 and 11. A significant difference between 10x11 vs haploid (P= 0.0198) and 11x10 vs haploid (P= 0.0019) is calculated. The cell size of the control disomic strains is the same size. The cell volume between11x10 and Disomy 10 is significant (P= 0.0447). Haploid … CCY7475; Diploid … CCY7434; Disomy 11… CCY5876; Disomy 10 …CCY5874; double disomic strains 10x11 (clones 1 to 3) and 11x10 (clones 1 to3) **D**: Cell sizes of the double disomy chromosome combination 8 and 16. No significant differences between the double disomy 16x8 and 8x16 are found. A significant difference in cell size is seen for haploid vs 8x16(P= 0.0002) and haploid vs 16x8 (P= 0.0003). 16x8 vs Disomy 8 (P= 0.0017). 16x8 vs Disomy 16 (P= <0.0001). 8x16 vs Disomy 8 (P= 0.0027). 8x16 vs Disomy 16 (P= <0.0001). Haploid … CCY7475; Diploid … CCY7434; Disomy 8 … CCY5866; Disomy 16 …CCY5888, double disomic strains 8x16 (clones 1 to 3) and 16x8 (clones 1 to3) **E**: The cell size of the disomic strains 10x14 and the controls was obtained via CASY analysis. Compared to the other measurements before no triplicate was measured. Only different strains, which are distinguishable by the different colors used. Two different media have been used in this experiment (YPAD and -HIS/-URA/-LYS/-LEU with media change to YPD). 10x14 vs haploid (P= 0.0020). 14x10 vs haploid (P= 0.0004). 10x14 vs Disomy 10 (P=0.0224).10x14 vs Disomy 14 (P=0.0092). 14x10 vs Disomy 14 (P=0.0033). 14x10 vs Disomy 14 (P=0.0011). Haploid …CCY 1895 (black) and CCY 5419(orange); Diploid…CCY803(black), CCY1914(orange) and CCY3837(red); Disomy 10… CCY1927(black), CCY6316 (orange), and CCY5841(red); Disomy 14… CCY6180 (black), CCY6181 (orange), and CCY6182 (red), CCY6183 (blue), and CCY5848 (purple); double disomic strains 10x14 (clones 1 to 3) and 14x10 (clones 2 to3)

4. Discussion

In this study, the aim was to gain a deeper understanding of how aneuploidy affects yeast cell size by identifying chromosome regions responsible for the larger cell size phenotypes. The initial focus was on understanding the synergetic effects of double disomic strains, specifically the chromosomal combination of chromosomes 11 and 16. Due to the strain diploidizing, the focus shifted to disomy 12 and understanding its cell size phenotype. There have been studies suspecting that the phenotype of disomy 12 is a result of the overexpressed rDNA region (Pérez-Ortín, 2021; Stanišić, 2023; Yordanov, 2024). To confirm this hypothesis, full and sequential partial chromosome arm deletions were engineered. The CASY method was optimized to clearly see the cell volume changes in aneuploid strains, as the influence of various auxotrophic marker combinations on cell size was determined.

4.1. Optimization of the CASY cell analyzer.

Overall, by implementing the adjusted parameters, the bulk cell size analysis via CASY has become more robust, and the reproducibility of the data has improved. The sample dilution range between $5.40x10^3$ to $5.40x10^4$ cells has been adjusted for the optimal cell size analysis. Although the growth media influences cell size, we were able to determine that the strain-to-strain differences are not affected by the media. Therefore, it is possible to grow the strains in selective media for active selection of aneuploidy either in -HIS/-URA/-LYS/-LEU or -HIS/-URA media, depending on the restored auxotrophic markers. Alternatively, growing the strains in YPAD is also an option if comparisons between various strains with different auxotrophic markers should be conducted. However, there is a possibility that the strains could lose their aneuploidy. A media change should be avoided, as it has been shown to cause a notable increase in cell size. The last parameter, which could influence cell size, is the incubation time. From this study's data, it was decided on an incubation time of 5 hours.

Future experiments can be conducted to fine-tune the parameters further. To keep the variability between analyses to a minimum, regardless of the operator, the incubation time, as well as the starting OD can be standardized. For example, to optimize the incubation times, an experiment can be conducted at the time intervals set at 4 hours,

5 hours, and 6 hours. By having multiple operators repeat the cell size analysis, it can be determined how robust the method has become.

To confirm all conclusions drawn in this thesis, the results have to be validated via an alternative method. One of the best-suited alternative method is microscopy.

4.2. Restored auxotrophic markers do not influence cell size when incorporated into the genome.

The lab yeast strains used in this thesis have been genetically manipulated to be auxotrophic for histidine, uracil, lysine, and leucine. To select for the aneuploidy, either histidine and uracil or lysine and leucine are reintegrated during this process. Both the single disomy and double disomy collections have been engineered to contain all four markers, making them closer to a wild type. The parent strains of the ACDC collection were induced with histidine and uracil, making them auxotrophic for lysine and leucine. Therefore, the haploid controls need to have the same auxotrophy as the aneuploid strains for the cell size comparison to be made.

It was found that uracil was not reintegrated into the genome. Instead, it is encoded on a centromeric plasmid, which was originally used to amplify the gene fragment. In the cell size analysis of all haploid and diploid control strains with various auxotrophic combinations, I discovered that cell size is not influenced by various marker combinations if the markers are integrated into the genome. As for the two haploid strains with the restored auxotrophic markers HIS/URA(plasmid) and HIS/LYS/LEU/URA(plasmid), where uracil is encoded on a plasmid, a size increase compared to the strains with the genome-integrated marker was seen. Overall, it can be concluded that the plasmid makes the haploid cells significantly larger. Diploids are not influenced by uracil encoded on the plasmid, suggesting diploids have a mechanism in place that compensates for the plasmid's effects. Diploids have improved cellular fitness over haploids under specific conditions (Harari, 2018). This may also play a role in counteracting the effects of the plasmid.

The cell size data does not provide conclusive evidence that either of the outliers strains discussed is free of problems. Therefore, I recommend confirming the diploid

and haploid background of the diploid LYS/LEU and the haploid strain with each marker via FACS. The LYS and LEU genes in each strain could be amplified via PCR, and the obtained fragments can be sent for sequencing to confirm that no mutations in the marker sequence are responsible for this change. If all results are inconclusive or no issues are found, mating of the haploid LYS/LEU strain with a non-marker strain can be performed to obtain a new LYS/LEU diploid strain for comparison with the original strain.

4.3. Cell size phenotypes in disomic strains are chromosome-specific.

Overall, previous lab members have confirmed that chromosome-specific effects are the main drivers of cell size (Nina Stanišić, 2023). The comparison between the previously obtained cell size data of the single disomy and the ACDC collection correlates. Therefore, the findings can be applied to both collections. Further, by measuring each strain in triplicates the reproducibility of the data will increase.

The main goal was to understand whether the genes involved in the cell size phenotypes are due to single genes or combinatorial effects on one chromosome. Various chromosomes result in larger or smaller cell size phenotypes. The smallest cell size phenotype, disomy 1, the main cell size regulator was identified as the CLN3 gene (Thorburn et al., 2013; Sommer, 2021). Control strains where CLN3 was either heterozygously deleted or fully knocked out showed an increase in cell volume compared to the disomy strains. These measurements have one minor limitation, which is the availability of only one clone for certain strains. The largest cell size phenotype in the disomy collection disomy 12 cell size, is highly dependent on the degree of aneuploidy. By increasing the copy numbers of chromosome 12, the cell size increases significantly.

The overall scheme to determine the individual cell size drivers a total of three steps have to be done (Koller et al. 2025). First, identify the main chromosome arm involved. Second, engineering sequential partial arm deletion strains, which will be used to narrow down the gene regions. Through the defined regions, it is possible to obtain a list of specific gene candidates that could play an important role in the cell size control

mechanism. Third, knockouts of predicted genes are performed to confirm their involvement. However, the single disomies with the largest phenotypes, full arm deletions, were analyzed. No partial arm deletions and therefore no gene candidates were found.

From the cell size data of the disomic strains of chromosomes 8, 10, 11, and 16 and their left and right chromosome arm deletions, it was possible to narrow down the chromosome arm responsible for the phenotype. The combinatorial effect of at least one gene located on each chromosome arm is responsible for the disomy 8 cell size phenotype. Disomy 11 left chromosome arm drives the cell size increase. Neither disomy 10 nor disomy 16 had a significant cell volume increase. The full arm deletions were inconclusive due to the high variability of the measurements. There may be genes located on the left arm of chromosome 16 involved in decreasing the cell size. For confirmation, further experiments need to be conducted. The next step is to measure the sequential partial arm deletion strains of disomy 8, 11, and 16 to further understand the underlying mechanism of cell size regulation in aneuploid strains.

In a future study, the disomy 7 and disomy 14 strain, which also exhibits larger cell size phenotypes, along with other strains showing smaller phenotypes, could be investigated. These strains may provide more insight into the mechanism regulating cell size phenotypes. However, a limitation of smaller cell size phenotypes is that the cell size change may not be as pronounced.

4.4. rDNA is not the only region involved in the cell size phenotype of Disomy 12.

The largest cell size phenotype was the disomy 12 strain. An increase in cell size independently of ploidy was observed (Figure 4C). This indicates that overexpressing this chromosome at various ploidy levels affects the regulatory pathway for cell size. This was the first time a correlation between increased ploidy levels of chromosome 12 caused a gradual size increase. Nevertheless, the exact mechanism driving the cell size phenotype of the disomy 12 is unknown.

A possible explanation for the increased cell size phenotype may be due to the formation of excess amounts of extracellular rDNA circles. Nina Stanišić (2023) has overexpressed rDNA circles and found that the cell size increases when a large number of circles are expressed in the cell. However, this result could be due to proliferation defects caused by the excessive amount of rDNA circles (Sinclair & Guarente, 1997; Shcheprova et al., 2008; Neurohr et al., 2018; Morlot et al., 2019). Due to the dynamic process of the cells forming rDNA circles, there was a concern that the cell size measurements lacked reproducibility. As the single colony experiment has shown, the concern is valid since a high day-to-day cell size variability for each colony was found (Figure 6B). The main cause of the variability is likely due to the dynamic mechanism of rDNA circles forming. Therefore, to obtain more accurate data, the cell size should be measured in triplicates.

However, it is not possible to differentiate between rDNA located on the chromosome and rDNA contained in the rDNA circles from this data. Therefore, to determine the amount of rDNA circles and the encoded rDNA on the chromosome, the topological differences, supercoiled and circular, can be used to separate the two states by agarose electrophoresis and Southern blotting (Sinclair and Guarente, 1997; Mansisidor et al. 2018).

Another way to monitor the rDNA copy numbers is by performing qPCR, as in this study. However, it is not possible to track only rDNA circles with this method. Instead, the entire rDNA in a population is measured, and overall changes can be observed. To measure both the rDNA copy numbers and the cell size, an additional step can be performed in the single-colony experiment. Before diluting the sample for CASY, a pellet of cells can be spun down and used to analyze the overall rDNA copy numbers in the cells. The total rDNA of each single colony can be determined either via electrophoresis or qPCR. Furthermore, the rDNA levels can be compared to the measured cell size of each single colony. With this setup, the previously observed day-to-day variability in cell size can be connected to the rDNA level changes.

To determine if the rDNA is the main driver of cell size, the engineered full and partial arm deletion cell size was measured. The right chromosome arm was identified as the main driver of the cell size phenotype. A total of four regions driving the phenotype

were identified, one of which corresponds to the location of the rDNA repeats. By engineering a partial arm deletion between the regions Disomy 12R-8 and Disomy 12R-10, further evidence could be obtained to support the hypothesis that the rDNA region is one of the main drivers. For the remaining regions, genes that were previously found to play a role in cell size regulation through a variety of cellular pathways were predicted (Figure S3 and Table S2). The majority of the encoded proteins are involved in cell wall synthesis and maintenance, and cell cycle progression. In the future, to identify the specific gene and the pathways involved in the disomy 12 phenotype, heterozygous deletions of these genes should be performed. The heterozygous deletion strain's cell size can be determined via CASY, and changes will be compared to the partial arm deletion strains and the disomic strain. If a gene regulating cell size is heterozygously deleted, a cell size decrease can be expected.

Additionally, the overexpressed rDNA locus may cause the transcription rate to increase. The study conducted by Wu (2010) discovered a correlation between cell size and transcription, for cells to maintain their homeostasis. Another study by Pérez-Ortín (2021) focused on the transcription rates from RNA polymerase I and II, and how these rates affect cell size in cln3 and whi5 mutation strains. Higher rDNA copy numbers and higher transcription rates were determined in the cln3 mutation strain, which had a significant cell size increase. The whi5 mutation strain had a decreased cell size, a lower transcription rate for nascent RNA, and fewer rDNA repeats. Hence, strains with increased rDNA repeats result in larger cell size (Pérez-Ortín et al., 2021). Therefore, the disomy 12 phenotype could be caused by higher transcription rates due to the larger number of encoded rDNA repeats. Consequently, due to increased transcription rates, the specific cell size regulators may increase expression levels.
To determine if the disomy 12 phenotype is a result of overexpressing ribosomal RNA, the cells are sorted according to their cell size via FACS. Each group's DNA content can then be analyzed through FACS with a DNA live-staining of the histone marker. However, for the cell size sorting to work, the size difference between each cell must be significant. If the sorting was a success, each cluster's RNA expression levels can be determined via qPCR. The qPCR expression data of various ploidy levels of chromosome 12 can provide information on whether an increase in ribosomal RNA drives the cell size change.

These results suggest that overexpressing genes of the cell cycle pathway are involved in the cell size phenotype, and if this is due to perturbed cell cycle progression. By enriching the disomy 12 cells via FACS and arresting them in the cell cycle stage G1 under the microscope, it is possible to track how long it takes for the cells to enter the G2+M phase. The haploid and diploid strains would be used as controls for this experiment.

Overall, the data obtained in this thesis proves that rDNA is in one of the four regions involved in the cell size phenotype of disomy 12. However, other pathways are highly likely involved as well. Therefore, to understand the cell size phenotype of disomy 12, additional experiments are necessary.

4.5. Synergetic effects of double disomic strains

To study synergistic effects between two chromosomes, double disomic strains were used. The double disomic strain 11x16 was determined to have the largest cell size phenotype in the collection. To understand which genes, interact for this phenotype to occur, the strain was studied in more detail. Through mating the disomic strains 11 and 16, a 0.5-fold overexpression of each chromosome was achieved. The cell size increase was not as significant as that of the double disomic strain. This led to the engineering of full chromosome arm deletion strains of both chromosomes in the double disomic background. All double disomic strains of 11x16 have diploidized. It is unclear if diploidization is favored by specific chromosome combinations. As a result of this discovery, double disomic strains showing unusual growth were analyzed via FACS to check for diploidization. It seems that some double disomic strains are prone to spontaneous diploidization, specifically chromosome combinations with chromosome 13, 14, or 16 (data not shown). Therefore, they must be monitored regularly via FACS. A study by Harari (2018) has investigated that spontaneous diploidization is a common occurrence for cells under stressful conditions. There are two possible mechanisms of diploidization. The first mechanism is endoreduplication, where the whole genome is duplicated (Harari, 2018). The second diploidization mechanism identified is caused by a mating type switch in some cells within the population, allowing them to mate with each other. Although laboratory strains have been designed to be only one mating type to avoid this (Harari, 2018). It is not possible to conclude which of the two proposed mechanisms of diploidization takes place in the

double disomic strains with the data obtained throughout this study. To determine which of these two proposed mechanisms is likely to cause diploidization, the strain's mating type should first be determined. These strains should have an a/α mating type, meaning no mating should occur between either a strain or the α strain used in this test. However, if a mating type switch did occur, the strain would mate with the mating type test strains, and growth would be observed. That would indicate a switch in the mating type has occurred. For further confirmation, the mutation in the HO gene (Harari, 2018; *Saccharomyces* Genome Database (SGD)), which prevents mating type switches, can be amplified and sent for sequencing to determine if a mutation has been lost.

This study has also provided data on other larger cell size double disomic strains. A significant increase in cell size was detected when two chromosomes are overexpressed. To identify the genes involved in these phenotypes in a future study, the same procedure as for the disomy strains can be applied. First, by determining which of the chromosomes is responsible for the phenotype. Second, through partial arm deletions, the regions can be narrowed down, and an initial prediction can be made. Lastly, the predicted genes are heterozygously deleted to confirm that they drive the cell size phenotype. However, performing full and partial arm deletion on double disomic strains is less efficient. Instead, the phenotype should be confirmed in a double trisomic strain (2N+2). This strain can be obtained through mating. If a 0.5-fold overexpression of the chromosomes is sufficient to observe the phenotype, the ACDC collection, containing all full and partial arm deletions in mating type a, can be used to mate with an aneuploid strain with an alpha mating type. As a result, various double trisomic strains for both chromosome arms can be obtained. However, as a precaution, all strain ploidy backgrounds should be confirmed via FACS.

5. Reference

1. Albert, B., Mathon, J., Shukla, A., Saad, H., Normand, C., Léger-Silvestre, I., Villa, D., Kamgoue, A., Mozziconacci, J., Wong, H., Zimmer, C., Bhargava, P., Bancaud, A., & Gadal, O. (2013). Systematic characterization of the conformation and dynamics of budding yeast chromosome XII. The Journal of cell biology, 202(2), 201–210. https://doi.org/10.1083/jcb.201208186
2. Anders, K. R., Kudrna, J. R., Keller, K. E., Kinghorn, B. A. A., Miller, E. M., Pauw, D., Peck, A. T., Shellooe, C. E., & Strong, I. J. T. (2009). A strategy for constructing aneuploid yeast strains by transient nondisjunction of a target chromosome. BMC Genetics, 10(1), 1–11. https://doi.org/10.1186/1471-2156-10-36
3. Anjur-Dietrich, M. I., Kelleher, C. P., & Needleman, D. J. (2021). Mechanical Mechanisms of Chromosome Segregation. Cells, 10(2), 465. https://doi.org/10.3390/cells10020465
4. Amon A. (1999). The spindle checkpoint. *Current opinion in genetics & development*, *9*(1), 69–75. https://doi.org/10.1016/s0959-437x(99)80010-0
5. Barber, F., Amir, A., & Murray, A. W. (2020). Cell-size regulation in budding yeast does not depend on linear accumulation of Whi5. Proceedings of the National Academy of Sciences of the United States of America, 117(25), 14243–14250.https://doi.org/10.1073/pnas.2001255117
6. Beach, R. R., Ricci-Tam, C., Brennan, C. M., Moomau, C. A., Hsu, P. H., Hua, B., Silberman, R. E., Springer, M., & Amon, A. (2017). Aneuploidy Causes Non-genetic Individuality. Cell, 169(2), 229–242.e21. https://doi.org/10.1016/j.cell.2017.03.021
7. Ben-David, U., & Amon, A. (2020). Context is everything: aneuploidy in cancer. Nature Reviews. Genetics, 21(1), 44–62. https://doi.org/10.1038/s41576-019-0171-x
8. Boveri T. (2008). Concerning the origin of malignant tumours by Theodor Boveri. Translated and annotated by Henry Harris. Journal of cell science, 121 Suppl 1, 1–84. https://doi.org/10.1242/jcs.025742
9. Chandler-Brown, D., Schmoller, K. M., Winetraub, Y., & Skotheim, J. M. (2017). The Adder Phenomenon Emerges from Independent Control of Pre- and Post-Start Phases of the Budding Yeast Cell Cycle. Current biology : CB, 27(18), 2774–2783.e3.https://doi.org/10.1016/j.cub.2017.08.015

10. Chen, G., Bradford, W. D., Seidel, C. W., & Li, R. (2012). Hsp90 stress potentiates rapid cellular adaptation through induction of aneuploidy. Nature, 482(7384), 246–250. https://doi.org/10.1038/nature10795
11. Chen, G., Mulla, W. A., Kucharavy, A., Tsai, H. J., Rubinstein, B., Conkright, J., McCroskey, S., Bradford, W. D., Weems, L., Haug, J. S., Seidel, C. W., Berman, J., & Li, R. (2015). Targeting the adaptability of heterogeneous aneuploids. Cell, 160(4), 771–784. https://doi.org/10.1016/j.cell.2015.01.026
12. Duncan, J. L., Bloomfield, M., Swami, N., Cimini, D., & Davalos, R. V. (2023). High-Frequency Dielectrophoresis Reveals That Distinct Bio-Electric Signatures of Colorectal Cancer Cells Depend on Ploidy and Nuclear Volume. Micromachines, 14(9), 1723. https://doi.org/10.3390/mi14091723
13. Facchetti, G., Chang, F., & Howard, M. (2017). Controlling cell size through sizer mechanisms. Current opinion in systems biology, 5, 86–92. https://doi.org/10.1016/j.coisb.2017.08.010
14. Gordon, D. J., Resio, B., & Pellman, D. (2012). Causes and consequences of aneuploidy in cancer. Nature reviews. Genetics, 13(3), 189–203. https://doi.org/10.1038/nrg3123
15. Harari, Y., Ram, Y., Rappoport, N., Hadany, L., & Kupiec, M. (2018). Spontaneous Changes in Ploidy Are Common in Yeast. Current biology : CB, 28(6), 825–835.e4. https://doi.org/10.1016/j.cub.2018.01.062
16. Hartwell, L. H., & Unger, M. W. (1977). Unequal division in Saccharomyces cerevisiae and its implications for the control of cell division. The Journal of cell biology, 75(2 Pt 1), 422–435.https://doi.org/10.1083/jcb.75.2.422
17. Hassold, T. J., & Jacobs, P. A. (1984). Trisomy in Man. Annual Review of Genetics, 18(1), 69– 97. https://doi.org/10.1146/annurev.ge.18.120184.000441
18. Hirano T. (2015). Chromosome Dynamics during Mitosis. Cold Spring Harbor perspectives in biology, 7(6), a015792. https://doi.org/10.1101/cshperspect.a015792
19. Ho, C. H., Magtanong, L., Barker, S. L., Gresham, D., Nishimura, S., Natarajan, P., Koh, J. L. Y., Porter, J., Gray, C. A., Andersen, R. J., Giaever, G., Nislow, C., Andrews, B., Botstein, D., Graham, T. R., Yoshida, M., & Boone, C. (2009). A molecular barcoded yeast ORF library enables mode-of-action analysis of bioactive compounds. Nature biotechnology, 27(4), 369–377. https://doi.org/10.1038/nbt.1534

20. Hsu, H. F., & Hou, J. W. (2007). Variable expressivity in Patau syndrome is not all related to trisomy 13 mosaicism. *American journal of medical genetics. Part A*, *143A*(15), 1739–1748. https://doi.org/10.1002/ajmg.a.31835
21. Ippolito, M. R., Martis, V., Martin, S., Tijhuis, A. E., Hong, C., Wardenaar, R., Dumont, M., Zerbib, J., Spierings, D. C. J., Fachinetti, D., Ben-David, U., Foijer, F., & Santaguida, S. (2021). Gene copy-number changes and chromosomal instability induced by aneuploidy confer resistance to chemotherapy. Developmental cell, 56(17), 2440-2454.e6. https://doi.org/10.1016/j.devcel.2021.07.006
22. Johnston, G. C., Pringle, J. R., & Hartwell, L. H. (1977). Coordination of growth with cell division in the yeast Saccharomyces cerevisiae. Experimental cell research, 105(1), 79–98.https://doi.org/10.1016/0014-4827(77)90154-9
23. Kobayashi T. (2014). Ribosomal RNA gene repeats, their stability and cellular senescence. Proceedings of the Japan Academy. Series B, Physical and biological sciences, 90(4), 119–129. https://doi.org/10.2183/pjab.90.119
24. Koller, M., Himmelbauer, C., Fink, S., Ravichandran, M., & Campbell, C. (2025). Combinatorial effects of multiple genes contribute to beneficial aneuploidy phenotypes. *bioRxiv*. https://doi.org/10.1101/2025.03.05.641640
25. Lin, H. Y., Lin, S. P., Chen, Y. J., Hung, H. Y., Kao, H. A., Hsu, C. H., Chen, M. R., Chang, J. H., Ho, C. S., Huang, F. Y., Shyur, S. D., Lin, D. S., & Lee, H. C. (2006). Clinical characteristics and survival of trisomy 18 in a medical center in Taipei, 1988-2004. *American journal of medical genetics. Part A*, *140*(9), 945–951. https://doi.org/10.1002/ajmg.a.31173
26. Linder, R. A., Greco, J. P., Seidl, F., Matsui, T., & Ehrenreich, I. M. (2017). The Stress-Inducible Peroxidase TSA2 Underlies a Conditionally Beneficial Chromosomal Duplication in Saccharomyces cerevisiae. G3 (Bethesda, Md.), 7(9), 3177–3184. https://doi.org/10.1534/g3.117.300069
27. Lukow, D. A., Sausville, E. L., Suri, P., Chunduri, N. K., Wieland, A., Leu, J., Smith, J. C., Girish, V., Kumar, A. A., Kendall, J., Wang, Z., Storchova, Z., & Sheltzer, J. M. (2021). Chromosomal instability accelerates the evolution of resistance to anti-cancer therapies. Developmental cell, 56(17), 2427–2439.e4. https://doi.org/10.1016/j.devcel.2021.07.009
28. Mansisidor, A., Molinar, T., Jr, Srivastava, P., Dartis, D. D., Pino Delgado, A., Blitzblau, H. G., Klein, H., & Hochwagen, A. (2018). Genomic Copy-Number

Loss Is Rescued by Self-Limiting Production of DNA Circles. Molecular cell, 72(3), 583–593.e4. https://doi.org/10.1016/j.molcel.2018.08.036

29. Morlot, S., Song, J., Léger-Silvestre, I., Matifas, A., Gadal, O., & Charvin, G. (2019). Excessive rDNA Transcription Drives the Disruption in Nuclear Homeostasis during Entry into Senescence in Budding Yeast. Cell reports, 28(2), 408–422.e4. https://doi.org/10.1016/j.celrep.2019.06.032
30. Muenzner, J., Trébulle, P., Agostini, F., Zauber, H., Messner, C. B., Steger, M., Kilian, C., Lau, K., Barthel, N., Lehmann, A., Textoris-Taube, K., Caudal, E., Egger, A. S., Amari, F., De Chiara, M., Demichev, V., Gossmann, T. I., Mülleder, M., Liti, G., Schacherer, J., … Ralser, M. (2024). Natural proteome diversity links aneuploidy tolerance to protein turnover. Nature, 630(8015), 149–157. https://doi.org/10.1038/s41586-024-07442-9
31. Nelson, J. O., Watase, G. J., Warsinger-Pepe, N., & Yamashita, Y. M. (2019). Mechanisms of rDNA Copy Number Maintenance. Trends in genetics : TIG, 35(10), 734–742. https://doi.org/10.1016/j.tig.2019.07.006
32. Neurohr, G. E., Terry, R. L., Sandikci, A., Zou, K., Li, H., & Amon, A. (2018). Deregulation of the G1/S-phase transition is the proximal cause of mortality in old yeast mother cells. Genes & development, 32(15-16), 1075–1084. https://doi.org/10.1101/gad.312140.118
33. Nittnaus K. (2024). Effects of aneuploidy on meiosis. Analysis of sporulation and chromosome segregation in meiosis of aneuploid yeast. Master Thesis; University of Vienna
34. OMNI Life Science GmbH & Co KG (2018). CASY C ELL COUNTER & ANALYZER Operators Guide
35. Oromendia, A. B., Dodgson, S. E., & Amon, A. (2012). Aneuploidy causes proteotoxic stress in yeast. Genes & development, 26(24), 2696–2708. https://doi.org/10.1101/gad.207407.112
36. Pérez, A. P., Artés, M. H., Moreno, D. F., Clotet, J., & Aldea, M. (2022). Mad3 modulates the G1 Cdk and acts as a timer in the Start network. Science advances, 8(18), eabm4086.https://doi.org/10.1126/sciadv.abm4086
37. Pérez-Ortín, J. E., Mena, A., Barba-Aliaga, M., Singh, A., Chávez, S., & García-Martínez, J. (2021). Cell volume homeostatically controls the rDNA repeat copy number and rRNA synthesis rate in yeast. PLoS genetics, 17(4), e1009520. https://doi.org/10.1371/journal.pgen.1009520

38. Peter, J., De Chiara, M., Friedrich, A., Yue, J. X., Pflieger, D., Bergström, A., Sigwalt, A., Barre, B., Freel, K., Llored, A., Cruaud, C., Labadie, K., Aury, J. M., Istace, B., Lebrigand, K., Barbry, P., Engelen, S., Lemainque, A., Wincker, P., Liti, G., … Schacherer, J. (2018). Genome evolution across 1,011 Saccharomyces cerevisiae isolates. Nature, 556(7701), 339–344. https://doi.org/10.1038/s41586-018-0030-5
39. Petes T. D. (1979). Yeast ribosomal DNA genes are located on chromosome XII. Proceedings of the National Academy of Sciences of the United States of America, 76(1), 410–414. https://doi.org/10.1073/pnas.76.1.410
40. Rojas, J., Hose, J., Dutcher, H. A., Place, M., Wolters, J. F., Hittinger, C. T., & Gasch, A. P. (2024). Comparative modeling reveals the molecular determinants of aneuploidy fitness cost in a wild yeast model. *Cell genomics*, *4*(10), 100656. https://doi.org/10.1016/j.xgen.2024.100656
41. Santaguida, S., & Amon, A. (2015). Short- and long-term effects of chromosome mis-segregation and aneuploidy. Nature reviews. Molecular cell biology, 16(8), 473–485. https://doi.org/10.1038/nrm4025
42. Santaguida, S., Vasile, E., White, E., & Amon, A. (2015). Aneuploidy-induced cellular stresses limit autophagic degradation. Genes & development, 29(19), 2010–2021. https://doi.org/10.1101/gad.269118.115
43. *Saccharomyces* Genome Database (SGD); https://www.yeastgenome.org (retrieved 08.08.2025)
44. Shcheprova, Z., Baldi, S., Frei, S. B., Gonnet, G., & Barral, Y. (2008). A mechanism for asymmetric segregation of age during yeast budding. Nature, 454(7205), 728–734. https://doi.org/10.1038/nature07212
45. Sheltzer, J. M., Blank, H. M., Pfau, S. J., Tange, Y., George, B. M., Humpton, T. J., Brito, I. L., Hiraoka, Y., Niwa, O., & Amon, A. (2011). Aneuploidy drives genomic instability in yeast. Science (New York, N.Y.), 333(6045), 1026–1030. https://doi.org/10.1126/science.1206412
46. Sinclair, D. A., & Guarente, L. (1997). Extrachromosomal rDNA circles--a cause of aging in yeast. Cell, 91(7), 1033–1042. https://doi.org/10.1016/s0092-8674(00)80493-6
47. Sirr, A., Cromie, G. A., Jeffery, E. W., Gilbert, T. L., Ludlow, C. L., Scott, A. C., & Dudley, A. M. (2015). Allelic variation, aneuploidy, and nongenetic mechanisms

suppress a monogenic trait in yeast. *Genetics*, *199*(1), 247–262. https://doi.org/10.1534/genetics.114.170563

48. Sommer, R. A., DeWitt, J. T., Tan, R., & Kellogg, D. R. (2021). Growth-dependent signals drive an increase in early G1 cyclin concentration to link cell cycle entry with cell growth. eLife, 10, e64364. https://doi.org/10.7554/eLife.64364
49. Stanišić N. (2023).Impact of ribosomal DNA on cell size in aneuploid yeast. Bachelor Thesis; University of Vienna
50. Stingele, S., Stoehr, G., Peplowska, K., Cox, J., Mann, M., & Storchova, Z. (2012). Global analysis of genome, transcriptome and proteome reveals the response to aneuploidy in human cells. Molecular systems biology, 8, 608. https://doi.org/10.1038/msb.2012.40
51. Tanaka T. U. (2002). Bi-orienting chromosomes on the mitotic spindle. Current opinion in cell biology, 14(3), 365–371. https://doi.org/10.1016/s0955-0674(02)00328-9
52. Thorburn, R. R., Gonzalez, C., Brar, G. A., Christen, S., Carlile, T. M., Ingolia, N. T., Sauer, U., Weissman, J. S., & Amon, A. (2013). Aneuploid yeast strains exhibit defects in cell growth and passage through START. Molecular biology of the cell, 24(9), 1274–1289. https://doi.org/10.1091/mbc.E12-07-0520
53. Thornton, K., Kwan, E. X., Bubb, K. L., Paleologu, L., Raghuraman, M. K., Brewer, B. J., Cuperus, J. T., & Queitsch, C. (2025). rDNA copy number variation affects yeast fitness in response to different environments. Genetics, 230(3), iyaf075. https://doi.org/10.1093/genetics/iyaf075
54. Torres, E. M., Sokolsky, T., Tucker, C. M., Chan, L. Y., Boselli, M., Dunham, M. J., & Amon, A. (2007). Effects of aneuploidy on cellular physiology and cell division in haploid yeast. Science (New York, N.Y.), 317(5840), 916–924. https://doi.org/10.1126/science.1142210
55. Torres, E. M., Williams, B. R., & Amon, A. (2008). Aneuploidy: cells losing their balance. Genetics, 179(2), 737–746. https://doi.org/10.1534/genetics.108.090878
56. Torres, E. M., Dephoure, N., Panneerselvam, A., Tucker, C. M., Whittaker, C. A., Gygi, S. P., Dunham, M. J., & Amon, A. (2010). Identification of aneuploidy-tolerating mutations. Cell, 143(1), 71–83. https://doi.org/10.1016/j.cell.2010.08.038

57. Tsai, H. J., Nelliat, A. R., Choudhury, M. I., Kucharavy, A., Bradford, W. D., Cook, M. E., Kim, J., Mair, D. B., Sun, S. X., Schatz, M. C., & Li, R. (2019). Hypo-osmotic-like stress underlies general cellular defects of aneuploidy. Nature, 570(7759), 117–121. https://doi.org/10.1038/s41586-019-1187-2
58. Turner, J. J., Ewald, J. C., & Skotheim, J. M. (2012). Cell size control in yeast. Current biology : CB, 22(9), R350–R359. https://doi.org/10.1016/j.cub.2012.02.041
59. van den Broek, M., Bolat, I., Nijkamp, J. F., Ramos, E., Luttik, M. A., Koopman, F., Geertman, J. M., de Ridder, D., Pronk, J. T., & Daran, J. M. (2015). Chromosomal Copy Number Variation in Saccharomyces pastorianus Is Evidence for Extensive Genome Dynamics in Industrial Lager Brewing Strains. Applied and environmental microbiology, 81(18), 6253–6267. https://doi.org/10.1128/AEM.01263-15
60. Yona, A. H., Manor, Y. S., Herbst, R. H., Romano, G. H., Mitchell, A., Kupiec, M., Pilpel, Y., & Dahan, O. (2012). Chromosomal duplication is a transient evolutionary solution to stress. Proceedings of the National Academy of Sciences of the United States of America, 109(51), 21010–21015. https://doi.org/10.1073/pnas.1211150109
61. Voordeckers, K., Kominek, J., Das, A., Espinosa-Cantú, A., De Maeyer, D., Arslan, A., Van Pee, M., van der Zande, E., Meert, W., Yang, Y., Zhu, B., Marchal, K., DeLuna, A., Van Noort, V., Jelier, R., & Verstrepen, K. J. (2015). Adaptation to High Ethanol Reveals Complex Evolutionary Pathways. *PLoS genetics*, *11*(11), e1005635. https://doi.org/10.1371/journal.pgen.1005635
62. Wang, H., Carey, L. B., Cai, Y., Wijnen, H., & Futcher, B. (2009). Recruitment of Cln3 cyclin to promoters controls cell cycle entry via histone deacetylase and other targets. PLoS biology, 7(9), e1000189. https://doi.org/10.1371/journal.pbio.1000189
63. Watson, E. V., Lee, J. J., Gulhan, D. C., Melloni, G. E. M., Venev, S. V., Magesh, R. Y., Frederick, A., Chiba, K., Wooten, E. C., Naxerova, K., Dekker, J., Park, P. J., & Elledge, S. J. (2024). Chromosome evolution screens recapitulate tissue-specific tumor aneuploidy patterns. *Nature genetics*, *56*(5), 900–912. https://doi.org/10.1038/s41588-024-01665-2

64. Weaver, B. A., & Cleveland, D. W. (2006). Does aneuploidy cause cancer?. Current opinion in cell biology, 18(6), 658–667. https://doi.org/10.1016/j.ceb.2006.10.002
65. Wu, C. Y., Rolfe, P. A., Gifford, D. K., & Fink, G. R. (2010). Control of transcription by cell size. PLoS biology, 8(11), e1000523. https://doi.org/10.1371/journal.pbio.1000523
66. Yordanov N. (2024) Characterising the cell size phenotype of chromosome XII disomy in yeast. Bachelor Thesis; University of Vienna
67. Zadrag-Tecza, R., Kwolek-Mirek, M., Alabrudzińska, M., & Skoneczna, A. (2018). Cell Size Influences the Reproductive Potential and Total Lifespan of the Saccharomyces cerevisiae Yeast as Revealed by the Analysis of Polyploid Strains. Oxidative medicine and cellular longevity, 2018, 1898421. https://doi.org/10.1155/2018/1898421
68. Zhu, Y. O., Sherlock, G., & Petrov, D. A. (2016). Whole Genome Analysis of 132 Clinical Saccharomyces cerevisiae Strains Reveals Extensive Ploidy Variation. G3 (Bethesda, Md.), 6(8), 2421–2434. https://doi.org/10.1534/g3.116.029397

6. Supplement

6.1. Supplementary methods

6.1.1. Confirmation of auxotrophic marker integration in haploid wild types

6.1.1.1. Amplification of the genome integrated auxotrophic marker via PCR and sequencing

The auxotrophic markers HIS, URA, LYS and LEU genome integration were confirmed PCR. The genomic material was extracted from the strains using the NaOH extraction protocol (chapter 2.3.8). The PCR was performed according to chapter 2.3.2.1. and the product was sent for sequencing (chapter 2.3.5.)

6.1.1.2. Selecting for the genome integrated URA3 marker via FOA plates

The haploid strain was diluted six times with 1x phosphate buffered saline buffer (PBS). The dilutions were plated on YPAD and 5-fluoroorotic acid (FOA) plates. If the plasmid was incorporated, the strain could not grow on FOA plates. However, if the strain grew, the strain lost the plasmid where the Ura3 gene was located.

6.1.2. Sporulation and Tetrad Dissection

Diploid strains, used to obtain haploid strains with various auxotrophic marker combinations, were freshly streaked out on yeast extract peptone dextrose (YPD) agar plates. Sporulation of diploid strains was induced by transferring a large number of cells onto sporulation media plates (SPM). The plate was left at room temperature over the weekend to allow the strains to sporulate. The progress of sporulation was checked under the light microscope by applying a small amount onto the slide and covering it with the cover glass. A large number of the cells were mixed with 3µL of the enzyme Zymolase (50%, Zymo Research) and 197µL of H_2O. The samples were incubated at 30°C for 20 min and placed on ice. A YPD plate for each sample was prepared beforehand and placed at 30°C to remove the excess water. 25µL of the digested culture solution was applied to the YPD plate, and the tetrads were dissected with the MSM 400 Micromanipulator/Tetrad dissector (Singer Instruments). The spores were grown for 2 days at 30°C.

The plate was replica plated on YPD and individual amino acid dropout plates to determine which marker has been inherited by which spore. The plate was used for

the mating type test. All plates were incubated at 30°C till colonies had formed. The colonies with the correct auxotrophic marker combinations were frozen for storage.

6.2. Supplementary Figures and Tables

Table S1: Final sample volume dilution table according to the OD values.

OD_{600} measurements	Number of cells in sample	Number of Cells normalized	Total V [mL]	V of culture [µL]
1.5	2.25E+07	1.01E+05	10	45.0
1.4	2.10E+07	1.01E+05	10	48.2
1.3	1.95E+07	1.01E+05	10	51.9
1.2	1.80E+07	1.01E+05	10	56.3
1.1	1.65E+07	1.01E+05	10	61.4
1	2E+07	1.01E+05	10	67.5
0.9	1.35E+07	1.01E+05	10	75.0
0.8	1.20E+07	1.01E+05	10	84.4
0.75	1.13E+07	1.01E+05	10	90.0
0.7	1.05E+07	1.01E+05	10	96.4
0.65	9.75E+06	1.01E+05	10	103.8
0.6	9.00E+06	1.01E+05	10	112.5
0.55	8.25E+06	1.01E+05	10	122.7
0.5	7.50E+06	1.01E+05	10	135.0
0.45	6.75E+06	1.01E+05	10	150.0
0.4	6.00E+06	1.01E+05	10	168.8
0.35	5.25E+06	1.01E+05	10	192.9
0.3	4.50E+06	1.01E+05	10	225.0
0.25	3.75E+06	1.01E+05	10	270.0
0.2	3.00E+06	1.01E+05	10	337.5
0.15	2.25E+06	1.01E+05	10	450.0
0.1	1.50E+06	1.01E+05	10	675.0

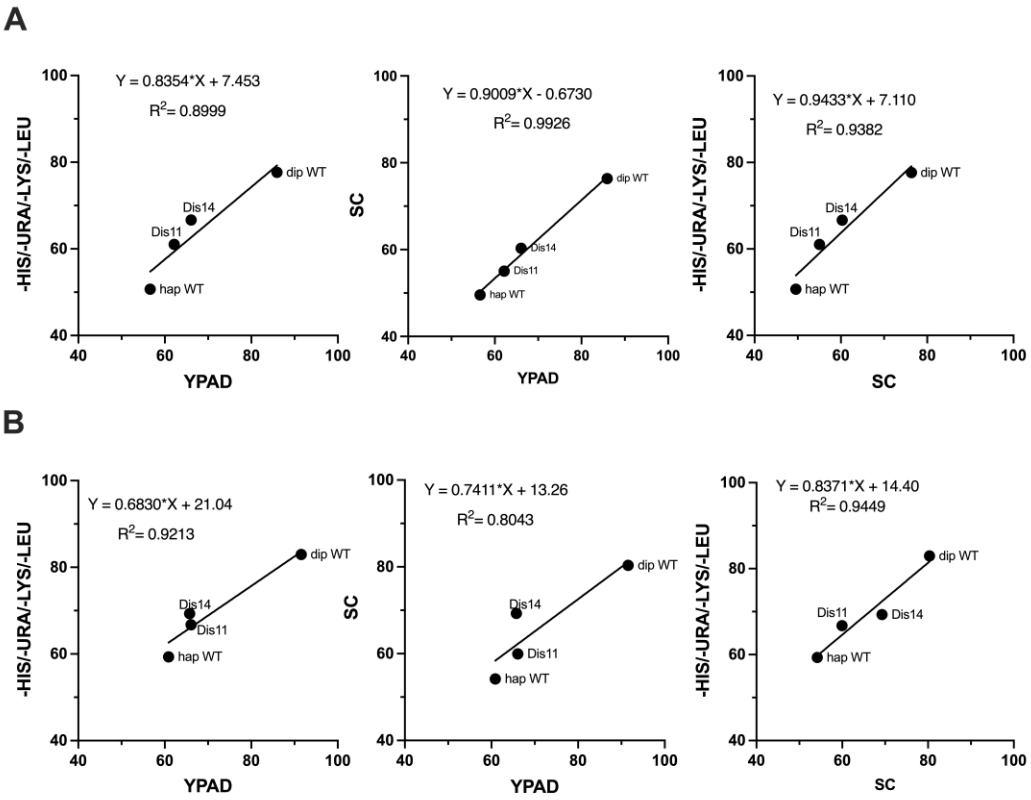

Figure S1: Correlation of cell volume between various media, YPAD, -HIS/-URA/-LYS/-LEU, and SC. **A:** Data set 1 n=1 **B**: Data set 2 n=1.

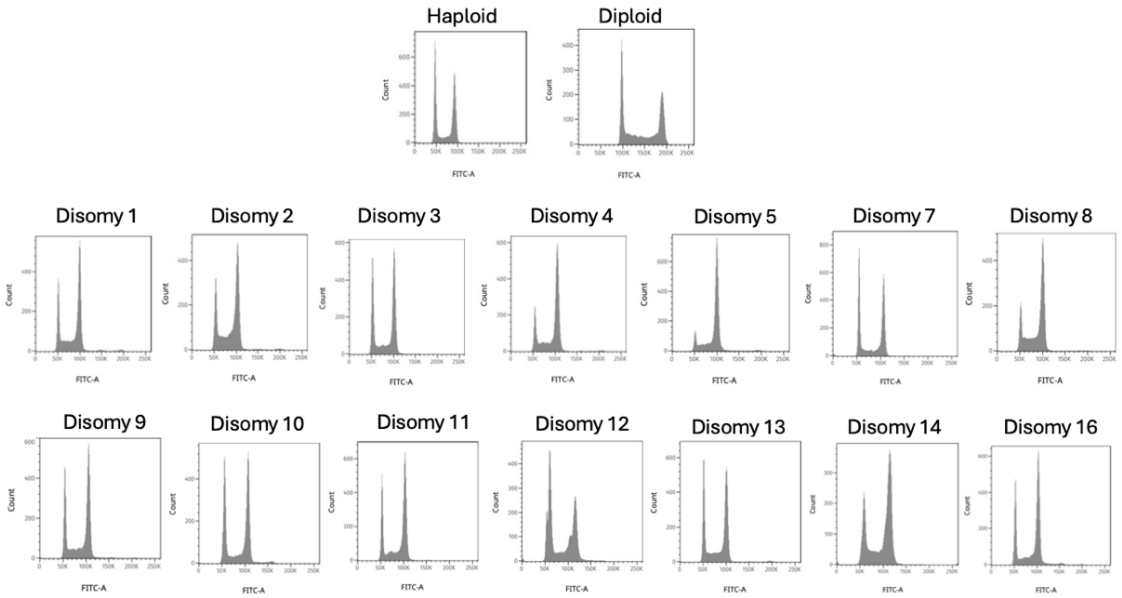

Figure S2: FACS data of disomy strains containing the restored auxotrophic markers HIS/URA. All 14 strains have a haploid background. The cell size was determined via the CASY cell counter analyzer. These 14 strains were the parent strain for the full and partial arm deletions for the ACDC collection.

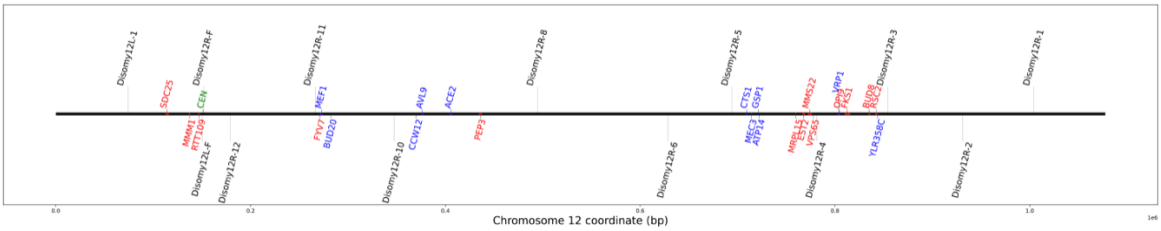

Figure S3: Annotation of genes located in the determined region involved in cell size regulation on Chromosome 12.

Table S2: List of genes located on chromosome 12 that have been found to play a role in cell size phenotypes. The gene name, a description, the systematic name, coordinates, and the strand location (from the Saccharomyces Genome Database (SGD)).

Gene	Description	Systematic Name	Coordinates	Strand
ACE2	Transcription factor required for septum destruction after cytokinesis; part of the RAM network that regulates polarity and morphogenesis; NES phosphorylation by RAM network kinase Cbk1p blocks nuclear exit in mother cells during the M/G1 transition, causing asymmetric localization to daughter cell nuclei, and increased Ace2p activity; phosphorylation by Cdc28p and Pho85p prevents nuclear import during cell cycle phases other than cytokinesis; Spt16p is required for nuclear exclusion during G1	YLR131C	404510-406822	-
ATP14	Subunit h of the F0 sector of mitochondrial F1F0 ATP synthase; F1F0 ATP synthase is a large, evolutionarily conserved enzyme complex required for ATP synthesis; protein abundance increases in response to DNA replication stress	YLR295C	721999-722373	-
AVL9	Conserved protein involved in exocytic transport from the Golgi; mutation is synthetically lethal with apl2 vps1 double mutation; member of a protein superfamily with orthologs in diverse organisms; relocalizes from bud neck to cytoplasm upon DNA replication stress	YLR114C	374944-377238	-
BUD20	C2H2-type zinc finger protein required for ribosome assembly; shuttling factor which associates with pre-60S particles in the nucleus, accompanying them to the cytoplasm; cytoplasmic dissociation of Bud20p	YLR074C	281956-282456	-

	requires Drg1p; N-terminus harbors a nuclear localization signal (NLS) and a nuclear export signal (NES); cytoplasmic Bud20p is reimported by Kap123-dependent pathway; involved in bud-site selection; diploid mutants display a random budding pattern; similar to human ZNF593			
BUD8	Protein involved in bud-site selection; diploid mutants display a unipolar budding pattern instead of the wild-type bipolar pattern, and bud at the proximal pole; BUD8 has a paralog, BUD9, that arose from the whole genome duplication	YLR353W	834352-836163	+
CCW12	Cell wall mannoprotein; plays a role in maintenance of newly synthesized areas of cell wall; localizes to periphery of small buds, septum region of larger buds, and shmoo tip; CCW12 has a paralog, YDR134C, that arose from the whole genome duplication	YLR110C	369697-370098	-
CTS1	Endochitinase; required for cell separation after mitosis; transcriptional activation during the G1 phase of the cell cycle is mediated by transcription factor Ace2p	YLR286C	708448-710136	-
EST2	Reverse transcriptase subunit of the telomerase holoenzyme; essential for telomerase core catalytic activity, involved in other aspects of telomerase assembly and function; mutations in human homolog are associated with aplastic anemia	YLR318W	766542-769196	+
FKS1	Catalytic subunit of 1,3-beta-D-glucan synthase; transfers glucose from UDP-glucose to growing chains of glucan via β-1,3-glycosidic linkages, translocating polymerized β-1,3-glucan to the extracellular space; role in cell wall synthesis and maintenance; functionally redundant with alternate catalytic subunit Gsc2p; activity regulated by Rho1p, a subunit of the synthase complex; localizes to sites of cell wall remodeling; contains a cellulose-synthase-like fold; antifungal drug target	YLR342W	809997-815627	+
FYV7	Nucleolar protein required for maturation of 18S rRNA; required for survival upon exposure to K1 killer toxin	YLR068W	271008-271463	+
GSP1	Ran GTPase; GTP binding protein (mammalian Ranp homolog) involved in the maintenance of nuclear organization, RNA processing and transport;	YLR293C	720771-721430	-

	regulated by Srm1p, Rna1p, Yrb1p, Yrb2p, Yrp4p, Yrb30p, Cse1p and Kap95p; GSP1 has a paralog, GSP2, that arose from the whole genome duplication			
MEC3	DNA damage and meiotic pachytene checkpoint protein; subunit of a heterotrimeric complex (Rad17p-Mec3p-Ddc1p) that forms a sliding clamp, loaded onto partial duplex DNA by a clamp loader complex; homolog of human and S. pombe Hus1	YLR288C	713480-714904	-
MEF1	Mitochondrial elongation factor involved in translational elongation	YLR069C	271630-273915	-
MMM1	ER integral membrane protein, ERMES complex subunit; ERMES links the ER to mitochondria and may promote inter-organellar calcium and phospholipid exchange as well as coordinating mitochondrial DNA replication and growth; required for mitophagy; ERMES complex is often co-localized with peroxisomes and with concentrated areas of pyruvate dehydrogenase; localizes to the peroxisome in glucose	YLL006W	136586-137866	+
MMS22	Subunit of E3 ubiquitin ligase complex involved in replication repair; stabilizes protein components of replication fork, such as fork-pausing complex and leading strand polymerase, preventing fork collapse and promoting efficient recovery during replication stress; Rtt101p-Mms22p ligase associates with replisome complex during S phase via Ctf4p; required for accurate meiotic chromosome segregation	YLR320W	771940-776304	+
MRPL15	Mitochondrial ribosomal protein of the large subunit	YLR312W-A	759480-760241	+
OPI9	Dubious open reading frame; unlikely to encode a functional protein, based on available experimental and comparative sequence data; partially overlaps the verified ORF VRP1/YLR337C	YLR338W	804346-805203	+
PEP3	Component of CORVET membrane tethering complex; vacuolar peripheral membrane protein that promotes vesicular docking/fusion reactions in conjunction with SNARE proteins, required for vacuolar biogenesis	YLR148W	434641-437397	+
RSC2	Component of the RSC chromatin remodeling complex; required for expression of mid-late sporulation-specific genes; involved in telomere	YLR357W	841331-844000	+

	maintenance; RSC2 has a paralog, RSC1, that arose from the whole genome duplication			
RTT109	Histone acetyltransferase; critical for cell survival in presence of DNA damage during S phase, required for recovery after DSB repair; acetylates H3K56, H3K9; H3K56 acetylation activity required for expression homeostasis, buffering of mRNA synthesis rate against changes in gene dosage during S phase; involved in non-homologous end joining and regulation of Ty1 transposition; prevents hyper-amplification of rDNA; interacts physically with Vps75p	YLL002W	146291-147601	+
SDC25	Non-essential Ras guanine nucleotide exchange factor (GEF); localized to the membrane; expressed in poor nutrient conditions and on nonfermentable carbon sources; contains a stop codon in S288C, full-length gene includes YLL017W; SDC25 has a paralog, CDC25, that arose from the whole genome duplication	YLL016W	112847-115993	+
VPS65	Dubious open reading frame; unlikely to encode a functional protein, based on available experimental and comparative sequence data; not conserved in closely related Saccharomyces species; 75% of ORF overlaps the verified gene SFH1; deletion causes a vacuolar protein sorting defect and blocks anaerobic growth	YLR322W	777628-777942	+
VRP1	Verprolin, proline-rich actin-associated protein; involved in cytoskeletal organization and cytokinesis; promotes actin nucleation and endocytosis; related to mammalian Wiskott-Aldrich syndrome protein (WASP)-interacting protein (WIP)	YLR337C	802653-805106	-
YLR358C	Protein of unknown function; expressed at both mRNA and protein levels; partially overlaps ORF RSC2/YLR357W	YLR358C	843487-844050	-

6.3. List of Figures

6.4. List of Tables

6.5. List of Abbreviation

Table S3: Abbreviation list

Abbreviation	Description
CCY	Yeast strains
CEN	Centromere
CHL	Chloramphenicol
ddH_2O	double distilled water
dNTP	Deoxynucleotide Triphosphate
EB	Elution Buffer
EDTA	Ethylenediaminetetraacetic acid
EtOH	Ethanol
FOA	5-Fluoroorotic Acid
G418	Kanamycin
HIS	Histidine
KAc	Potassium acetate
LB	Lysogeny Broth/ Luria-Bertani
LEU	Leucin
LicAc	Lithium acetate
LYS	Lysin
Mat	Mating type
MoBY	Molecular Barcoded Yeast ORF Library
NaCl	Sodium Chloride
NaOH	Sodium Hydroxide
OCC	Oligo /primer
ON	Overnights
ORF	Open reading frame
PCR	Polymerase chain reaction

PBS	Phosphate Buffered Saline buffer
PEG	Polyethylene glycol
pGAL	Galactose promoter
qPCR	Quantitative polymerase chain reaction
rpm	Rounds per minute
SC	Synthetic complete media
SG	Single chromosome gain
ssDNA	Salmon sperm DNA
SPM	sporulation medium
TE	Tris- EDTA
URA	Uracil
WT	Wildtype
YPA	Yeast peptone adenine medium
YPAD	Yeast Extract Peptone Adenine Dextrose

6.6. List of yeast strains

Table S4: List of yeast strains found in the Christopher Campbell Lab Yeast (CCY) collection. The strains CCY number, strain background, mating type (MAT), genotype and a short description is provided.

CCY	Background	Mat	Genotype	Description
433	W303	α	ura3-1; leu2,3-112; his3-11; trp1-1; ade2-1	used to obtain URA3 fragment
801	SSY1	α	trp1D63; ura3-52; his3D200	used to obtain URA3 fragment
803	S288c	a/α	trp1D63; ura3-52; his3D200	Diploid (2n) WT with no auxotrophic markers
1894	S288c	a	his3D1; leu2D0; lys2D0; ura3D0	Haploid (1n) WT with no auxotrophic markers
1895	S288c	α	his3D1; leu2D0; lys2D0; ura3D0	Haploid (1n) WT with no auxotrophic markers
1914	S288c	a/α	his3D1/his3D1; leu2D0/leu2D0; lys2D0/lys2D0; ura3D2/ura3D2	Diploid (2n) WT with no auxotrophic markers
3862	S288c	a	HIS3; leu2D0; lys2D0; URA3	Haploid (1n) WT with URA3 and HIS3 auxotrophic markers; URA3 on a plasmid
3863	S288c	α	his3D1; LEU2; LYS2; MET15/ ura3D0	Haploid (1n) WT with LEU2 and LYS2 auxotrophic markers

3837	S288c	a/α	HIS3/his3D1; LEU2/leu2D0; LYS2/lys2D0; MET15/met15D0; URA3/ura3D0	Diploid (2n) WT with LEU2, LYS2, URA3 and HIS3 auxotrophic markers; URA3 on a plasmid
5419	S288c	α	HIS3 LEU2; LYS2; ura3Δ0, pRS316	Haploid (1n) WT with LYS2, LEU2, URA3 and HIS3 auxotrophic markers; URA3 on a plasmid
6265	S288c	a/α	his3D1/his3D1/his3D1/his3D1; leu2D0/leu2D0/leu2D0/leu2D0; lys2D0/lys2D0/lys2D0/lys2D0; ura3D2/ura3D2/ura3D2/ura3D2; pGalCEN12::lys2::pCC644::LEU2/pGalCEN12::LYS2/pGalCEN12::ura3::HIS3(pCC631)/pGalCEN12::URA3; MATa/mataD::G418; MATα/matαD::G418	Tetraploid (4n) WT with LYS2, LEU2, URA3 and HIS3 auxotrophic markers
6269	S288c	a/α	his3D1/his3D1/his3D1/his3D1; leu2D0/leu2D0/leu2D0/leu2D0; lys2D0/lys2D0/lys2D0/lys2D0; ura3D2/ura3D2/ura3D2/ura3D2; pGalCEN4::lys2::pCC644::LEU2/pGalCEN4::LYS2/pGalCEN4::ura3::HIS3(pCC631)/pGalCEN4::URA3; MATa/mataD::G418; MATα/matαD::G418	Tetraploid (4n) WT with LYS2, LEU2, URA3 and HIS3 auxotrophic markers
7312	S288c	a	HIS3; leu2D0; lys2D0; ura3D2	Haploid (1n) WT with HIS3 auxotrophic markers
7372	S288c	a	HIS3; leu2D0; lys2D0; URA3	Haploid (1n) WT with URA3 and HIS3 auxotrophic markers
7373	S288c	α	his3D1; leu2D0; lys2D0; URA3	Haploid (1n) WT with URA3 auxotrophic markers
7433	S288c	a/α	his3D1/HIS3; leu2D0; lys2D0; ura3D0/URA3	Diploid (2n) WT with URA3 and HIS3 auxotrophic markers
7434	S288c	a/α	his3D1/HIS3; leu2D0/LEU2; lys2D0/LYS; ura3D0/URA3	Diploid (2n) WT with LYS2, LEU2, URA3 and HIS3 auxotrophic markers
7435	S288c	a/α	his3D1; leu2D0/LEU2; lys2D0/LYS; MET15/ ura3D0/ura3D0	Diploid (2n) WT with LYS2, LEU2 auxotrophic markers

7475	S288c	α	HIS3; LEU2; LYS; URA3	Haploid (1n) WT with LYS2, LEU2, URA3 and HIS3 auxotrophic markers
7476	S288c	a	his3D1; leu2D0; LYS2; MET15/ ura3D0/ura3D0	Haploid (1n) WT with LYS2 auxotrophic markers
7477	S288c	a	his3D1; leu2D0; LYS2; MET15/ ura3D0/ura3D0	Haploid (1n) WT with LYS2 auxotrophic markers
7478	S288c	α	his3D1; LEU2; lys2D0; MET15/ ura3D0/ura3D0	Haploid (1n) WT with LEU2 auxotrophic markers
7479	S288c	α	his3D1; LEU2; lys2D0; MET15/ ura3D0/ura3D0	Haploid (1n) WT with LEU2 auxotrophic markers
7492	S288c	α	HIS3; LEU2; LYS; URA3	Haploid (1n) WT with LYS2, LEU2, URA3 and HIS3 auxotrophic markers
6157	S288C	a	his3D1; leu2D0; lys2D0; ura3D2; pGalCEN5::URA3::HIS3 (pCC631)	Disomic chromosome 1 with HIS and URA marker
1956	S288C	a	his3D1; leu2D0; lys2D0; ura3D2; pGalCEN2::URA3::HIS3 (pCC631)	Disomic chromosome 2 with HIS and URA marker
1959	S288C	a	his3D1; leu2D0; lys2D0; ura3D2; pGalCEN3::URA3::HIS3 (pCC631)	Disomic chromosome 3 with HIS and URA marker
6144	S288C	a	his3D1; leu2D0; lys2D0; ura3D2; pGalCEN4::URA3::HIS3 (pCC631)	Disomic chromosome 4 with HIS and URA marker
6178	S288C	a	his3D1; leu2D0; lys2D0; ura3D2; pGalCEN1::URA3::HIS3 (pCC631)	Disomic chromosome 5 with HIS and URA marker
6312	S288C	a	his3D1; leu2D0; lys2D0; ura3D2; pGalCEN7::URA3::HIS3 (pCC631)	Disomic chromosome 7 with HIS and URA marker
1909	S288C	a	his3D1; leu2D0; lys2D0; ura3D2; pGalCEN8::URA3::HIS3 (pCC631)	Disomic chromosome 8 with HIS and URA marker
6530	S288C	a	his3D1; leu2D0; lys2D0; ura3D2; pGalCEN9::URA3::HIS3 (pCC631)	Disomic chromosome 9 with HIS and URA marker
1927	S288C	a	his3D1; leu2D0; lys2D0; ura3D2; pGalCEN10::URA3::HIS3 (pCC631)	Disomic chromosome 10 with HIS and URA marker
6223	S288C	a	his3D1; leu2D0; lys2D0; ura3D2; pGalCEN11::URA3::HIS3 (pCC631)	Disomic chromosome 11 with HIS and URA marker
6103	S288C	a	his3D1; leu2D0; lys2D0; ura3D2; pGalCEN12::URA3::HIS3 (pCC631)	Disomic chromosome 12 with HIS and URA marker
6317	S288C	a	his3D1; leu2D0; lys2D0; ura3D2; pGalCEN13::URA3::HIS3 (pCC631)	Disomic chromosome 13 with HIS and URA marker
6180	S288C	a	his3D1; leu2D0; lys2D0; ura3D2; pGalCEN14::URA3::HIS3 (pCC631)	Disomic chromosome 14 with HIS and URA marker

6160	S288C	a	his3D1; leu2D0; lys2D0; ura3D2; pGalCEN16::URA3::HIS3 (pCC631)	Disomic chromosome 16 with HIS and URA marker
5859	S288C	a	his3D1;LEU2; LYS2; ura3D2; pGalCEN4::URA3::pCC631::HIS3	Disomic chromosome 4 with HIS, URA, LYS and LEU marker
5866	S288C	a	his3D1;LEU2; LYS2; ura3D2; pGalCEN8::URA3::HIS3 (pCC631); MET15	Disomic chromosome 8 with HIS, URA, LYS and LEU marker
5874	S288C	a	his3D1;LEU2; LYS2; ura3D2; pGalCEN10::URA3::HIS3 (pCC631); MET15	Disomic chromosome 10 with HIS, URA, LYS and LEU marker
5876	S288C	a	his3D1;LEU2; LYS2; ura3D2; pGalCEN11::URA3::pCC631::HIS3	Disomic chromosome 11 with HIS, URA, LYS and LEU marker
5888	S288C	a	his3D1/his3D1; leu2D0/LEU2; lys2D0/LYS2; ura3D2/ura3D2; pGalCEN16::URA3::pCC631::HIS3	Disomic chromosome 16 with HIS, URA, LYS and LEU marker
7196	S288C	a	his3D1; leu2D0; lys2D0; ura3D2; pGalCEN1::URA3::HIS3 (pCC631); Chr8R-457kb::uptag::G418::down tag::artificial telomer	Disomic chromosome 8 Plasmid used from moby collection YOR042W::10NP_C6 Chr 8R-full arm deletion cut site at 106,467bp
7304	S288C	a	his3D1; leu2D0; lys2D0; ura3D2; pGalCEN1::URA3::HIS3 (pCC631); Chr10L-436.307kb::uptag::G418::down tag::artificial telomer	Disomic chromosome 10 Plasmid used from moby collection YOR049C::10NP_C11 Chr 10L-full arm deletion cut site at 435.981bp
7306	S288C	a	his3D1; leu2D0; lys2D0; ura3D2; pGalCEN1::URA3::HIS3 (pCC631); Chr10R-309kb::uptag::G418::down tag::artificial telomer	Disomic chromosome 10 Plasmid used from moby collection YOR051C::10NP_C12 Chr 10R-full arm deletion cut site at 436.802 bp
7079	S288C	a	his3D1; leu2D0; lys2D0; ura3D2; pGalCEN11::URA3::HIS3 (pCC631); Chr11L-439::uptag::G418::down tag::artificial telome	Disomic chromosome 11 Plasmid used from moby collection YOR006C::10NP_A5 Chr 11L-full arm deletion cut site at 439,009 bp

7080	S288C	a	his3D1; leu2D0; lys2D0; ura3D2; pGalCEN11::URA3::HIS3 (pCC631); Chr11R-441::uptag::G418::down tag::artificial telome	Disomic chromosome 11 Plasmid used from moby collection YOR007C::10NP_A6 Chr 11R-full arm deletion cut site at 441,049 bp
7077	S288C	a	his3D1; leu2D0; lys2D0; ura3D2; pGalCEN16::URA3::HIS3 (pCC631); Chr16L-555kb::uptag::G418::down tag::artificial telomer	Disomic chromosome 16 Plasmid used from moby collection YOR009W::10NP_A8 Chr 16L-full arm deletion cut site at 555,188bp
7147	S288C	a	his3D1; leu2D0; lys2D0; ura3D2; pGalCEN16::URA3::HIS3 (pCC631); 16R-557::uptag::G418::down tag::artificial telome	Disomic chromosome 16 Plasmid used from moby collection YOR010C::10NP_A9 Chr 16R-full arm deletion cut site at 556, 919bp
7474	S288C	a	his3D1; leu2D0; lys2D0; ura3D2; pGalCEN12::URA3::HIS3 (pCC631); Chr12R 900kb::uptag::G418::down tag::artificial telomer	Disomic chromosome 12 Plasmid used from moby collection YLR017W::32NP_F12 Chr 12R-12 partial arm deletion cut site at 178,373bp
7446	S288C	a	his3D1; leu2D0; lys2D0; ura3D2; pGalCEN12::URA3::HIS3 (pCC631); Chr12R 900kb::uptag::G418::down tag::artificial telomer	Disomic chromosome 12 Plasmid used from moby collection YLR017W::32NP_F12 Chr12R-12 partial arm deletion cut site at 178,373 bp
7445	S288C	a	his3D1; leu2D0; lys2D0; ura3D2; pGalCEN12::URA3::HIS3 (pCC631); Chr12R 812 kb::uptag::G418::down tag::artificial telomer	Disomic chromosome 12 Plasmid used from moby collection YLR064W::38NP_F4 Chr12R-11 partial arm deletion cut site at 265,995 bp
7444	S288C	a	his3D1; leu2D0; lys2D0; ura3D2; pGalCEN12::URA3::HIS3 (pCC631);	Disomic chromosome 12 Plasmid used from moby collection

			Chr12R 812kb::uptag::G418::down tag::artificial telomer	YLR064W::38NP_F4Chr12 R-11 partial arm deletion cut site at 265,995 bp
7473	S288C	a	his3D1; leu2D0; lys2D0; ura3D2; pGalCEN12::URA3::HIS3 (pCC631); Chr12R 732kb::uptag::G418::down tag::artificial telomer	Disomic chromosome 12 Plasmid used from moby collection YLR104W::33NP_B11 Chr12R-10 partial arm deletion cut site at 346,669 bp
7443	S288C	a	his3D1; leu2D0; lys2D0; ura3D2; pGalCEN12::URA3::HIS3 (pCC631); Chr12R 732kb::uptag::G418::down tag::artificial telomer	Disomic chromosome 12 Plasmid used from moby collection YLR104W::33NP_B11 Chr12R-10 partial arm deletion cut site at 346,669 bp
7442	S288C	a	his3D1; leu2D0; lys2D0; ura3D2; pGalCEN12::URA3::HIS3 (pCC631); Chr12R 584kb::uptag::G418::down tag::artificial telomer	Disomic chromosome 12 Plasmid used from moby collection YLR164W::8NP_E11 Chr12R-8 partial arm deletion cut site at 494168 bp
7441	S288C	a	his3D1; leu2D0; lys2D0; ura3D2; pGalCEN12::URA3::HIS3 (pCC631); Chr12R 584kb::uptag::G418::down tag::artificial telomer	Disomic chromosome 12 Plasmid used from moby collection YLR164W::8NP_E11 Chr12R-8 partial arm deletion cut site at 494168 bp
7533	S288C	a	his3D1; leu2D0; lys2D0; ura3D2; pGalCEN12::URA3::HIS3 (pCC631); Chr12R 450kb::uptag::G418::down tag::artificial telomer	Disomic chromosome 12 Plasmid used from moby collection YLR017W::32NP_F12 Chr12R-6 partial arm deletion cut site at 627,956 bp
7532	S288C	a	his3D1; leu2D0; lys2D0; ura3D2; pGalCEN12::URA3::HIS3 (pCC631);	Disomic chromosome 12 Plasmid used from moby collection

			Chr12R 450kb::uptag::G418::down tag::artificial telomer	YLR017W::32NP_F12 Chr12R- 6 partial arm deletion cut site at 627,956 bp confirmed by qPCR
7537	S288C	a	his3D1; leu2D0; lys2D0; ura3D2; pGalCEN12::URA3::HIS3 (pCC631); Chr12R 383 kb::uptag::G418::down tag::artificial telomer	Disomic chromosome 12 Plasmid used from moby collection YLR017W::32NP_F12 -> mutation in gene sequence used for deletion Chr12R- 5 partial arm deletion cut site at 694,800 bp
7536	S288C	a	his3D1; leu2D0; lys2D0; ura3D2; pGalCEN12::URA3::HIS3 (pCC631); Chr12R 383 kb::uptag::G418::down tag::artificial telomer	Disomic chromosome 12 Plasmid used from moby collection YLR017W::32NP_F12 -> mutation in gene sequence used for deletionChr12R- partial arm deletion cut site at 694,800 bp
7472	S288C	a	his3D1; leu2D0; lys2D0; ura3D2; pGalCEN12::URA3::HIS3 (pCC631); Chr12R 298kb::uptag::G418::down tag::artificial telomer	Disomic chromosome 12 Plasmid used from moby collection YLR324W::33NP_C9 Chr12R-4 partial arm deletion cut site at 780,528 bp
7440	S288C	a	his3D1; leu2D0; lys2D0; ura3D2; pGalCEN12::URA3::HIS3 (pCC631); Chr12R 298kb::uptag::G418::down tag::artificial telomer	Disomic chromosome 12 Plasmid used from moby collection YLR324W::33NP_C9 Chr12R-4 partial arm deletion cut site at 780,528 bp
7439	S288C	a	his3D1; leu2D0; lys2D0; ura3D2; pGalCEN12::URA3::HIS3 (pCC631); Chr12R 225kb::uptag::G418::down tag::artificial telomer	Disomic chromosome 12 Plasmid used from moby collection YLR363W-A::45NP_B2 Chr12R-3 partial arm deletion cut site at 853,546 bp

7438	S288C	a	his3D1; leu2D0; lys2D0; ura3D2; pGalCEN12::URA3::HIS3 (pCC631); Chr12R 225 kb::uptag::G418::down tag::artificial telomer	Disomic chromosome 12 Plasmid used from moby collection YLR363W-A::45NP_B2 Chr12R-3 partial arm deletion cut site at 853,546 bp
7535	S288C	a	his3D1; leu2D0; lys2D0; ura3D2; pGalCEN12::URA3::HIS3 (pCC631); Chr12R 148kb::uptag::G418::down tag::artificial telomer	Disomic chromosome 12 Plasmid used from moby collection YLR017W::32NP_F12 Chr12R-2 partial arm deletion cut site at 931,185 bp
7534	S288C	a	his3D1; leu2D0; lys2D0; ura3D2; pGalCEN12::URA3::HIS3 (pCC631); Chr12R 148kb::uptag::G418::down tag::artificial telomer	Disomic chromosome 12 Plasmid used from moby collection YLR017W::32NP_F12 Chr12R-2 partial arm deletion cut site at 931,185 bp
7437	S288C	a	his3D1; leu2D0; lys2D0; ura3D2; pGalCEN12::URA3::HIS3 (pCC631); Chr12R 74 kb::uptag::G418::down tag::artificial telomer	Disomic chromosome 12 Plasmid used from moby collection YLR432W::37NP_C10 Chr12R-1 partial arm deletion cut site at 1,003,894 bp
7436	S288C	a	his3D1; leu2D0; lys2D0; ura3D2; pGalCEN12::URA3::HIS3 (pCC631); Chr12R 74kb::uptag::G418::down tag::artificial telomer	Disomic chromosome 12 Plasmid used from moby collection YLR432W::37NP_C10 Chr12R-1 partial arm deletion cut site at 1,003,894 bp
7205	S288C	a	his3D1; leu2D0; lys2D0; ura3D2; pGalCEN1::URA3::HIS3 (pCC631); Chr12R-927kb::uptag::G418::down tag::artificial telomer	Disomic chromosome 12 Plasmid used from moby collection YOR058C::10NP_D3

				Chr12R-full arm deletion cut site at 151,726 bp
7204	S288C	a	his3D1; leu2D0; lys2D0; ura3D2; pGalCEN1::URA3::HIS3 (pCC631); Chr12R-927kb::uptag::G418::down tag::artificial telomer	Disomic chromosome 12 Plasmid used from moby collection YOR058C::10NP_D3 Chr12R-full arm deletion cut site at 151,726 bp
7203	S288C	a	his3D1; leu2D0; lys2D0; ura3D2; pGalCEN1::URA3::HIS3 (pCC631); Chr12L-151kb::uptag::G418::down tag::artificial telomer	Disomic chromosome 12 Plasmid used from moby collection YOR052C::10NP_D1 Chr12L-full arm deletion cut site at 150,253 bp
7202	S288C	a	his3D1; leu2D0; lys2D0; ura3D2; pGalCEN1::URA3::HIS3 (pCC631); Chr12L-151kb::uptag::G418::down tag::artificial telomer	Disomic chromosome 12 Plasmid used from moby collection YOR052C::10NP_D1 Chr12L-full arm deletion cut site at 150,253bp
7321	S288C	a	his3D1; leu2D0; lys2D0; ura3D2; pGalCEN12::URA3::HIS3 (pCC631); Chr12L- 74 kb::uptag::G418::down tag::artificial telomer	Disomic chromosome 12 Plasmid used from moby collection YLL032C::32NP_D7 Chr12L- 1 partial arm deletion cut site at 73,932 bp
7320	S288C	a	his3D1; leu2D0; lys2D0; ura3D2; pGalCEN12::URA3::HIS3 (pCC631); Chr12L- 74kb ::uptag::G418::down tag::artificial telomer	Disomic chromosome 12 Plasmid used from moby collection YLL032C::32NP_D7 Chr12L-1 partial arm deletion cut site at 73,932 bp
6135	S288C	a/α	his3D1/his3D1; leu2D0/leu2D0; lys2D0/lys2D0; ura3D2/ura3D2; pGalCEN12::LYS2::pCC644::LEU2; pGalCEN12::URA3::HIS3 (pCC631)	Tetrasomic chromosome 12
6105	S288C	a/α	his3D1/his3D1; leu2D0/leu2D0; lys2D0/lys2D0; ura3D2/ura3D2;	Tetrasomic chromosome 12

			pGalCEN12::LYS2::pCC644::LEU2; pGalCEN12::URA3::HIS3 (pCC631)	
6269	S288C	a/α	his3D1/his3D1/his3D1/his3D1; leu2D0/leu2D0/leu2D0/leu2D0; lys2D0/lys2D0/lys2D0/lys2D0; ura3D2/ura3D2/ura3D2/ura3D2; pGalCEN4::lys2::pCC644::LEU2/pGalCEN4::LYS2/pGalCEN4::ura3::HIS3(pCC631)/pGalCEN4::URA3; MATa/mataD::G418; MATα/matαD::G418	Tetraploid (4N)
5845	S288C	α	HIS3;leu2D0; lys2D0;URA3; pGalCEN12::LYS2::pCC644::LEU2	Disomic chromosome 12
6102	S288C	α	his3D1; leu2D0; lys2D0; ura3D2; pGalCEN12::LYS2::pCC644::LEU2	Made disomic for chromosome 12 by growing in galactose/raffinose for 3 hours and selected on -LYS -LEU plates
6162	S288C	α	his3D1; leu2D0; lys2D0; ura3D2; pGalCEN16::LYS2::pCC644::LEU2	Made disomic for chromosome 16 by growing in galactose/raffinose for 3 hours and selected on -LYS -LEU plates. Checked by q-PCR
6225	S288C	α	his3D1; leu2D0; lys2D0; ura3D2; pGalCEN11::LYS2::pCC644::LEU2	Made disomic for chromosome 11 by growing in galactose/raffinose for 3 hours and selected on -LYS -LEU plates. Checked by q-PCR
6104	S288C	a/α	his3D1/his3D1; leu2D0/leu2D0; lys2D0/lys2D0; ura3D2/ura3D2; pGalCEN12::LYS2::pCC644::LEU2; pGalCEN12::URA3::HIS3 (pCC631)	Trisomic chromosome 12
6106	S288C	a/α	his3D1/his3D1; leu2D0/leu2D0; lys2D0/lys2D0; ura3D2/ura3D2; pGalCEN12::LYS2::pCC644::LEU2; pGalCEN12::URA3::HIS3 (pCC631)	Trisomic chromosome 12
6297	S288C	a/α	his3D1/his3D1; leu2D0/leu2D0; lys2D0/lys2D0; ura3D2/ura3D2;	Made disomic for chromosome 11 by growing in galactose/raffinose for 2

			pGalCEN11::LYS2::pCC644::LEU2; pGalCEN11::URA3::HIS3 (pCC631)	hours and selecting for -URA -HIS colonies. Disomic chromosome 11 confirmed by qPCR.Made disomic for chromosome 11 by growing in galactose/raffinose for 2 hours and selecting for -LYS -LEU colonies. Disomic chromosome 11 confirmed by qPCR.Should be tetrasomic for chromosome 11
6298	S288C	a/α	his3D1/his3D1; leu2D0/leu2D0; lys2D0/lys2D0; ura3D2/ura3D2; pGalCEN11::LYS2::pCC644::LEU2; pGalCEN11::URA3::HIS3 (pCC631)	Made disomic for chromosome 11 by growing in galactose/raffinose for 2 hours and selecting for -URA -HIS colonies. Disomic chromosome 11 confirmed by qPCR.Made disomic for chromosome 11 by growing in galactose/raffinose for 2 hours and selecting for -LYS -LEU colonies. Disomic chromosome 11 confirmed by qPCR.Should be tetrasomic for chromosome 11
80		a		a-tester for use with minimal plates. thr4. From D. Norris 1989 (only α-types will mate with this strain)
81		α		α-tester for use with minimal plates. thr4. From D. Norris 1989 (only a-types will mate with this strain)
180		a	a; dot strain Bir1+, Sli15del2-227	Mating test
181		a	MATa; dot strain Bir1+, Sli15del2-227	Mating test
2188	S288C	α	his3D1; leu2D0; lys2D0; ura3D2; pGalCEN1::LYS::pCC644::LEU	Made disomic for chromosome 1 by growing in galactose/raffinose for 3 hours and selected on -LYS

				-LEU plates. Checked by q-PCR (M5)
3146	S288C	a/α	his3D1/his3D1; leu2D0/leu2D0; lys2D0/lys2D0; ura3D2/ura3D2; pGal-CEN13::URA3; TUB2D0; ::HYGRO	PCR OCC1949/1950check for deletion: OCC282/1951; OCC1951/1952
5563	S288C	a/α	a/α HIS3/his3D1; LEU2/leu2D0; LYS2/lys2D0; MET15/met15D0; URA3/ura3D00; CLN3(+/-):G418	CLN3 was heterozygouslz deleted. (+/-):G418tested with PCR
5564	S288C	α	α HIS3 LEU2; LYS2; ura3,àÜ0, pRS316 cln3,àÜ::G418	URA3, LEU2,HIS3 transformed back into their original locus-Some of the markers might be on a plasmid! URA3 is on a CEN plasmid (pCC250-pRS316)CLN3 was deleted.tested with PCR
5565	S288C	a	his3D1; leu2D0; lys2D0; ura3D2; pGal-CEN1::URA3::pCC631::HIS3; CLN3/cln3,àÜ::G418	pCC631 StuICLN3 was deleted in the induced version of this strain. The strain is aneuploid for chromosome 1.
5843	S288C	α	HIS3;leu2D0; lys2D0;URA3; pGalCEN11::LYS2::pCC644::LEU2	Made disomic for chromosome 11 by growing in galactose/raffinose for 4 and 3 hours and selecting for -LYS -LEU colonies. Disomic chromosome 11 confirmed by qPCR.
5845	S288C	α	HIS3;leu2D0; lys2D0;URA3; pGalCEN12::LYS2::pCC644::LEU2	Made disomic for chromosome 12 by growing in galactose/raffinose for 4 and 3 hours and selecting for -LYS -LEU colonies. Disomic chromosome 12 confirmed by qPCR.
5848	S288C	α	HIS3;leu2D0; lys2D0;URA3; pGalCEN14::LYS2::pCC644::LEU2	Made disomic for chromosome 14 by growing in galactose/raffinose for 4 and 3 hours and selecting for -LYS -LEU colonies.

				Disomic chromosome 14 confirmed by qPCR.
5851	S288C	a	his3D1;LEU2; LYS2; ura3D2; pGal-CEN1::URA3::pCC631::HIS3	Made disomic for chromosome 1 by growing in galactose/raffinose for 4 and 3 hours and selecting for -URA-HIS colonies. Disomic chromosome 1 confirmed by qPCR.
5886	S288C	a	his3D1/his3D1; leu2D0/LEU2; lys2D0/LYS2; ura3D2/ura3D2; pGalCEN16::URA3::pCC631::HIS3	Made disomic for chromosome 16 by growing in galactose/raffinose for 4 and 3 hours and selecting for -URA-HIS colonies. Disomic chromosome confirmed by qPCR.
6156	S288C	a	his3D1; leu2D0; lys2D0; ura3D2; pGalCEN1::URA3::HIS3 (pCC631)	Made disomic for chromosome 1 by growing in galactose/raffinose for 3 hours and selecting for -URA -HIS colonies. Disomic chromosome 1 confirmed by qPCR.has 3 copies of chr1 (Clara qPCR arm del.- trafo)
6181	S288C	a	his3D1; leu2D0; lys2D0; ura3D2; pGalCEN14::URA3::HIS3 (pCC631)	Made disomic for chromosome 14 by growing in galactose/raffinose for 3 hours and selecting for -URA -HIS colonies. Disomic chromosome 14 confirmed by qPCR.
6182	S288C	α	his3D1; leu2D0; lys2D0; ura3D2; pGalCEN14::LYS2::pCC644::LEU2	Made disomic for chromosome 14 by growing in galactose/raffinose for 3 hours and selected on -LYS -LEU plates. Checked by q-PCR
6183	S288C	α	his3D1; leu2D0; lys2D0; ura3D2; pGalCEN14::LYS2::pCC644::LEU2	Made disomic for chromosome 14 by growing in galactose/raffinose for 3 hours and selected on -LYS

				-LEU plates. Checked by q-PCR
6230	S288C	a/α	his3D1/his3D1; leu2D0/leu2D0; lys2D0/lys2D0; ura3D2/ura3D2; pGalCEN1::LYS2::pCC644::LEU2; pGalCEN1::URA3::HIS3 (pCC631)	Made disomic for chromosome 1 by growing in galactose/raffinose for 2 hours and selecting for -URA -HIS colonies. Disomic chromosome 1 confirmed by qPCR.Chr. 1 LYS/LEU uninducedShould be trisomic for chromosome 1
6231	S288C	a/α	his3D1/his3D1; leu2D0/leu2D0; lys2D0/lys2D0; ura3D2/ura3D2; pGalCEN1::LYS2::pCC644::LEU2; pGalCEN1::URA3::HIS3 (pCC631)	Made disomic for chromosome 1 by growing in galactose/raffinose for 2 hours and selecting for -URA -HIS colonies. Disomic chromosome 1 confirmed by qPCR.Chr. 1 LYS/LEU uninducedShould be trisomic for chromosome 1
6232	S288C	a/α	his3D1/his3D1; leu2D0/leu2D0; lys2D0/lys2D0; ura3D2/ura3D2; pGalCEN1::LYS2::pCC644::LEU2; pGalCEN1::URA3::HIS3 (pCC631)	Made disomic for chromosome 1 by growing in galactose/raffinose for 2 hours and selecting for -URA -HIS colonies. Disomic chromosome 1 confirmed by qPCR.Made disomic for chromosome 1 by growing in galactose/raffinose for 2 hours and selecting for -LYS -LEU colonies. Disomic chromosome 1 confirmed by qPCR.Should be tetrasomic for chromosome 1
6233	S288C	a/α	his3D1/his3D1; leu2D0/leu2D0; lys2D0/lys2D0; ura3D2/ura3D2; pGalCEN1::LYS2::pCC644::LEU2; pGalCEN1::URA3::HIS3 (pCC631)	Made disomic for chromosome 1 by growing in galactose/raffinose for 2 hours and selecting for -URA -HIS colonies. Disomic chromosome 1 confirmed by qPCR.Made disomic for

				chromosome 1 by growing in galactose/raffinose for 2 hours and selecting for -LYS -LEU colonies. Disomic chromosome 1 confirmed by qPCR.Should be tetrasomic for chromosome 1
6234	S288C	a/α	his3D1/his3D1; leu2D0/leu2D0; lys2D0/lys2D0; ura3D2/ura3D2; pGalCEN1::LYS2::pCC644::LEU2; pGalCEN1::URA3::HIS3 (pCC631)	Chr. 16 URA/HIS uninducedMade disomic for chromosome 1 by growing in galactose/raffinose for 2 hours and selecting for -LYS -LEU colonies. Disomic chromosome 1 confirmed by qPCR.Should be trisomic for chromosome 1
6236	S288C	a/α	his3D1/his3D1; leu2D0/leu2D0; lys2D0/lys2D0; ura3D2/ura3D2; pGalCEN1::LYS2::pCC644::LEU2; pGalCEN1::URA3::HIS3 (pCC631)	Chr. 1 URA/HIS uninducedChr. 1 LYS/LEU uninducedShould be disomic for chromosome 1
6237	S288C	a/α	his3D1/his3D1; leu2D0/leu2D0; lys2D0/lys2D0; ura3D2/ura3D2; pGalCEN1::LYS2::pCC644::LEU2; pGalCEN1::URA3::HIS3 (pCC631)	Chr. 1 URA/HIS uninducedChr. 1 LYS/LEU uninducedShould be disomic for chromosome 1
6958	S288C	a/α	his3D1; leu2D0; lys2D0; ura3D2; pGalCEN11::URA3::HIS3 (pCC631); his3D1; leu2D0; lys2D0; ura3D2; pGalCEN16::LYS2::pCC644::LEU2	CCY6223: Made disomic for chromosome 11 by growing in galactose/raffinose for 3 hours and selecting for -URA -HIS colonies. Disomic chromosome 11 confirmed by qPCR.CCY6162: Made disomic for chromosome 16 by growing in galactose/raffinose for 3 hours and selected on -LYS -LEU plates. Checked by q-PCR
6959	S288C	a/α	his3D1; leu2D0; lys2D0; ura3D2; pGalCEN11::URA3::HIS3 (pCC631); his3D1; leu2D0; lys2D0; ura3D2; pGalCEN16::LYS2::pCC644::LEU2	CCY6223: Made disomic for chromosome 11 by growing in galactose/raffinose for 3 hours and selecting for -

				URA -HIS colonies. Disomic chromosome 11 confirmed by qPCR.CCY6162: Made disomic for chromosome 16 by growing in galactose/raffinose for 3 hours and selected on -LYS -LEU plates. Checked by q-PCR
6960	S288C	a/α	his3D1; leu2D0; lys2D0; ura3D2; pGalCEN11::URA3::HIS3 (pCC631); his3D1; leu2D0; lys2D0; ura3D2; pGalCEN16::LYS2::pCC644::LEU2	CCY6223: Made disomic for chromosome 11 by growing in galactose/raffinose for 3 hours and selecting for -URA -HIS colonies. Disomic chromosome 11 confirmed by qPCR.CCY6162: Made disomic for chromosome 16 by growing in galactose/raffinose for 3 hours and selected on -LYS -LEU plates. Checked by q-PCR
7194	S288C	a	his3D1; leu2D0; lys2D0; ura3D2; pGalCEN1::URA3::HIS3 (pCC631); Chr8L-106kb::uptag::G418::down tag::artificial telomer	Made disomic for chromosome 8 by growing in galactose/raffinose for 3 hours and selecting for -URA -HIS colonies. Disomic chromosome 8 confirmed by qPCR.plasmid used from moby collection YOR040W::10NP_C5Chr8L-full arm deletion cut site at 104,937, confirmed by qPCR
5843	S288C	α	HIS3;leu2D0; lys2D0;URA3; pGalCEN11::LYS2::pCC644::LEU2	Made disomic for chromosome 11 by growing in galactose/raffinose for 4 and 3 hours and selecting for -LYS -LEU colonies. Disomic chromosome 11 confirmed by qPCR.

5848	S288C	α	HIS3;leu2D0; lys2D0;URA3; pGalCEN14::LYS2::pCC644::LEU2	Made disomic for chromosome 14 by growing in galactose/raffinose for 4 and 3 hours and selecting for -LYS -LEU colonies. Disomic chromosome 14 confirmed by qPCR.

Table S5: List of yeast strain from the double disomy collection. The strains abriviation, strain background, mating type (MAT), genotype and a short description is provided.

strain	Background	Mat	Genotype	Description
11x16-1	S288C	α	his3D1;leu2D0; lys2D0;ura3D2; pGalCEN16::LYS2::pCC644::LEU2 ; pGalCEN11::URA3::pCC631::HIS3	Made disomic for chromosome 11 and 16 Diploidized ! 1n+2 uninduced Single gains were mated and again sporulated to generate the strains inducible for aneuploidy. Part of the GG collection URA3+, HIS3+, LEU2+, LYS2+
11x16-2	S288C	α	his3D1;leu2D0; lys2D0;ura3D2; pGalCEN16::LYS2::pCC644::LEU2 ; pGalCEN11::URA3::pCC631::HIS3	Made disomic for chromosome 11 and 16 Diploidized ! 1n+2 uninduced Single gains were mated and again sporulated to generate the strains inducible for aneuploidy. Part of the GG collection URA3+, HIS3+, LEU2+, LYS2+
11x16-3	S288C	α	his3D1;leu2D0; lys2D0;ura3D2; pGalCEN16::LYS2::pCC644::LEU2 ; pGalCEN11::URA3::pCC631::HIS3	Made disomic for chromosome 11 and 16 Diploidized ! 1n+2 uninduced Single gains were mated and again

				sporulated to generate the strains inducible for aneuploidy. Part of the GG collection URA3+, HIS3+, LEU2+, LYS2+
16x11-1	S288C	α	his3D1;leu2D0; lys2D0;ura3D2; pGalCEN11::LYS2::pCC644::LEU2 ; pGalCEN16::URA3::pCC631::HIS3	Made disomic for chromosome 11 and 16 Diploidized ! 1n+2 uninduced Single gains were mated and again sporulated to generate the strains inducible for aneuploidy. Part of the GG collection URA3+, HIS3+, LEU2+, LYS2+
16x11-2	S288C	α	his3D1;leu2D0; lys2D0;ura3D2; pGalCEN11::LYS2::pCC644::LEU2 ; pGalCEN16::URA3::pCC631::HIS3	Made disomic for chromosome 11 and 16 Diploidized ! 1n+2 uninduced Single gains were mated and again sporulated to generate the strains inducible for aneuploidy. Part of the GG collection URA3+, HIS3+, LEU2+, LYS2+
16x11-3	S288C	α	his3D1;leu2D0; lys2D0;ura3D2; pGalCEN11::LYS2::pCC644::LEU2 ; pGalCEN16::URA3::pCC631::HIS3	Made disomic for chromosome 11 and 16 Diploidized ! 1n+2 uninduced Single gains were mated and again sporulated to generate the strains inducible for aneuploidy. Part of the GG collection URA3+, HIS3+, LEU2+, LYS2+
11x10-1	S288C	α	his3D1;leu2D0; lys2D0;ura3D2; pGalCEN10::LYS2::pCC644::LEU2 ;	Made disomic for chromosome 11 and 10 1n+2

			pGalCEN11::URA3::pCC631::HIS3	uninduced Single gains were mated and again sporulated to generate the strains inducible for aneuploidy. Part of the GG collection URA3+, HIS3+, LEU2+, LYS2+
11x10-2	S288C	α	his3D1;leu2D0; lys2D0;ura3D2; pGalCEN10::LYS2::pCC644::LEU2 ; pGalCEN11::URA3::pCC631::HIS3	Made disomic for chromosome 11 and 10 1n+2 uninduced Single gains were mated and again sporulated to generate the strains inducible for aneuploidy. Part of the GG collection URA3+, HIS3+, LEU2+, LYS2+
11x10-3	S288C	α	his3D1;leu2D0; lys2D0;ura3D2; pGalCEN10::LYS2::pCC644::LEU2 ; pGalCEN11::URA3::pCC631::HIS3	Made disomic for chromosome 11 and 10 1n+2 uninduced Single gains were mated and again sporulated to generate the strains inducible for aneuploidy. Part of the GG collection URA3+, HIS3+, LEU2+, LYS2+
10x11-1	S288C	α	his3D1;leu2D0; lys2D0;ura3D2; pGalCEN11::LYS2::pCC644::LEU2 ; pGalCEN10::URA3::pCC631::HIS3	Made disomic for chromosome 11 and 10 1n+2 uninduced Single gains were mated and again sporulated to generate the strains inducible for aneuploidy. Part of the GG collection URA3+, HIS3+, LEU2+, LYS2+
10x11-2	S288C	α	his3D1;leu2D0; lys2D0;ura3D2; pGalCEN11::LYS2::pCC644::LEU2 ;	Made disomic for chromosome 11 and 10 1n+2

			pGalCEN10::URA3::pCC631::HIS3	uninduced Single gains were mated and again sporulated to generate the strains inducible for aneuploidy. Part of the GG collection URA3+, HIS3+, LEU2+, LYS2+
10x11-3	S288C	α	his3D1;leu2D0; lys2D0;ura3D2; pGalCEN11::LYS2::pCC644::LEU2 ; pGalCEN10::URA3::pCC631::HIS3	Made disomic for chromosome 11 and 10 1n+2 uninduced Single gains were mated and again sporulated to generate the strains inducible for aneuploidy. Part of the GG collection URA3+, HIS3+, LEU2+, LYS2+
11x16-1	S288C	α	his3D1;leu2D0; lys2D0;ura3D2; pGalCEN16::LYS2::pCC644::LEU2 ; pGalCEN11::URA3::pCC631::HIS3	Made disomic for chromosome 11 and 16 1n+2 uninduced Single gains were mated and again sporulated to generate the strains inducible for aneuploidy. Part of the GG collection URA3+, HIS3+, LEU2+, LYS2+
11x16-2	S288C	α	his3D1;leu2D0; lys2D0;ura3D2; pGalCEN16::LYS2::pCC644::LEU2 ; pGalCEN11::URA3::pCC631::HIS3	Made disomic for chromosome 11 and 16 1n+2 uninduced Single gains were mated and again sporulated to generate the strains inducible for aneuploidy. Part of the GG collection URA3+, HIS3+, LEU2+, LYS2+
11x16-3	S288C	α	his3D1;leu2D0; lys2D0;ura3D2; pGalCEN16::LYS2::pCC644::LEU2 ;	Made disomic for chromosome 11 and 16 1n+2

			pGalCEN11::URA3::pCC631::HIS3	uninduced Single gains were mated and again sporulated to generate the strains inducible for aneuploidy. Part of the GG collection URA3+, HIS3+, LEU2+, LYS2+
16x11-1	S288C	α	his3D1;leu2D0; lys2D0;ura3D2; pGalCEN11::LYS2::pCC644::LEU2 ; pGalCEN16::URA3::pCC631::HIS3	Made disomic for chromosome 11 and 16 1n+2 uninduced Single gains were mated and again sporulated to generate the strains inducible for aneuploidy. Part of the GG collection URA3+, HIS3+, LEU2+, LYS2+
16x11-2	S288C	α	his3D1;leu2D0; lys2D0;ura3D2; pGalCEN11::LYS2::pCC644::LEU2 ; pGalCEN16::URA3::pCC631::HIS3	Made disomic for chromosome 11 and 16 1n+2 uninduced Single gains were mated and again sporulated to generate the strains inducible for aneuploidy. Part of the GG collection URA3+, HIS3+, LEU2+, LYS2+
16x11-3	S288C	α	his3D1;leu2D0; lys2D0;ura3D2; pGalCEN11::LYS2::pCC644::LEU2 ; pGalCEN16::URA3::pCC631::HIS3	Made disomic for chromosome 11 and 16 1n+2 uninduced Single gains were mated and again sporulated to generate the strains inducible for aneuploidy. Part of the GG collection URA3+, HIS3+, LEU2+, LYS2+
10x14-1	S288C	α	his3D1;leu2D0; lys2D0;ura3D2; pGalCEN14::LYS2::pCC644::LEU2 ;	Made disomic for chromosome 10 and 14 1n+2

			pGalCEN10::URA3::pCC631::HIS3	uninduced Single gains were mated and again sporulated to generate the strains inducible for aneuploidy. Part of the GG collection URA3+, HIS3+, LEU2+, LYS2+
10x14-2	S288C	α	his3D1;leu2D0; lys2D0;ura3D2; pGalCEN14::LYS2::pCC644::LEU2 ; pGalCEN10::URA3::pCC631::HIS3	Made disomic for chromosome 10 and 14 1n+2 uninduced Single gains were mated and again sporulated to generate the strains inducible for aneuploidy. Part of the GG collection URA3+, HIS3+, LEU2+, LYS2+
10x14-3	S288C	α	his3D1;leu2D0; lys2D0;ura3D2; pGalCEN14::LYS2::pCC644::LEU2 ; pGalCEN10::URA3::pCC631::HIS3	Made disomic for chromosome 10 and 14 1n+2 uninduced Single gains were mated and again sporulated to generate the strains inducible for aneuploidy. Part of the GG collection URA3+, HIS3+, LEU2+, LYS2+
14x10-1	S288C	α	his3D1;leu2D0; lys2D0;ura3D2; pGalCEN10::LYS2::pCC644::LEU2 ; pGalCEN14::URA3::pCC631::HIS3	Made disomic for chromosome 10 and 14 1n+2 uninduced Single gains were mated and again sporulated to generate the strains inducible for aneuploidy. Part of the GG collection URA3+, HIS3+, LEU2+, LYS2+
14x10-2	S288C	α	his3D1;leu2D0; lys2D0;ura3D2; pGalCEN10::LYS2::pCC644::LEU2 ;	Made disomic for chromosome 10 and 14 1n+2

			pGalCEN14::URA3::pCC631::HIS3	uninduced Single gains were mated and again sporulated to generate the strains inducible for aneuploidy. Part of the GG collection URA3+, HIS3+, LEU2+, LYS2+
14x10-3	S288C	α	his3D1;leu2D0; lys2D0;ura3D2; pGalCEN10::LYS2::pCC644::LEU2 ; pGalCEN14::URA3::pCC631::HIS3	Made disomic for chromosome 10 and 14 1n+2 uninduced Single gains were mated and again sporulated to generate the strains inducible for aneuploidy. Part of the GG collection URA3+, HIS3+, LEU2+, LYS2+
10x8-1	S288C	α	his3D1;leu2D0; lys2D0;ura3D2; pGalCEN8::LYS2::pCC644::LEU2 ; pGalCEN10::URA3::pCC631::HIS3	Made disomic for chromosome 10 and 8 1n+2 uninduced Single gains were mated and again sporulated to generate the strains inducible for aneuploidy. Part of the GG collection URA3+, HIS3+, LEU2+, LYS2+
10x8-2	S288C	α	his3D1;leu2D0; lys2D0;ura3D2; pGalCEN8::LYS2::pCC644::LEU2 ; pGalCEN10::URA3::pCC631::HIS3	Made disomic for chromosome 10 and 8 1n+2 uninduced Single gains were mated and again sporulated to generate the strains inducible for aneuploidy. Part of the GG collection URA3+, HIS3+, LEU2+, LYS2+
10x8-3	S288C	α	his3D1;leu2D0; lys2D0;ura3D2; pGalCEN8::LYS2::pCC644::LEU2 ;	Made disomic for chromosome 10 and 8 1n+2

			pGalCEN10::URA3::pCC631::HIS3	uninduced Single gains were mated and again sporulated to generate the strains inducible for aneuploidy. Part of the GG collection URA3+, HIS3+, LEU2+, LYS2+
8x10-1	S288C	α	his3D1;leu2D0; lys2D0;ura3D2; pGalCEN10::LYS2::pCC644::LEU2 ; pGalCEN8::URA3::pCC631::HIS3	Made disomic for chromosome 10 and 8 1n+2 uninduced Single gains were mated and again sporulated to generate the strains inducible for aneuploidy. Part of the GG collection URA3+, HIS3+, LEU2+, LYS2+
8x10-2	S288C	α	his3D1;leu2D0; lys2D0;ura3D2; pGalCEN10::LYS2::pCC644::LEU2 ; pGalCEN8::URA3::pCC631::HIS3	Made disomic for chromosome 10 and 8 1n+2 uninduced Single gains were mated and again sporulated to generate the strains inducible for aneuploidy. Part of the GG collection URA3+, HIS3+, LEU2+, LYS2+
8x10-3	S288C	α	his3D1;leu2D0; lys2D0;ura3D2; pGalCEN10::LYS2::pCC644::LEU2 ; pGalCEN8::URA3::pCC631::HIS3	Made disomic for chromosome 10 and 8 1n+2 uninduced Single gains were mated and again sporulated to generate the strains inducible for aneuploidy. Part of the GG collection URA3+, HIS3+, LEU2+, LYS2+
16x8-1	S288C	α	his3D1;leu2D0; lys2D0;ura3D2; pGalCEN8::LYS2::pCC644::LEU2 ;	Made disomic for chromosome 16 and 8 1n+2

			pGalCEN16::URA3::pCC631::HIS3	uninduced Single gains were mated and again sporulated to generate the strains inducible for aneuploidy. Part of the GG collection URA3+, HIS3+, LEU2+, LYS2+
16x8-2	S288C	α	his3D1;leu2D0; lys2D0;ura3D2; pGalCEN8::LYS2::pCC644::LEU2 ; pGalCEN16::URA3::pCC631::HIS3	Made disomic for chromosome 16 and 8 1n+2 uninduced Single gains were mated and again sporulated to generate the strains inducible for aneuploidy. Part of the GG collection URA3+, HIS3+, LEU2+, LYS2+
16x8-3	S288C	α	his3D1;leu2D0; lys2D0;ura3D2; pGalCEN8::LYS2::pCC644::LEU2 ; pGalCEN16::URA3::pCC631::HIS3	Made disomic for chromosome 16 and 8 1n+2 uninduced Single gains were mated and again sporulated to generate the strains inducible for aneuploidy. Part of the GG collection URA3+, HIS3+, LEU2+, LYS2+
8x16-1	S288C	α	his3D1;leu2D0; lys2D0;ura3D2; pGalCEN16::LYS2::pCC644::LEU2 ; pGalCEN8::URA3::pCC631::HIS3	Made disomic for chromosome 16 and 8 1n+2 uninduced Single gains were mated and again sporulated to generate the strains inducible for aneuploidy. Part of the GG collection URA3+, HIS3+, LEU2+, LYS2+
8x16-2	S288C	α	his3D1;leu2D0; lys2D0;ura3D2; pGalCEN16::LYS2::pCC644::LEU2 ; pGalCEN8::URA3::pCC631::HIS3	Made disomic for chromosome 16 and 8 1n+2

				uninduced Single gains were mated and again sporulated to generate the strains inducible for aneuploidy. Part of the GG collection URA3+, HIS3+, LEU2+, LYS2+
8x16-3	S288C	α	his3D1;leu2D0; lys2D0;ura3D2; pGalCEN16::LYS2::pCC644::LEU2 ; pGalCEN8::URA3::pCC631::HIS3	Made disomic for chromosome 16 and 8 1n+2 uninduced Single gains were mated and again sporulated to generate the strains inducible for aneuploidy. Part of the GG collection URA3+, HIS3+, LEU2+, LYS2+
8x4-1	S288C	α	his3D1;leu2D0; lys2D0;ura3D2; pGalCEN4::LYS2::pCC644::LEU2 ; pGalCEN8::URA3::pCC631::HIS3	Made disomic for chromosome 4 and 8 1n+2 uninduced Single gains were mated and again sporulated to generate the strains inducible for aneuploidy. Part of the GG collection URA3+, HIS3+, LEU2+, LYS2+
8x4-2	S288C	α	his3D1;leu2D0; lys2D0;ura3D2; pGalCEN4::LYS2::pCC644::LEU2 ; pGalCEN8::URA3::pCC631::HIS3	Made disomic for chromosome 4 and 8 1n+2 uninduced Single gains were mated and again sporulated to generate the strains inducible for aneuploidy. Part of the GG collection URA3+, HIS3+, LEU2+, LYS2+
8x4-3	S288C	α	his3D1;leu2D0; lys2D0;ura3D2; pGalCEN4::LYS2::pCC644::LEU2 ; pGalCEN8::URA3::pCC631::HIS3	Made disomic for chromosome 4 and 8 1n+2

				uninduced Single gains were mated and again sporulated to generate the strains inducible for aneuploidy. Part of the GG collection URA3+, HIS3+, LEU2+, LYS2+
4x8-1	S288C	α	his3D1;leu2D0; lys2D0;ura3D2; pGalCEN8::LYS2::pCC644::LEU2 ; pGalCEN4::URA3::pCC631::HIS3	Made disomic for chromosome 4 and 8 1n+2 uninduced Single gains were mated and again sporulated to generate the strains inducible for aneuploidy. Part of the GG collection URA3+, HIS3+, LEU2+, LYS2+
4x8-2	S288C	α	his3D1;leu2D0; lys2D0;ura3D2; pGalCEN8::LYS2::pCC644::LEU2 ; pGalCEN4::URA3::pCC631::HIS3	Made disomic for chromosome 4 and 8 1n+2 uninduced Single gains were mated and again sporulated to generate the strains inducible for aneuploidy. Part of the GG collection URA3+, HIS3+, LEU2+, LYS2+
4x8-3	S288C	α	his3D1;leu2D0; lys2D0;ura3D2; pGalCEN8::LYS2::pCC644::LEU2 ; pGalCEN4::URA3::pCC631::HIS3	Made disomic for chromosome 4 and 8 1n+2 uninduced Single gains were mated and again sporulated to generate the strains inducible for aneuploidy. Part of the GG collection URA3+, HIS3+, LEU2+, LYS2+

6.7. List of primers

Table S6: List of primers. Oligo number, Sequence and description

Oligos	Sequence	Description
OCC1614	TTCTATTACTCTTGGCCTCCT	Amplification of HIS3 gene
OCC1615	CAGCTTTAAATAATCGGTGTCACTA	Amplification of HIS3 gene
OCC4081	CAGTTAAGCCGCTAAAGG	Amplification of URA3 gene fragment (template: CCY801)
OCC4082	CTGTTACTTGGTTCTGGC	Amplification of URA3 gene fragment (template: CCY801)
OCC4083	CAAAAGGCCTCTAGGTTC	Amplification of URA3 gene fragment (template: CCY433)
OCC4084	TGCGAGGCATATTTATGG	Amplification of URA3 gene fragment (template: CCY433)
OCC3939	CCCCAACCCCAACCCCAACCCCAACCCCAACCCCA ACTACTCAGACAATGCGATGC	universal rev Primer Artificial Telomere sequence
OCC3940	CAGCTGAAGCTTCGTACGCTGCAGAGACCTATCGT GATGTGGT	universal Moby Primer for chromosome arm deletions
OCC4037	CCATCGATAATACCAGCC	cutting SG12L-1/1
OCC4038	GAATTGTGTCAAACTGCG	cutting SG12L-1/2
OCC4087	CAGACAGTGTTTTGGTCG	cutting SG12R-1/1
OCC4088	CCTGAGCAGGAAAAATCC	cutting SG12R-1/2
OCC4089	CGTTTACGATGAAGAATGG	cutting SG12R-2/1
OCC4090	CAAAAACCCTTTAAGTGTCC	cutting SG12R-2/2
OCC4091	ATTTGAGAAAAGCTGCCC	cutting SG12R-3/1
OCC4092	CTGCGTCTATGCTAATTCC	cutting SG12R-3/2
OCC4093	AGCACGAATGGTTTAACC	cutting SG12R-4/1
OCC4094	GTTGAGAATCGCAGATGG	cutting SG12R-4/2
OCC4095	GATCTTTTGCAAAAGGACG	cutting SG12R-5/1
OCC4096	CTATGGTGACAAGAACACC	cutting SG12R-5/2
OCC4097	TCAGCAAACAACAAGGG	cutting SG12R-6/1
OCC4098	CTCGCTACTGTTTTCACC	cutting SG12R-6/2

OCC4099	CTCAGCAAAATCCTACTGG	cutting SG12R-7/1
OCC4100	GGCTTCCGAGATTTTGG	cutting SG12R-7/2
OCC4101	ACATTTCTTTCCTTGGTCC	cutting SG12R-8/1
OCC4102	GGTCTTGAGATTGAGAGG	cutting SG12R-8/2
OCC4103	ATGTTCTTCCGTGTACG	cutting SG12R-9/1
OCC4104	TCTGTCCACAGCTAATCC	cutting SG12R-9/2
OCC4105	AGGATACCTCTGTGATCC	cutting SG12R-10/1
OCC4106	TGCCTTCTTCAATTTCGG	cutting SG12R-10/2
OCC4107	ATACAGATCTCACTCCCC	cutting SG12R-11/1
OCC4108	TGAGATTATCTGCGGCC	cutting SG12R-11/2
OCC4109	TGTCTACCGATTACGACG	cutting SG12R-12/1
OCC4110	TGGATATTGGCAACATGG	cutting SG12R-12/2
OCC4329	GGCAATGTCCTTTTACCAG	cutting SG12R-7/4
OCC4330	TGTTGGGGCAATTACTAGG	cutting SG12R-9/4
OCC4331	CGTATGGAACCAGATTTGC	cutting SG12R-9/5
OCC4358	CGGCTTAAATCAAGCAAGC	cutting SG12R-5/3
OCC4359	TAGCTGAGAAAGGTCAGG	cutting SG12R-5/4
OCC4183	CGAGAGTGAAAGCTTTCG	cutting SG12R-5/2
OCC4184	ACGTTCTTATTTGGCCAG	cutting SG12R-7/3
OCC4185	CGAAACCCACAGAGTTG	cutting SG12R-9/3
OCC4186	GCTTGCCTTTTCAATTGG	cutting SG12R-2/3
OCC949	AAAGTTGGCGCTGGGTACTTTGAG	ChrIX Left arm (Forward)
OCC950	AGAACTGATGGCATTTGATGGCCG	ChrIX Left arm (Reverse)
OCC4075	TGGGGTTGTTCACCATCCTCC	qPCR primer Chr XII R tip
OCC4076	AAAGGGTCAAAGGATTCACGGC	qPCR primer Chr XII R tip
OCC3531	CCTGCGAATCTGTGATGCAAGAACG	qPCR primer for tip of ChrXIIL
OCC3532	GCTGTGGATGTTAGAAAACGGCTAGG	qPCR primer for tip of ChrXIIL
OCC957	TGGAGATGAAGGGTTGTCGTTGGT	ChrXII Left arm (Forward)
OCC958	ACGTGTAGCGTTTCTGCTGGTCTT	ChrXII Left arm (Reverse)
OCC1471	TAGGCTTCCGGAACCACACAAGAT	ChrXI Right arm (Forward)

OCC1472	AGAGGCAGCTTCCCTTCTGATTCT	ChrXI Right arm (Reverse)
OCC955	AGCTGGTGATGAGCCAAATGTCGT	ChrXI Left arm (Forward)
OCC956	TTTAGAGCAAGCGCCTTTGTGAGC	ChrXI Left arm (Reverse)
OCC967	AAGAGCCTTGAACTTCTCGGGTGA	ChrXVI Left arm (Forward)
OCC968	TGATGTTCCTCTCGTTTGGCACTC	ChrXVI Left arm (Reverse)
OCC1471	TAGGCTTCCGGAACCACACAAGAT	ChrXI Right arm (Forward)
OCC1472	AGAGGCAGCTTCCCTTCTGATTCT	ChrXI Right arm (Reverse)
OCC1479	ACATGTGGAGCATAGCAGGCTCTT	ChrXVI Right arm (Forward)
OCC1480	ATTACCTCTTTCCCACAACCGGCA	ChrXVI Right arm (Reverse)
OCC961	GGGATTAACAATACGGTAAAGGGACG	ChrXIV Left arm (Forward)
OCC962	CAACCACTGTCAGCACAAACTCCT	ChrXIV Left arm (Reverse)
OCC963	TCGCTCAGAACATCAGCGAGAGTT	ChrXIV Right arm (Forward)
OCC964	GTTTCTGCGAAGGCCCTTTGTTCT	ChrXIV Right arm (Reverse)
OCC3949	ACGATTCGTTAACAGATGCTCCT	Chr XVI left qPCR tip (do not use – incorrect design)
OCC3950	ACCTCGGCACCCCTATAACTG	Chr XVI left qPCR tip (do not use – incorrect design)
OCC3951	CCGCTCAGGCTATCCGTTCT	Chr XVI left qPCR tip
OCC3952	TGCAGTTCCCAGGAAGCGTT	Chr XVI left qPCR tip
OCC4002	CTGGAAGCGGGTTAGGTGGT	qPCR primer Chr XI L tip
OCC4003	GTTGACGTAGGCCTTGATGTGTTG	qPCR primer Chr XI L tip
OCC4073	GCCAGTCAGCCCGTTTCG	qPCR primer Chr XI R tip

OCC4074	CGGACAGCAGCAAAGGATTGC	qPCR primer Chr XI R tip
OCC3430	CTGCAGCGTACGAAGCTTCAGCTGGTATTGGCACTACCTTGG	deleting 554kb chr16L
OCC3431	CACTTTGATGATCATCTCG	deleting 554kb chr16L
OCC3432	CCACACTGAAAATGGATG	deleting 389kb chr16R
OCC3433	CTGCAGCGTACGAAGCTTCAGCTGTGTAGCAAAGAGGGATCC	deleting 389kb chr16R
OCC3428	GGACCATTGAGGTATTAGG	deleting 226kb chr11R
OCC3429	CTGCAGCGTACGAAGCTTCAGCTGGACGGGTAAACCATTACC	deleting 226kb chr11R
OCC3941	TGTAGCAGATAACTCTGC	deleting 438kb chr11L
OCC3942	CTGCAGCGTACGAAGCTTCAGCTGTGAACTTCAAACCAGCCT	deleting 438kb chr11L
OCC3862	TGCGGCCATCAAAATGTATG	Sequencing primer for the amplified plasmid fragments
OCC3104	TCGTTCCAATTTACGCTGGTT	qPCR reference gene ACT1 Forward
OCC3105	CGGCCAAATCGATTCTCAA	qPCR reference gene ACT1 Reverse
OCC3106	GTTGCGGCCATATCTACCAG	qPCR 5S rDNA F Perez-Ortin
OCC3107	AGCACCTGAGTTTCGCGTAT	qPCR 5S rDNA R Perez-Ortin
OCC3108	CATGGCCGTTCTTAGTTGGT	qPCR 18S rDNA F Perez-Ortin
OCC3109	ATTGCCTCAAACTTCCATCG	qPCR 18S rDNA R Perez-Ortin
OCC3116	TCCCCACCTGACAATGTCTT	qPCR 35S 3' F Horigome
OCC3117	GCCAGTGAAATACCACTACC	qPCR 35S 3' R Horigome

6.8. Lists of MoBy plasmids

Table S7: List of MoBy plasmids. MoBy identifier and description of its use.

MoBy identifier	Description
YOR006C::10NP_A5	Plasmid used for Disomy 11 cut site Disomy11L-F (left full arm deletion)
YOR007C::10NP_A6	Plasmid used for Disomy 11 cut site Disomy 11R-F (right full arm deletion)
YLL032C::32NP_D7	Plasmid used for Disomy 12 cut site Disomy 12L-1
YOR052C::10NP_D1	Plasmid used for Disomy 12 cut site Disomy 12L-F (left full arm deletion)
YLR432W::37NP_C10	Plasmid used for Disomy 12 cut site Disomy 12R-1
YLR405W::33NP_F7	Plasmid used for Disomy 12 cut site Disomy 12R-2
YLR363W-A::45NP_B2	Plasmid used for Disomy 12 cut site Disomy 12R-3
YLR324W::33NP_C9	Plasmid used for Disomy 12 cut site Disomy 12R-4
YLR275W::8EP_A5	Plasmid used for Disomy 12 cut site Disomy 12R-5
YLR246W::2NP_B1	Plasmid used for Disomy 12 cut site Disomy 12R-6
YLR164W::8NP_E11	Plasmid used for Disomy 12 cut site Disomy 12R-8
YLR104W::33NP_B11	Plasmid used for Disomy 12 cut site Disomy 12R-10
YLR064W::38NP_F4	Plasmid used for Disomy 12 cut site Disomy 12R-11
YLR017W::32NP_F12	Plasmid used for Disomy 12 cut site Disomy 12R-12
YOR058C::10NP_D3	Plasmid used for Disomy 12 cut site Disomy 12R-F (right full arm deletion)
YOR009W::10NP_A8	Plasmid used for Disomy 16 cut site Disomy 16L-F (left full arm deletion)
YOR010C::10NP_A9	Plasmid used for Disomy 16 cut site Disomy 16R-F (right full arm deletion)

6.9. Lists of Media

Table S8: List of Media and their compositions

Media	Composition
Amino acid dropout media -LEU/-HIS/-URA/-LYS (-All4)	H_2O, 1.7 g/L Bacto-yeast nitrogen base without amino acids and without ammonium sulfate; 5 g/L ammonium sulfate; 20 g/L agar, 55 mg/L Tyrosine, 55mg/L Adenine; 20 g/L glucose; amino acid dropout solution (0.1 g/L Arg, 1.5 g/L Ile, 0.1 g/L Met, 0.25 g/ Phe, 2 g/L Ser, 1 g/L Thr, 0.3 g/L Trp, 0.7 g/L Val)
Amino acid dropout media -HIS/-URA	H_2O, 1.7 g/L Bacto-yeast nitrogen base without amino acids and without ammonium sulfate; 5 g/L ammonium sulfate; 20 g/L agar, 55 mg/L Tyrosine, 55mg/L Adenine; 20 g/L glucose; 0.4 g/L Leu and 0.2 g/L Lys in amino acid dropout solution (0.1 g/L Arg, 1.5 g/L Ile, 0.1 g/L Met, 0.25 g/ Phe, 2 g/L Ser, 1 g/L Thr, 0.3 g/L Trp, 0.7 g/L Val)

Amino acid dropout media -LEU/-LYS	H_2O, 1.7 g/L Bacto-yeast nitrogen base without amino acids and without ammonium sulfate; 5 g/L ammonium sulfate; 20 g/L agar, 55 mg/L Tyrosine, 55mg/L Adenine; 20 g/L glucose; 0.1 g/L His; 55 mg/L Uracil in amino acid dropout solution (0.1 g/L Arg, 1.5 g/L Ile, 0.1 g/L Met, 0.25 g/ Phe, 2 g/L Ser, 1 g/L Thr, 0.3 g/L Trp, 0.7 g/L Val)
Amino acid dropout media -HIS	H_2O, 1.7 g/L Bacto-yeast nitrogen base without amino acids and without ammonium sulfate; 5 g/L ammonium sulfate; 20 g/L agar, 55 mg/L Tyrosine, 55mg/L Adenine; 20 g/L glucose; 55 mg/L Uracil; 0.4 g/L Leu and 0.2 g/L Lys in amino acid dropout solution (0.1 g/L Arg, 1.5 g/L Ile, 0.1 g/L Met, 0.25 g/ Phe, 2 g/L Ser, 1 g/L Thr, 0.3 g/L Trp, 0.7 g/L Val)
Amino acid dropout media -LEU	H_2O, 1.7 g/L Bacto-yeast nitrogen base without amino acids and without ammonium sulfate; 5 g/L ammonium sulfate; 20 g/L agar, 55 mg/L Tyrosine, 55mg/L Adenine; 20 g/L glucose; 0.1 g/L His; 55 mg/L Uracil and 0.2 g/L Lys in amino acid dropout solution (0.1 g/L Arg, 1.5 g/L Ile, 0.1 g/L Met, 0.25 g/ Phe, 2 g/L Ser, 1 g/L Thr, 0.3 g/L Trp, 0.7 g/L Val)
Amino acid dropout media -URA	H_2O, 1.7 g/L Bacto-yeast nitrogen base without amino acids and without ammonium sulfate; 5 g/L ammonium sulfate; 20 g/L agar, 55 mg/L Tyrosine, 55mg/L Adenine; 20 g/L glucose; 0.1 g/L His, 0.4 g/L Leu and 0.2 g/L Lys in amino acid dropout solution (0.1 g/L Arg, 1.5 g/L Ile, 0.1 g/L Met, 0.25 g/ Phe, 2 g/L Ser, 1 g/L Thr, 0.3 g/L Trp, 0.7 g/L Val)
Amino acid dropout media -LYS	H_2O, 1.7 g/L Bacto-yeast nitrogen base without amino acids and without ammonium sulfate; 5 g/L ammonium sulfate; 20 g/L agar, 55 mg/L Tyrosine, 55mg/L Adenine; 20 g/L glucose; 0.1 g/L His; 55 mg/L Uracil and 0.4 g/L Leu in amino acid dropout solution (0.1 g/L Arg, 1.5 g/L Ile, 0.1 g/L Met, 0.25 g/ Phe, 2 g/L Ser, 1 g/L Thr, 0.3 g/L Trp, 0.7 g/L Val)
FOA media	H_2O; 1g FOA; 1.7 g/L Bacto-yeast nitrogen base without amino acids and ammonium sulfate; 5g/L ammonium sulfate; 20g/L glucose; 20g/L agar; Amino acid (20mg/L Ade, 160mg/L Arg, 80mg/L Asp, 80mg/L Glu, 80mg/L Gly, 80mg/L His, 100mg/L Ile, 160mg/L Leu, 80mg/L Lys, 80mg/L Met, 20mg/L Phe, 320mg/L Ser, 160mg/L Thr, 80mg/L Trp, 80mg/L Tyr, 160mg/L Val, 48mg/L Ura)
Kanamycin (G418) media	H_2O; 10 g/L yeast extract; 20 g/L Bacto peptone; 20 g/L Agar; 20 g/L Glucose; 200mg/mL G418
LB with kanamycin (G418) and chloramphenicol (CHL)	H_2O; 20 g/L Agar; 10 g/L yeast extract; 20 g/L Bacto peptone; 10g/L NaCl; 100 µg/mL G418; 12.5 µg/mL CHL

Synthetic complete media (SC)	H_2O; 1.7 g Bacto-yeast nitrogen base without amino acids and ammonium sulfate; 5g ammonium sulfate; 20g glucose; 20g agar; amino acid (20mg Ade, 160mg Arg, 80mg Asp, 80mg Glu, 80mg Gly, 80mg His, 100mg Ile, 160mg Leu, 80mg Lys, 80mg Met, 20mg Phe, 320mg Ser, 160mg Thr, 80mg Trp, 80mg Tyr, 160mg Val, 48mg Ura)
Sporulation media (SPM)	H_2O; 20 g/L Bacto agar; 20 g/L KAc
Yeast Peptone Adenine Dextrose medium (YPAD)	H_2O; 10 g/L yeast extract; 20 g/L Bacto peptone; 20 g/L agar; 20 g/L glucose; 55 mg/L adenine

6.10. Lists of equipment and materials

Table S9: List of equitpment and materials

Name	Company
5X Phusion HF Reaction Buffer	Thermo Fisher
Agarose	GERBU
Biometra TOne 96 thermal cycler	Analytik Jena
Biorender	Biorender
Breath easy optical clear foil	Diversified Biotech
Canon EOS DIGITAL REBEL XSi	Canon
CASYclean	OLS OMNI Life Science
CASY Cell counter and analyzer	OLS OMNI Life Science
CASYton	OLS OMNI Life Science
Cuvettes	SARSTEDT AG & Co. KG
Deoxynucleotide (dNTP) Solution Mix	New England BioLabs Inc.
DNPI	Biolabs
DS-11 Spectrophotometer/Fluorometer	Denovix
EDTA	AppliChem
EZ plateTM beads	Sunrise Science Product
Fisherbrand TM Standard Minicentrifuge	Thermo Fisher Scientific
Gel DocTM XR+	BIO RAD
Glass Beads, acid washed	Sigma Aldrich
GraphPad Prism xxx	GraphPad Software
Image J / Fiji	National Institute of Health
Lithium Acetate dihydrate	Merck
Luna Universal qPCR Master Mix	New England BioLabs Inc.
Lyticase from Arthrobacter Luteus	Sigma Aldrich
Mastercycler realplex4 epgradient S	Eppendorf

Megafuge 1.0 R	Thermo Fischer Scientific
Microplate 96 well, PS, F-BOTTOM, CLEAR	Greiner bio-one
Microscope Slides Ground Edges	VWR
Microsoft Excel	Microsoft
MiniPEx kit 3 in 1 Plasmid isolation, PCR purification, Gel extraction	MiniPEx
MSM 400 Micromanipulator/Tetrad dissector	Singer Instruments
Orange G	AppliChem
PCR 8-tube strips, with separate domed cap strips	VWR
PeqGreen	VWR
Phusion High-Fidelity DNA Polymerase	Thermo fisher
Polyethylenglycol 4,000 (PEG 4,000)	AppliChem
QIAquick® PCR purification Kit	Quiagen
QIAquick® Spin Miniprep Kit by Quiagen	Quiagen
Quick-Load® Purple 1 kb DNA Ladder	New England Biolabs
Sodium Citrate Dihydrate	Sigma Aldrich
Sonicator Sonopuls	Bandelin
Twin.tec real-time PCR Plate 96, skirted	Eppendorf
Wizard Genomic Purification Kit	Promega
Zymolyase	Zymo Research